TO MY WIFE

THE SHORT-TERM STABILITY OF SLOPES IN LONDON CLAY

Thesis submitted to the
University of London

by

PIERRE LAROCHELLE

B.Sc., M.Sc.(Laval University)

for the degree of

Doctor of Philosophy in the Faculty of Engineering

April, 1960

TABLE OF CONTENTS

TABLE OF CONTENTS i

ABSTRACT iii

ACKNOWLEDGMENTS iv

CHAPTER I

Introduction 1

Description of Excavations and Slips ... 4

CHAPTER II: Site Investigation and Soil Tests

1. Original Investigation 9

2. Investigation after the Slip 13

(a) Undrained Tests 13

(b) Drained Tests 22

(c) Consolidated Undrained Tests 26

(d) Comparison of Drained and Undrained Tests 31

(e) Summary of A values 32

(f) Field Permeability Measurement 37

CHAPTER III: Total Stress Analysis 39

1. Reactor Excavation, Slip I 39

2. Reactor Excavation, Slip II 43

3. Turbine House Excavation 44

4. Pump House Excavation 45

5. Comparison with Long-Term Failure ... 46

CHAPTER IV: Effective Stress Analysis 48

1. Use of Elastic Stress Distribution ... 48

2. Use of "Plastic" Stress Distribution ... 50

3. Considerations on the value of σ' 53

4. Preliminary conclusions 55

MORE DETAILED CONCLUSIONS 57

CONCLUSIONS 63

APPENDIX A Tables of Results 66

APPENDIX B Rubber Membrane, Drain and Area Correction 67

APPENDIX C Details of Ø = 0 Analysis 79

APPENDIX D Photoelastic Analysis of Stresses .. 83

REFERENCES 103

ABSTRACT

Two slips which occurred in the banks of the excavation for the Reactor House in Bradwell, Essex, have given the opportunity to study the behaviour of London Clay under "short-term" conditions.

The site, excavations and slips are first described and this is followed by the test results from an intensive site investigation. Many drained and consolidated undrained tests were made on samples of London Clay taken from the site, in order to determine the effective stress parameters c' and $\emptyset'$ and the coefficient of pore water pressure A.

A total stress analysis of the slip shows that a few days after the excavation was completed the strength had dropped to about 50% of its measured value. The reduction of strength due to the mechanical effect of the fissures is estimated to be about 15% of the strength and cannot account for the whole decrease in strength. In order to try and explain this phenomenon, some effective stress analyses were made, using predicted pore pressures based on an elastic and a "plastic" stress distribution.

From the results of the analyses and of the tests, it is suggested that the decrease in strength is mainly due to the migration of water towards the thin zone of failure. This migration might be accelerated in the field by the presence of a continuous network of fissures.

ACKNOWLEDGMENTS

The research presented in this thesis was carried out in the Civil Engineering Department of the Imperial College of Science and Technology under the supervision of Professor A. W. Skempton.

It was made possible by the successive awards of an Athlone Fellowship by the British Ministry of Education and Special Scholarships by the National Research Council of Canada. These grants were supplemented by financial aid from the Government of the Province of Quebec, Canada.

The author wishes to express his gratitude to Professor A. W. Skempton who has inspired this research and has been of considerable help in the redaction of this thesis, to Dr. D. J. Henkel who has directed parts of this work, and to Dr. E. H. Brown who has directed the work on photoelasticity.

The site investigation has been carried out with the permission of the Central Electricity Board Authorities in collaboration with the Nuclear Power Plant Company and McAlpine & Sons who have been most cooperative. The author is also indebted to George Wimpey & Co. and to Simon-Carves

Ltd. for permission to use their test results.

We wish also to acknowledge the cooperation of Dr. A. W. Bishop whose many suggestions were greatly appreciated, of Dr. R. E. Gibson and Mr. Nordie Morgenstern with whom we had stimulating discussions and who occasionally carried out some calculations, of Mr. John Brown who greatly helped in the testing of gelatine models, and of Dr. N. N. Ambraseys and Mr. I. Donald who helped in the later stage of the testing.

Many thanks must be expressed to Miss C. L. Hacker, Miss P. O'Reilly, Miss J. Gurr and Mr. E. W. Harris for their assistance in presenting this thesis, and to Mr. S. F. Hillis, Mr. A. T. Webster and Mr. A. Strmac for their assistance with some of the calculations.

The author is most grateful to his friend, Professeur Guillaume Piette, from Laval University, for his constant encouragement which has greatly facilitated the undertaking of this research.

CHAPTER I

INTRODUCTION

The London Clay is a heavily over-consolidated clay, of the Eocene age, and one of its outstanding characteristics is the network of fissures which are found at all depths and at all sites so far investigated. In the natural state, where the ground is level, the fissures are closed. But they constitute potential planes of weakness, and when an excavation is made some of the fissures open, in the zone subject to stress changes caused by the excavation. It is probable that the opening of fissures leads to stress concentrations and certainly ground water can penetrate and come into contact with the clay now, on the surface of an open fissure, under zero effective pressure. As a consequence there is a tendency for the clay to absorb water and

soften. This effect will be additional to the more general tendency for softening in over-consolidated clays even when these clays are not fissured. For in all over-consolidated clays, when an excavation is made the pore pressures will at once drop to very small values, due to the low values of the pore pressure coefficient A, and there is bound to be an increase in time in pore pressure as the pore water comes into equilibrium with the new ground-water conditions corresponding to the state of steady seepage.

In the course of time the softening can lead to failure of the slope, and this effect is well known in cuttings in the London Clay (Skempton 1948, Henkel 1957, DeLory 1957, and others). But all the existing information relates to long-term failures, taking place many years after the cutting was excavated. And it seems quite clear that the softening is progressive.

Moreover from an engraving made in 1836 during the construction of retaining walls just outside Euston, it can be seen that the London Clay was excavated to a steep slope and remained stable during the period of building the walls. A section of the wall (Brees, 1837)

shows that the excavation was 23 ft. deep and inclined at about ½:1 (i.e. about 60°). Cuttings of this depth are known to have failed even at slopes of 3:1 after several decades: so the progressive increase of the softening action is very marked.

Until recently, however, no opportunity had arisen for studying the short-term stability in London Clay. Open excavations are very rare in the London area, owing to the proximity of houses and other buildings. But during excavation for the Reactors, Turbine House and Pump House at the Bradwell Nuclear Power Station, in Essex, such an opportunity presented itself. These excavations, made 1957, were typically about 30 ft. deep with steep slopes. Some remained stable, but two moderate sized slips occurred in the excavation for Reactor No.1.

The present thesis is concerned with a detailed site investigation and analysis of these slopes.

DESCRIPTION OF EXCAVATIONS AND SLIPS

The Power Station at Bradwell is built on flat land lying behind the river wall of the Blackwater Estuary. From borings, which will be described in more detail later, the ground consists in general, of a thin deposit of post-glacial "marsh clay" overlying London Clay. The London Clay extends to about -160 ft. O.D. This is followed by a bed of fine sand, possibly the lowest part of the so-called Basement Bed of the London Clay. The Woolwich and Reading Beds, consisting of hard mottled clay start at about -175 ft. O.D. but their thickness is not known. A plan is given in Fig.1, and a general section through the site is shown in Fig.2.

There were three principal excavations, for the Reactors, Turbine House and Pump House. Excavation for the Reactors started at the north end where the depth was to be 37 ft. below ground level at +6 O.D. The marsh clay was removed by 1 April 1957 (i.e. to -3 ft. O.D.). A fortnight (14.4.57) later the northern end had been taken down to -23 ft. O.D. The last 8 ft. was removed in strips and 12 ins. concrete immediately placed. The most northerly strip 12 ft. 6 ins. wide was opened up by 16 April, the next strip 17 ft. 6 ins. wide by 18th April, and the next, 15 ft. wide, by

River Blackwater

River Wall

Pump House

Reactor No 1

Reactor No 2

Turbine House

Cooling Pond

Brook

+6

+10

+20

N

SCALE : 1" = 200'

Bore Holes:

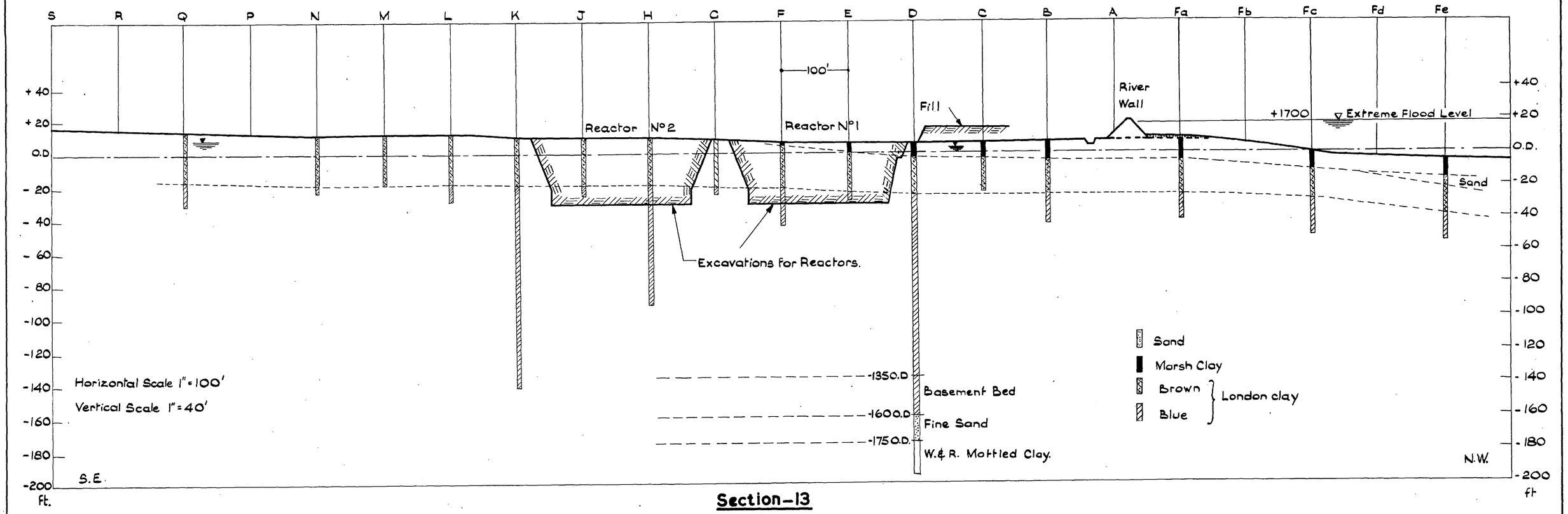
- ● London Clay at surface.
- ○ Marsh Clay " "

Contour lines : Elev. O.D.

NUCLEAR POWER PLANT BRADWELL

SITE PLAN

FIG- 1



Section–13

GEOLOGICAL PROFILE

FIG.- 2

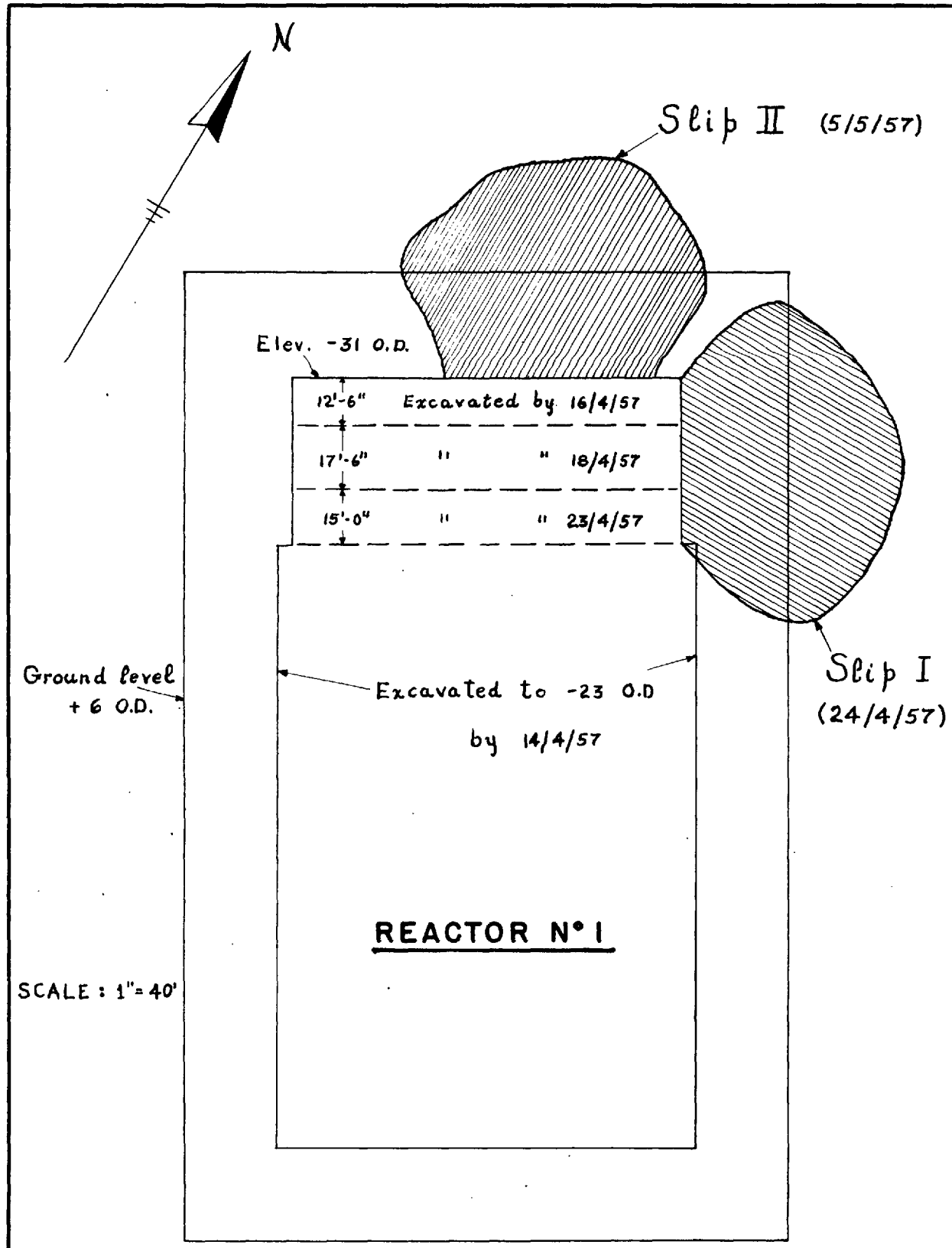
23 April (see Fig.3). Effectively, this part of the excavation was therefore completed on about 19 April. The spoil was placed as a fill behind the slope, up to a level of +17.5 O.D. (Fig.4).

The first sign of instability noticed was the opening up of cracks about 3 ft. above the bottom of the excavation, in the face of the slope, on the morning of 24th April. At 5 p.m. the same day a slip occurred, extending up to the berm at -3 O.D. This was followed at 9 p.m. the same evening by a slip extending back another 20 ft. and up to ground level. The derrick which was being erected on the fill was removed just in time, for a further slip occurred at 2 p.m. on 25 April extending well into the fill. The plan (Fig.3) shows the extent of the slip; but there were some slight cracks further back.

During excavation a small amount of water had seeped out of the marsh clay, but this was led away in a ring drain on the berm at -3 O.D. Throughout the period of excavation the weather had been very dry.

The slope was cut back to an inclination of about 40° by 27 April, and remained stable.

On 5 May 1957, however, a second slip occurred in



PLAN OF EXCAVATION FOR REACTOR N°I

FIG-3

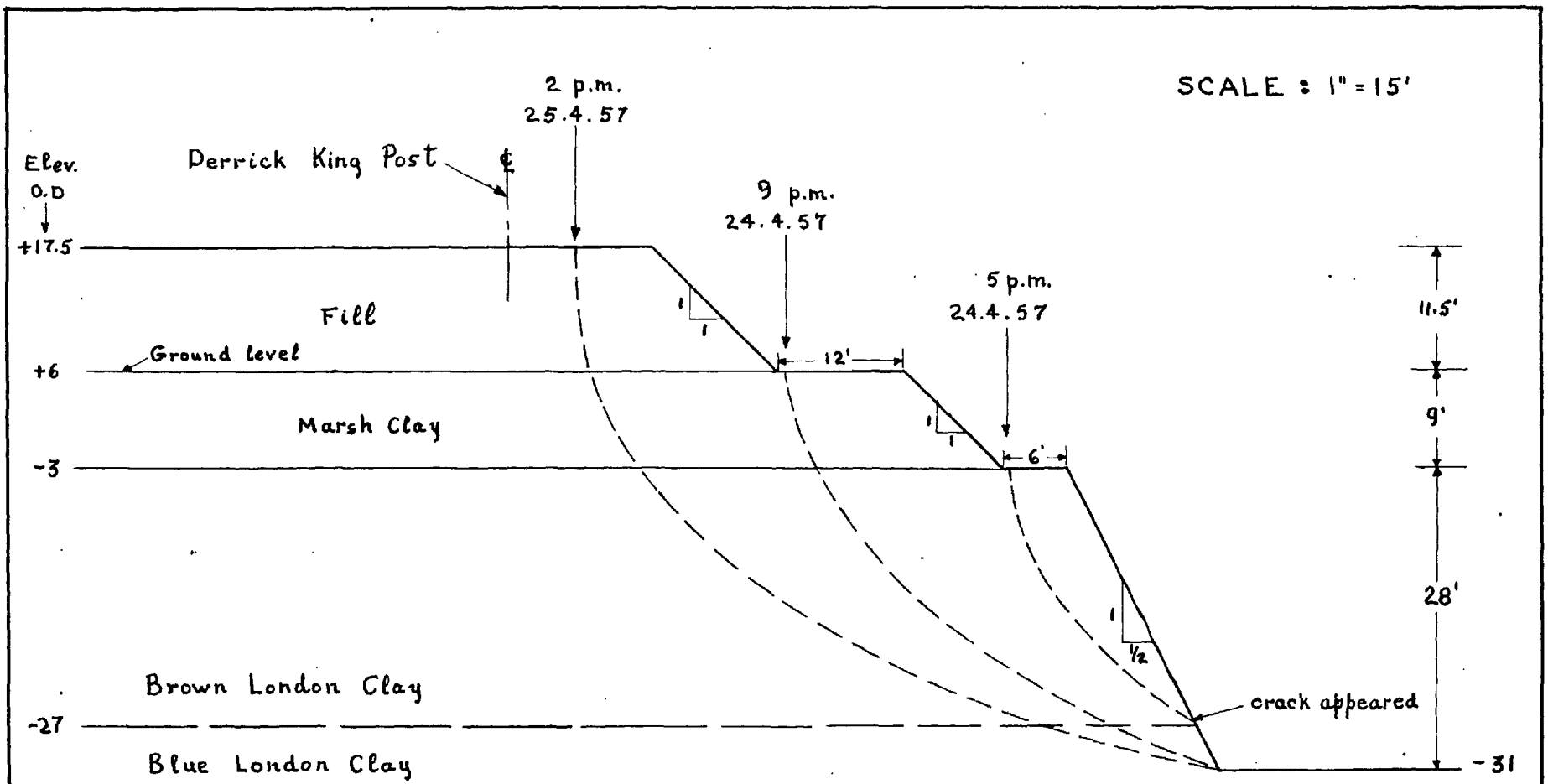


FIG-4

PROFILE OF EXCAVATION FOR REACTOR N°I, (EAST SIDE)

SLIP-I

the north slope (Fig.3). The conditions here were identical with those at the first slip except that the fill had been raised to +14 O.D. instead of +17.5 O.D. No rain had occurred throughout the period since the excavation had been completed.

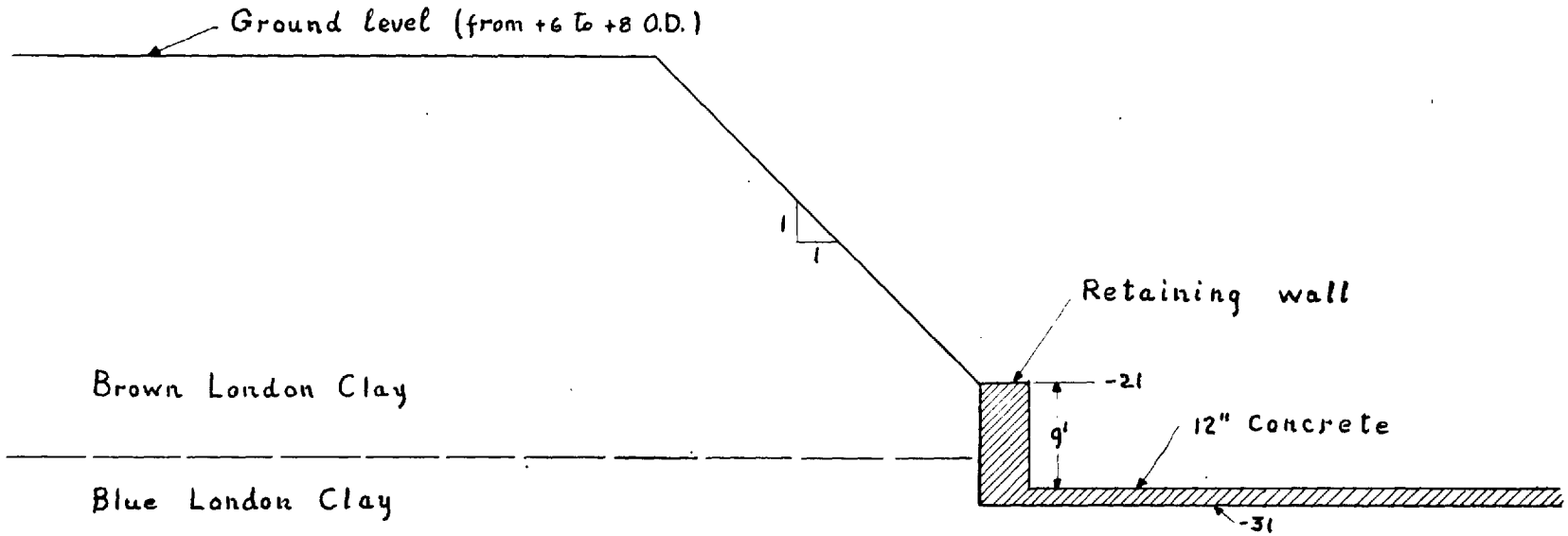
It was then decided to adopt a slope of 1:1 and to build a small retaining wall, and this scheme was used for the north half of Reactor No.1 and for the whole of the excavation for Reactor No.2 (Fig.5).

Excavation for Reactor No.2 was completed between 16 June and 21 July 1957. The slopes were still stable in October 1957 except for a small movement in the south east corner where a land drain was situated.

At various places on the site, where small excavations had been made, minor slips had occurred, but these were really no more than "falls" of clay along very shallow slip surfaces. An example is shown in Fig.6. This was in the Steam Pipe Tunnel excavation, completed 30 April 1957, and it occurred on 9 May 1957.

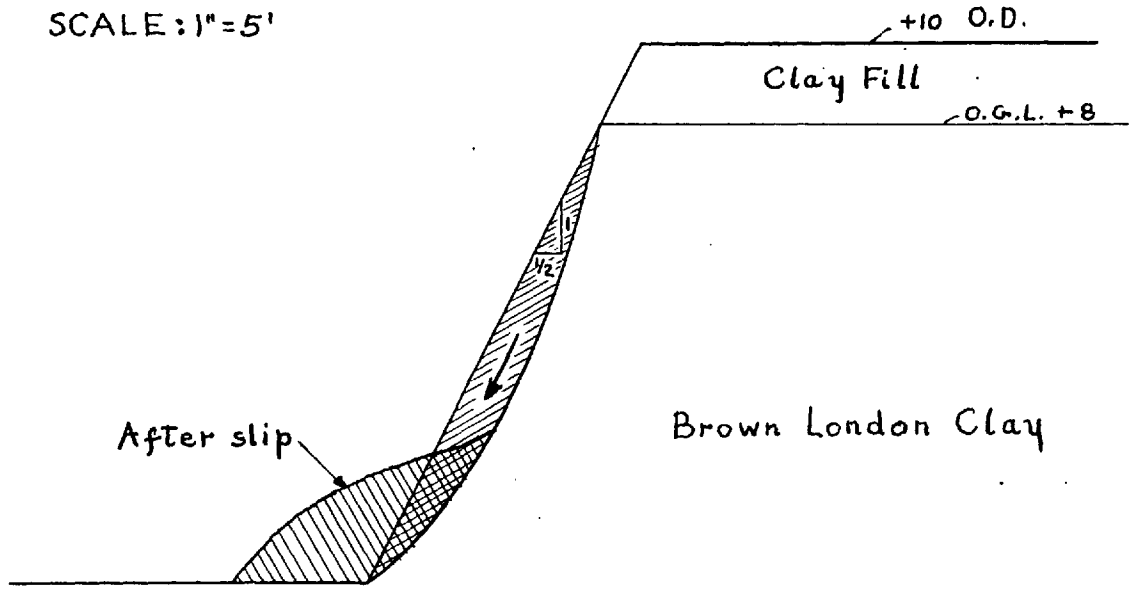
The Turbine House excavation was entirely in the London Clay and had a depth of 23 ft. at the south end. Excavation at this end was completed on 8 April 1957. The

SCALE : 1" = 15'



REVISED PROFILE OF EXCAVATIONS FOR REACTORS

FIG-5



Excavation completed by 30/4/57.

Slip occurred on 9/5/57.

EXAMPLE OF MINOR SLIP

STEAM PIPE TUNNEL EXCAVATION.

FIG-6

slope (Fig.7) was still stable when, on 21 August 1957 a concrete raft 10 ft. thick was placed, in strips, the ground being excavated a further 8 ft. before concreting. After this date, therefore, the slope was only 21 ft. deep. In this state it was still stable in October 1957.

On May 10 1957 Professor Skempton visited the site to study the slips and to advise on the slope to be adopted for the Pump House excavation, which was to be 39 ft. below ground level.

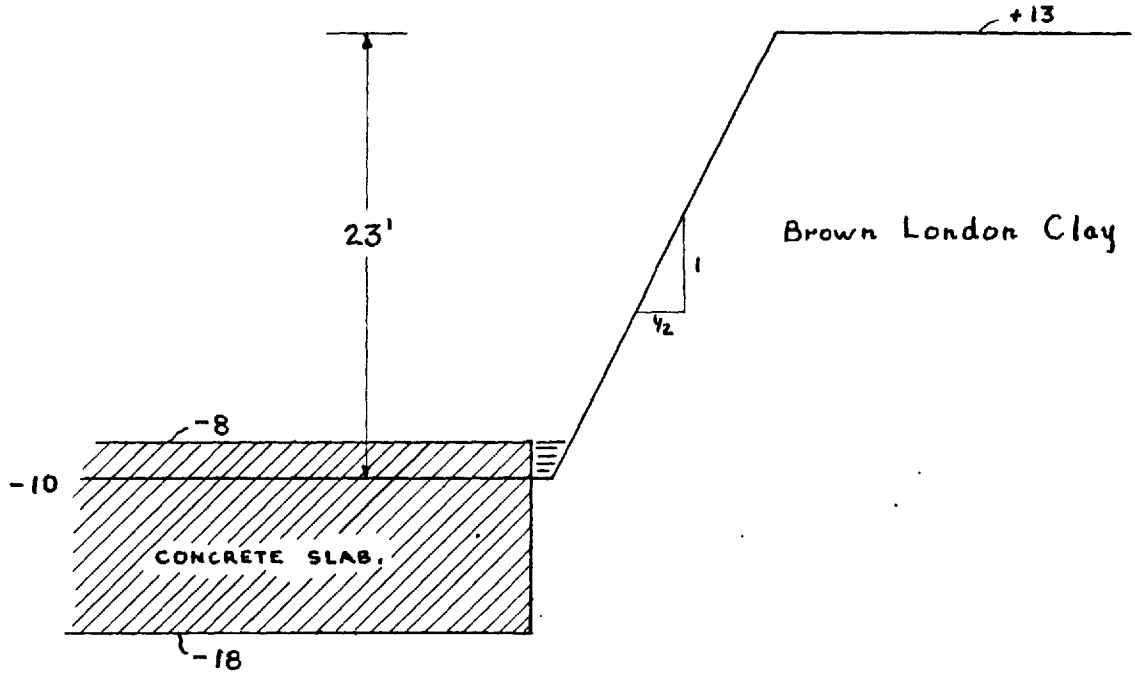
In a report dated July 1957 he showed that, for the Reactor excavation, the ratio of the strength required for a factor of safety of 1.0 to the strength measured on samples of the clay, was 0.60 (for Slip I) and 0.55 for Slip II. He recommended a slope of 1:1 for the Pump House, which corresponded to a strength ratio of 0.45. A plan and section of the Pump House excavation as carried out are shown in Fig.8. The slope remained stable from August 1957, when completed, until December 1957 when the excavation was backfilled against the structure.

The history of these various slopes is summarised in Table I.

TABLE I

Slope	Depth below Original Ground	Total Depth	Slope in London Clay	Time to Slip (days)		Stable for at least (months)
				Since beginning of excavation	Since completion of excavation	
Reactor No.1, Slip I	37'	48.5'	½:1	23	5	-
Reactor No.1, Slip II	37'	45'	½:1	34	19	-
Reactor No.2	39'	39'	1:1	-	-	4
Turbine House	23'	23'	½:1	-	-	4½
Pump House	39'	39'	1:1	-	-	4

SCALE : 1" = 10'

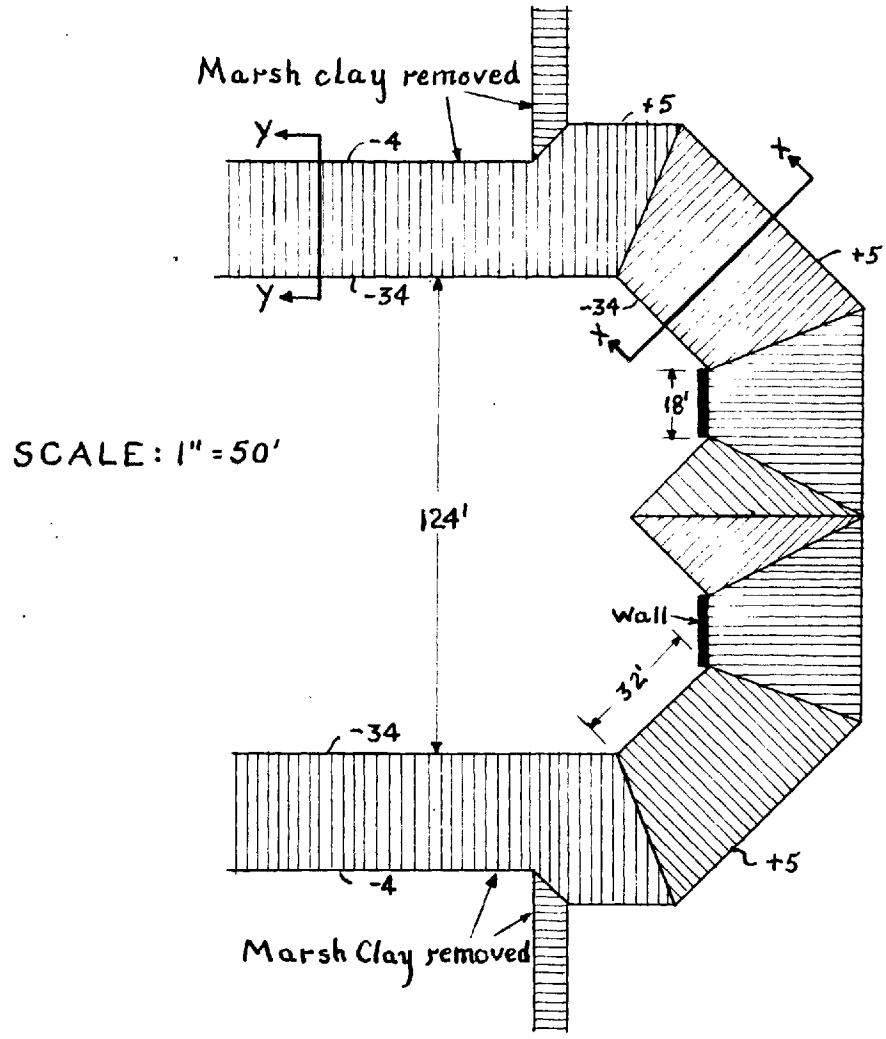


Excavated to -10 O.D. by 8/4/57

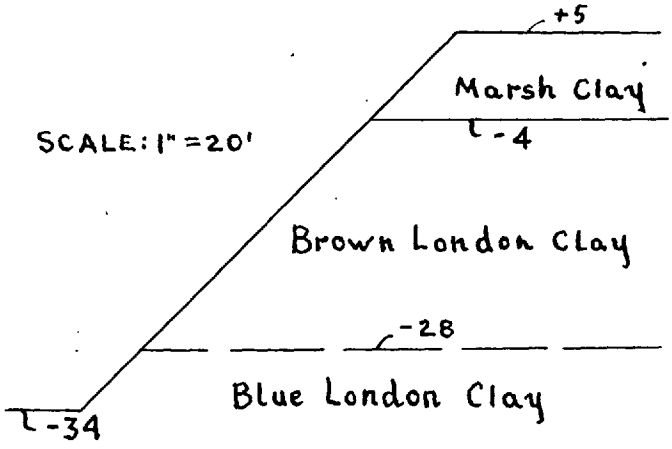
Concrete slab completed by 21/8/57

TURBINE HOUSE EXCAVATION, SOUTH SIDE.

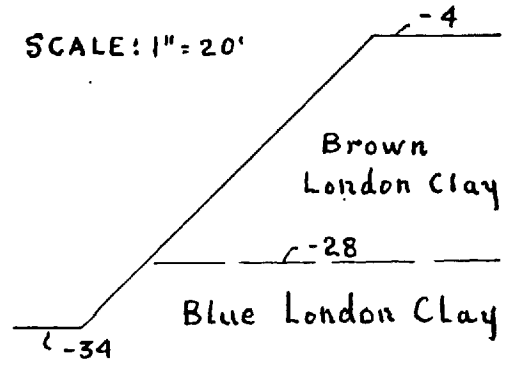
FIG-7



PLAN OF PUMPHOUSE EXCAVATION



SECTION X-X



SECTION Y-Y

FIG-8

CHAPTER II

SITE INVESTIGATION AND SOIL TESTS*

1. ORIGINAL INVESTIGATION

The site investigation was carried out in two stages. Firstly, borings and tests were made by George Wimpey & Co. for Messrs. Rendel, Palmer and Tritton, consulting engineers to the Central Electricity Authority and the programme was supplemented by two additional deep borings, also made by Messrs. Wimpey, for Simon Carves Ltd. who tested the samples in their laboratory. All the site work was carried out between October 1955 and March 1956. The position of the borings is shown in Fig.1, and the two additional borings were alongside those at position K.9 and K.13.

From most of the boreholes the undrained strength was determined by triaxial tests on specimens 4 in. diameter

---

* All the test results are tabulated in Appendix A.

with the cell pressure equal approximately to the total overburden pressure at the depth of the sample. In boreholes F.14 and G.16 specimens 1½ ins. diameter were also tested, whilst all the tests from boreholes K.9/2 and K.13/2 were on 1½ ins. diameter specimens. Tests were also made to determine the consolidation characteristics, the density, Atterberg Limits and particle size distribution. All the samples were taken with the usual 4 ins. diameter open-drive sampler. These tests are referred to as Series I.

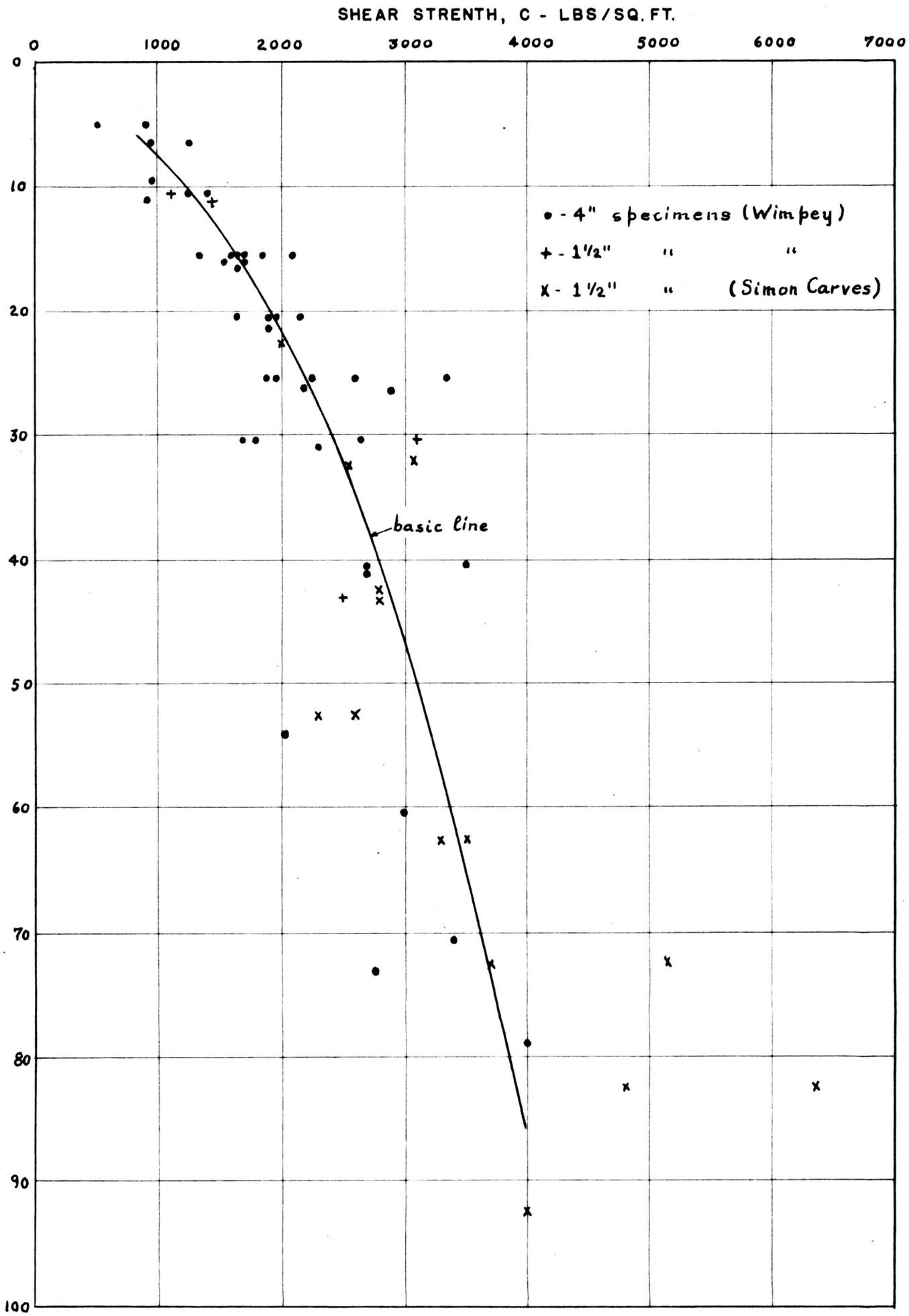
The borings can be separated into two groups; those where the London Clay extends to ground surface, and those where it is covered by marsh clay - typically about 9 ft. of this soft post-glacial clay. The relation between shear strength and depth for the first group is shown in Fig.9 together with the water contents and Atterberg Limits. Down to 60 ft. there seems to be no significant difference between the strengths of the different sized specimens, although at greater depths the smaller specimens appear to give higher strengths*. There is the usual scatter in

---

* In Boring D.12 the 1½ ins. specimens are all considerably higher in strength than those from any other borehole. Unfortunately no 4 ins. specimens were tested from D.12. No explanation has been found for this anomaly, and the results have been ignored.

TEST RESULTS, BRADWELL. (SERIES-1)

LONDON CLAY AT SURFACE



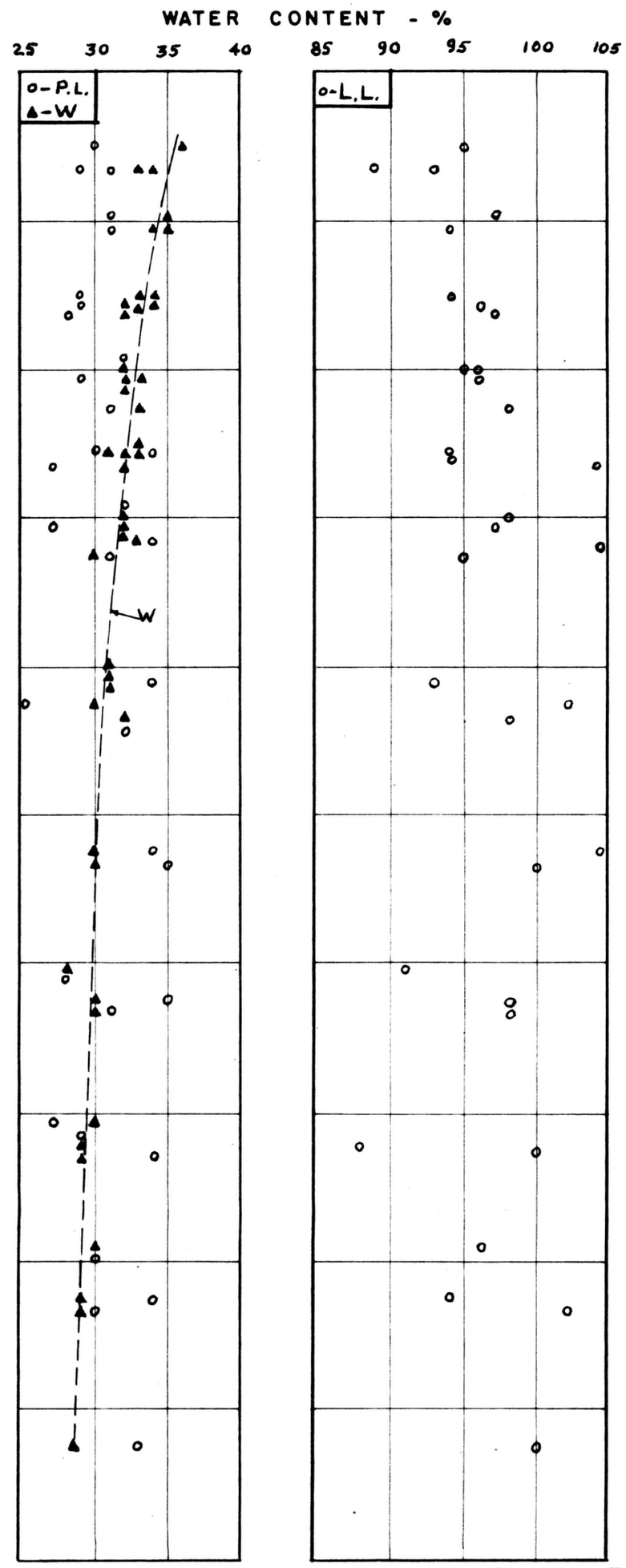


FIG - 9

the results, but the "basic line" in Fig.9 clearly represents the strength-depth relation with reasonable accuracy.

It may be noted at once that the strength at any particular depth, at Bradwell, is conspicuously less than in London*. The explanation may well be that the clay has been less heavily overconsolidated in Essex due to a smaller thickness of sediments having deposited, and subsequently eroded (Jukes-Brown 1911).

The water contents decrease steadily with depth, being decidedly above the plastic limit within the top 20 ft. and thereafter equal or even smaller than the plastic limit: the average value of which is about 30. The liquid limit, with few exceptions, lies in the range 90 to 100 and averages about 95.

Where the London Clay is overlain by marsh clay the strength at a particular depth below ground surface is less than when the London Clay extends up to the ground (Fig.10). This is also found in London, where the clay is covered by river gravels (Skempton 1959). In that case,

---

* see A. W. Skempton "Cast In-situ Bored Piles in London Clay" Geotechnique, vol.9, pp.153-73, 1959 (Fig.2).

TEST RESULTS, BRADWELL. (SERIES - I)

MARSH CLAY AT SURFACE

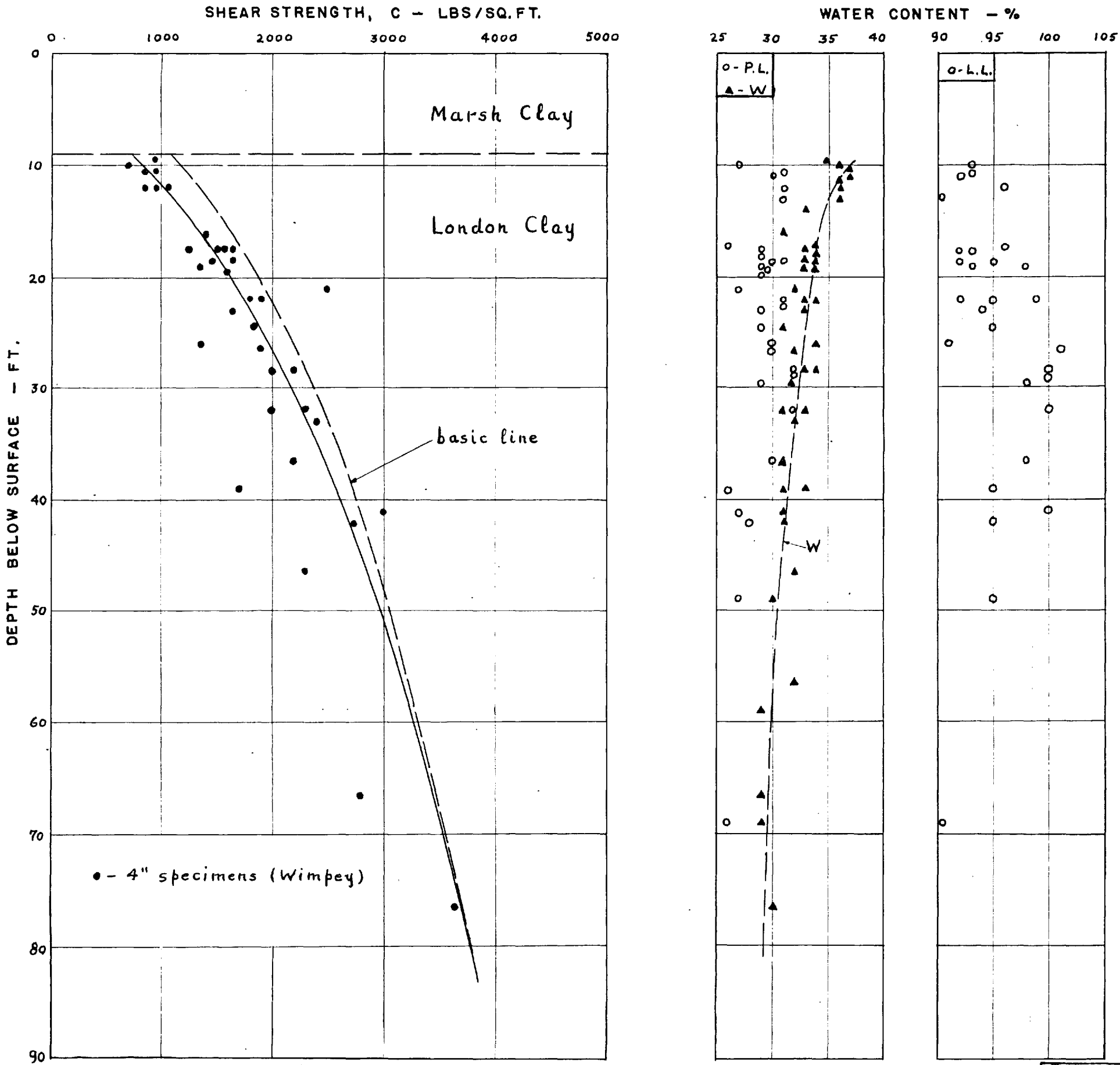


FIG - 10

however, there is evidence that the strengths at depths of more than about 50 ft. are unaffected by the presence or otherwise of gravels, and there is no reason to suppose that the strength differences at Bradwell persist below depths of this magnitude. Consequently the relation between strength and depth, for the London Clay, where it is beneath marsh clay, has been drawn to merge into the "basic line" at about 50 ft.

There is no difference in the Atterberg Limits, between the two groups of borings, but there is an indication that the water contents are slightly higher where the clay is covered by marsh clay.

The activity of the clay has an average value of 1.27 (mean of 12 tests), the corresponding values of PI and clay fraction being 67 and 53%. This activity is appreciably greater than for the clay in London (typically 0.95, Skempton 1953) and may indicate some mineralogical difference: possibly the Bradwell clay was deposited in deeper water and contains more montmorillonite.

As usual, the upper zone of the London Clay is brown, whilst the deeper part is grey. The junction is fairly well defined and occurs at a depth of about 30 ft.

where the clay extends to ground surface, and about 33 ft. below ground where there is marsh clay.

The London Clay is decidedly fissured throughout the full depth.

The density of the brown London Clay is 120 lb/cu.ft. (average of 42 tests) whilst the average value for the grey clay is 121 lb./cu.ft. (average of 40 tests).

The marsh clay is a typical soft post-glacial deposit, the average properties of which are:-

water content	56 %
liquid limit	88 %
plastic limit	27 %
density	105 lb./cu.ft.
shear strength	400 lb./sq.ft.

Ground water level, in the neighbourhood of the Reactors and Turbine House varies between 3' and 5'6" below the surface, the average depth being 4 ft.

2. INVESTIGATION AFTER THE SLIP

(a) Undrained Triaxial Tests

The two slips in the excavation for Reactor No.1 occurred on 24 April 1957 and 5 May 1957. As

mentioned before, Professor Skempton visited the site on May 10th, and reported on the slips and on the new slope to be adopted in July. The author took up the problem as a research investigation in September and visited the site October 3rd 1957. On this occasion four U.4 samples were taken from small benches cut into the freshly excavated slope of the Pump House, approximately at location c-9. These are referred to as Tubes A, B, C and D, and they were taken at depths of 2.1, 6.6, 8.4 and 11.1 ft. below the top of the London Clay. The thickness of marsh clay was 10.5 ft. Undrained triaxial tests (cell pressure = total overburden pressure) were done on 1½" specimens. Some of the specimens were trimmed from the samples, others were jacked into 1½ in. diameter brass tubes. The results are given in Table 2 (each figure being the average of two or three individual tests).

The values of c are plotted in Fig.11, where the curve is the strength-depth relation from Series I (Fig.10). The points lie quite close to this curve, as might be expected as the samples in Series I and II were all taken in open-drive samplers. The strength of the trimmed specimens, however, is consistently lower than that of

TABLE 2

Series II

Sample	Depth below top of London Clay	Total overburden pressure lb./sq.in.	Consistency			γ	c	% Strain at failure	E	*
			LL	PL	w	lb./cu.ft.	lb./sq.ft.		ton/sq.ft.	
A	2.1'	10	93	31	34.5	120.1	1150	6.3	62	J
					34.6	119.0	830	3.2	55	T
B	6.6'	14	91	32	35.1	120.8	1390	5.4	82	J
					32.6	119.5	1140	3.0	85	T
C	8.4'	15	94	32	32.9	120.1	1340	4.8	83	J
					33.3	119.9	1360	3.6	135	T
D	11.1'	17	95	33	32.4	122.2	1660	4.4	85	J
					31.6	120.7	1630	3.0	93	T

* J = Jacked Specimens T = Trimmed Specimens.

TEST RESULTS, BRADWELL.

SERIES II, III & IV.

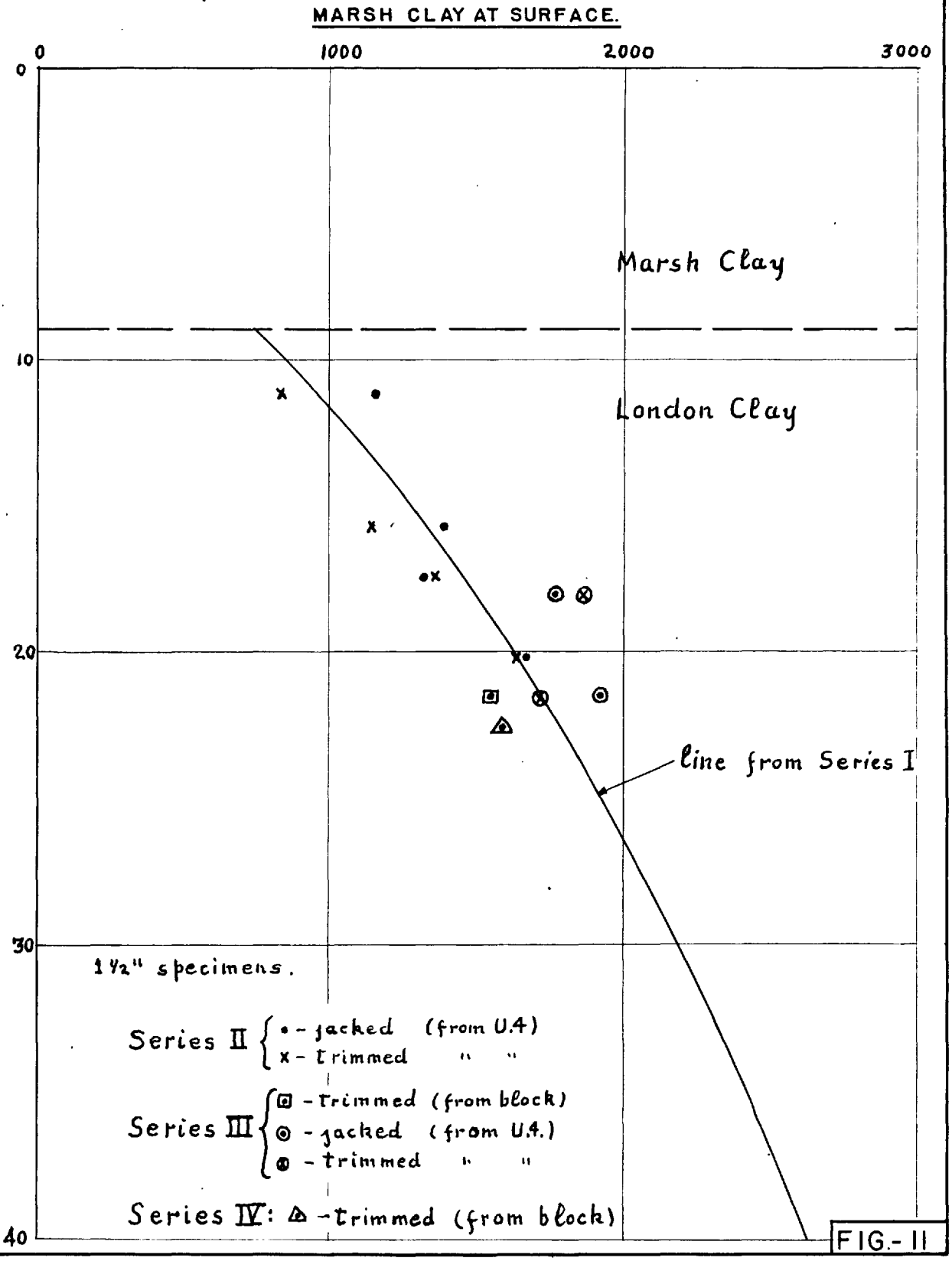


FIG.- II

the jacked specimens, and the strain at failure in the former is decidedly smaller.

On November 28th another visit was made to the site, when two blocks of clay were carefully obtained from benches in the Pump House excavation, together with two adjacent U.4 samples approximately at location D-10. From each of the blocks and from each of the tubes a number of specimens were prepared by jacking and by trimming. The thickness of marsh clay was 10.5 ft.

Unfortunately the clay in Block 2 had dried out slightly before the tests were made, although it had been sealed in paraffin wax, and the results have therefore been discarded. The other results are summarized in Table 3 (each figure being the average of three tests).

These results also lie within the usual scatter about the previously determined strength-depth curve (Fig.11).

The average figures for the six pairs of jacked and trimmed specimens are summarised in Table 4. The differences in strength and in E are not statistically significant, but the strains at failure are markedly different.

TABLE 3

Series III

Sample	Depth below top of London Clay	Total overburden pressure lb./sq.in.	Consistency			γ	c	% Strain at failure	E	*
			LL	PL	w	lb./cu.ft.	lb./sq.ft.		ton/sq.ft.	
Tube 1	12.5'	18	93	30	32.5	119.9	1920	5.6	109	J
					32.0	119.8	1710	4.1	110	T
Block 1	12.5'	18	93	30	-	-	-	-	-	J
					32.3	118.3	1550	4.2	117	T
Tube 2	9'	15	92	30	33.8	116.9	1770	6.5	92	J
					33.3	117.5	1870	4.3	95	T

* J = Jacked specimens T = Trimmed

TABLE 4

	Jacked	Trimmed
w	33.2	32.9
γ lb./cu.ft.	120.0	119.4
c lb./sq.ft.	1540	1420
E ton/sq.ft.	86	96
% Strain at failure	5.5	3.6

Drained tests were also carried out in Block 1 but the results will be considered later.

On 18 March, 1958, a further visit was made to the site, and Block 3 was obtained immediately below the position of Block 1 at a depth of 13.5 ft. below the top of the London Clay. On specimens trimmed from this block 14 undrained triaxial tests were made, (referred to as Series IV) with the object of studying the post-failure stress-strain characteristics. For this purpose small cell pressures were used corresponding to the reduced ground pressures obtaining after the excavation had been made.

First of all, the strength (as usually defined at the peak of the stress-strain curve), water content and density, have the average values:

w = 32.8 %

γ = 120.0 lb./cu.ft.

c = 1590 lb./sq.ft.

E = 152 tons/sq.ft.

strain at failure = 3.7 %

The strength is consistent with all the previous results (see Fig.11).

Stress-strain curves are shown in Figs. 12 and 13, the heavy lines being a somewhat idealized average for each cell pressure. The experimental difficulties in the triaxial apparatus, when large strains are applied to specimens which fail on a single plane, are considerable - especially regarding the correction to be applied for the restraining effect of the rubber membrane (Appendix B). Thus the post-failure curves are only rough approximations to the truth. Nevertheless it is clear that what might be called the "residual strength" increases with increasing cell pressure, although it seems to become practically indistinguishable from the peak strength at pressures of about 15 lb./sq.in. - as noted in other tests.

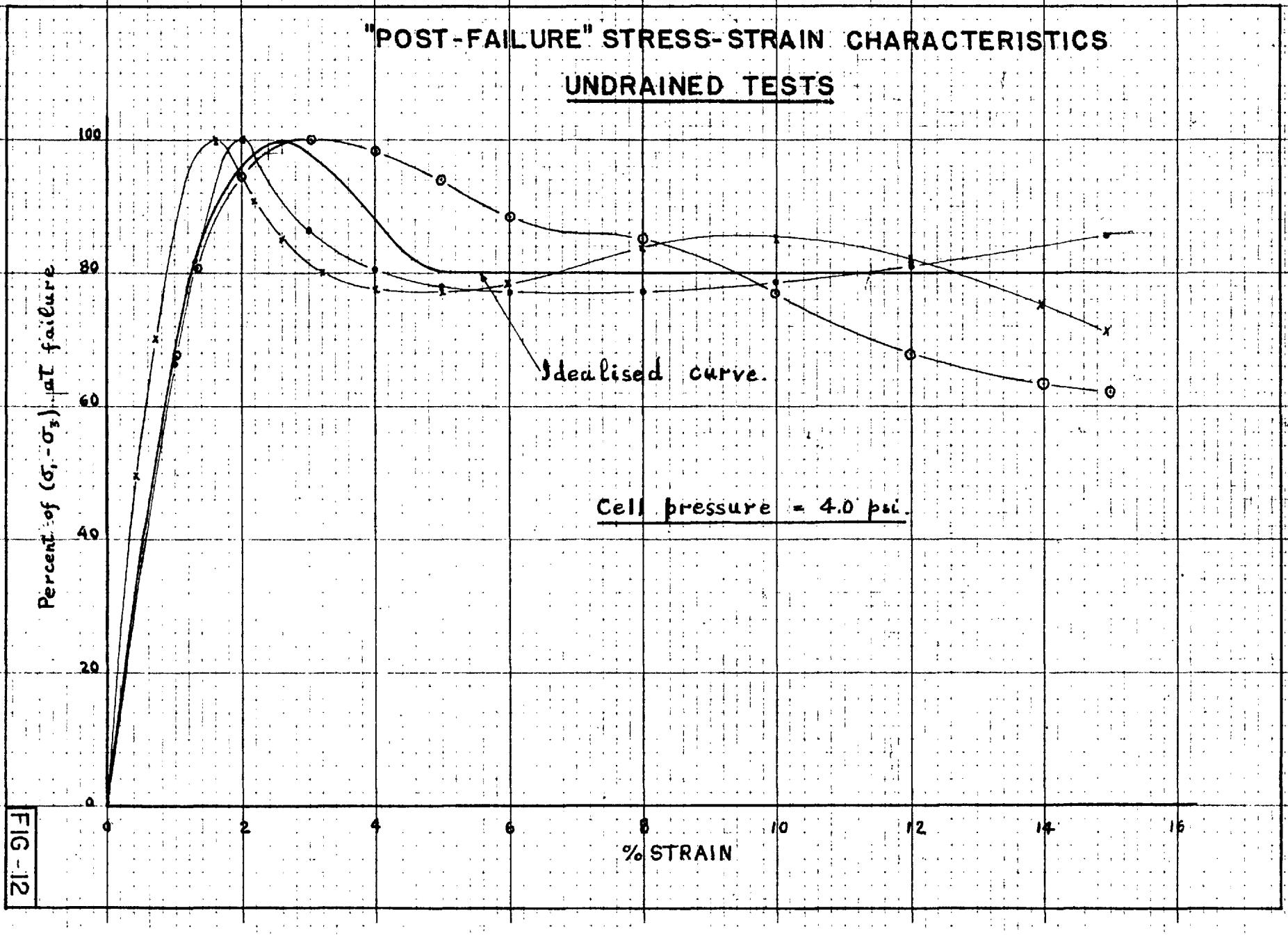

"POST-FAILURE" STRESS-STRAIN CHARACTERISTICS
UNDRAINED TESTS
Idealised curve.
Cell pressure = 4.0 psi.
Percent of $(\sigma_1 - \sigma_3)$ at failure
100
80
60
40
20
0
0
2
4
6
8
10
12
14
16
% STRAIN

FIG-12

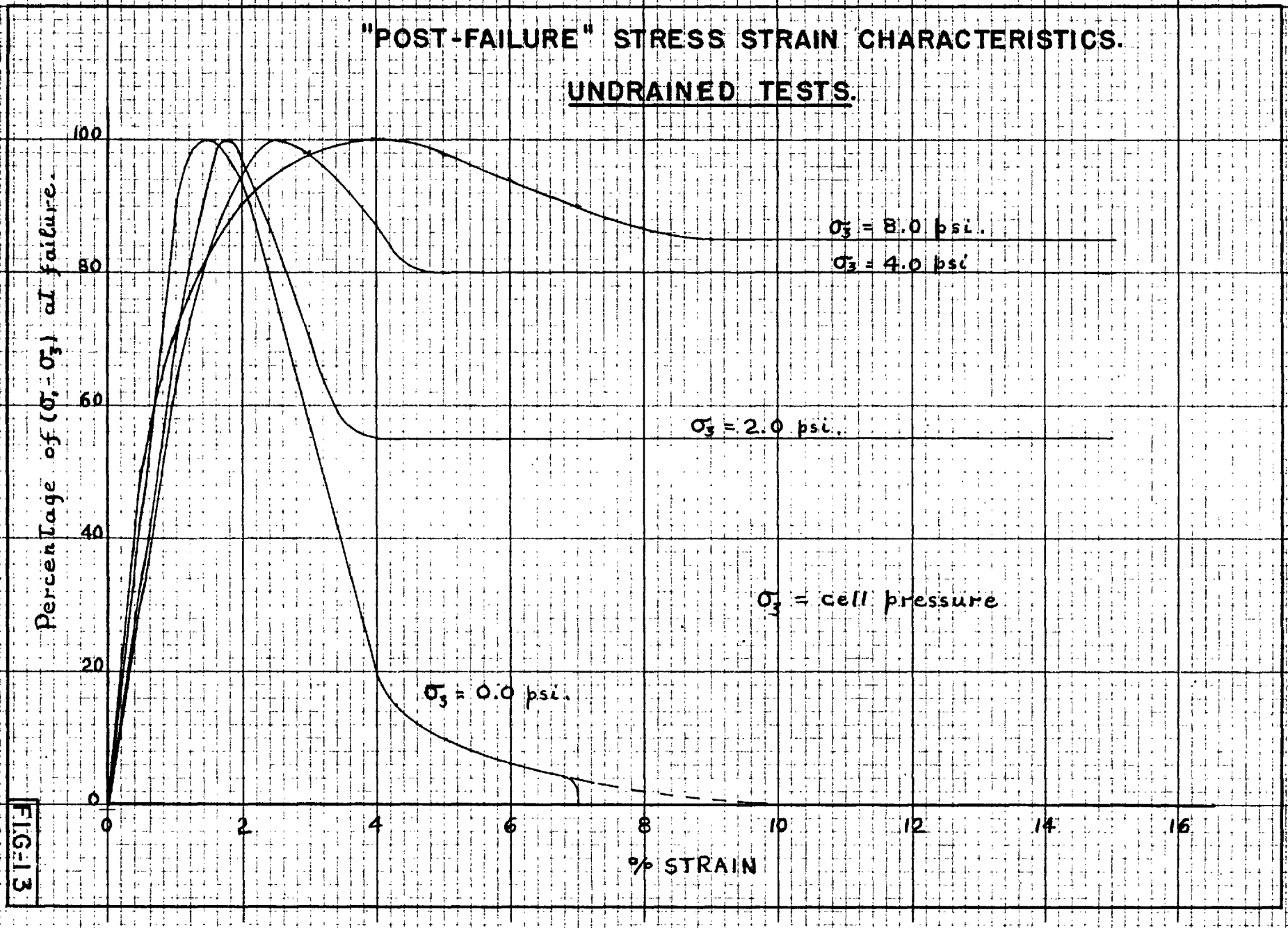

"POST-FAILURE" STRESS STRAIN CHARACTERISTICS.
UNDRAINED TESTS.
Percentage of $(\sigma_1 - \sigma_3)$ at failure.
100
80
60
40
20
0
0
2
4
6
8
10
12
14
16
% STRAIN
σ_3 = 8.0 psi.
σ_3 = 4.0 psi
σ_3 = 2.0 psi.
σ_3 = cell pressure
σ_3 = 0.0 psi.

FIG-13

On the same visit Block 4 was obtained, just beneath Block 3, but this could not be tested until months after sampling, and the clay had definitely reduced in water content.

Lastly, in April 1959 two visits were made to obtain further samples (Blocks 5, 6, 7 and 8 and Tube 5 and 6). These were taken at location G-15 from a bench in the slopes of the Cooling Pond excavation (5 and 6) and from a bench left in the base of this excavation (7 and 8). This material was used chiefly for drained and consolidated undrained tests (with pore pressure measurements) - which will be described later - but in addition the following undrained tests were made.

From Tube 6 a specimen was tested 4 ins. diameter, and after test three 1½ ins. specimens were trimmed from this specimen. Two other 1½ ins. specimens were trimmed from the original sample but, as it happened, these had a lower water content. (All these tests were made within a few days of sampling). Nevertheless, taking into account the variation of water content, there is no marked difference of strength between these specimens. From Block 7 four undrained tests on 1½ ins. trimmed specimens were made. The results are given in Table 5.

TABLE 5

Series V

Sample	Depth below top of London Clay	Consistency			γ	c	E	Specimen
		LL	PL	w	lb./cu.ft.	lb./sq.ft.	ton/sq.ft.	
Tube 6	85'	95	31	36.5	-	1110	193	4"
		95	31	35.9	120.0	1070	129	1½"
		95	31	33.6	120.0	1360	157	1½"
Block 7	18.5'	95	33	33.0	121.5	1640	156	1½"

At the Reading Farm the London Clay rises to ground surface. Consequently the above results should be compared with the "basic curve" of Fig.9. This curve has been re-plotted in Fig.14 with the grand average for Tube 6 and Block 7. The results lie quite close to the curve: showing that these samples are perfectly normal.

(b) Drained Tests

Drained triaxial tests were carried out on 1½ in. diameter specimens trimmed from Blocks 1, 5, 6 and 7, and drained shear box tests have been made on specimens cut from Tube 5 and Block 5. In the triaxial tests the specimens were fully consolidated under a given cell pressure, with filter paper drains along the sides, and the rate of strain in the subsequent shearing process was arranged so that failure occurred in no cases in a time of less than 2 days. Typically the time to failure was 3 or 4 days.

The results are summarised in Table 6. Some typical stress-strain and volume change curves are given in Fig. 12, 13, and 14.

TEST RESULTS, BRADWELL.

SERIES V

LONDON CLAY AT SURFACE

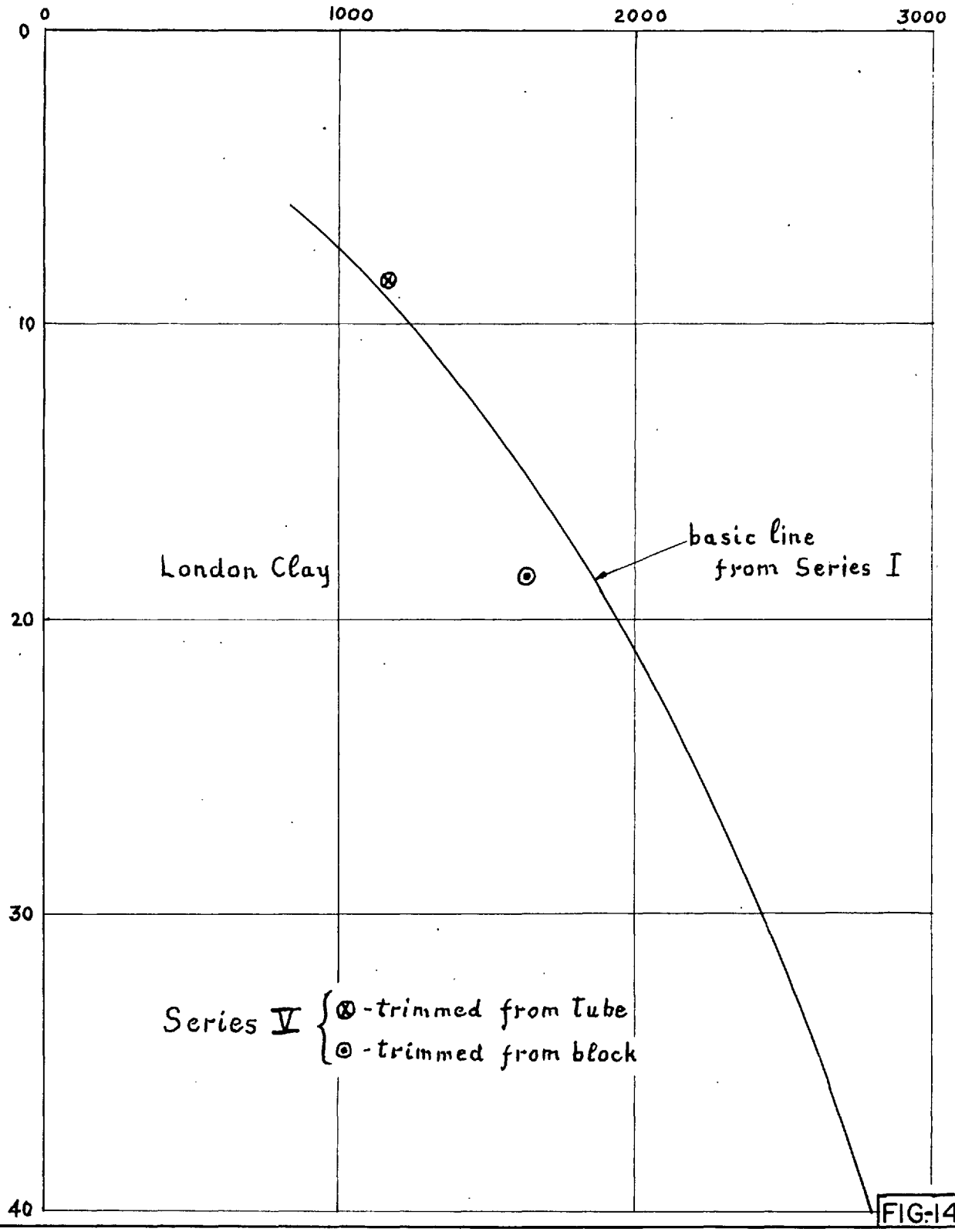


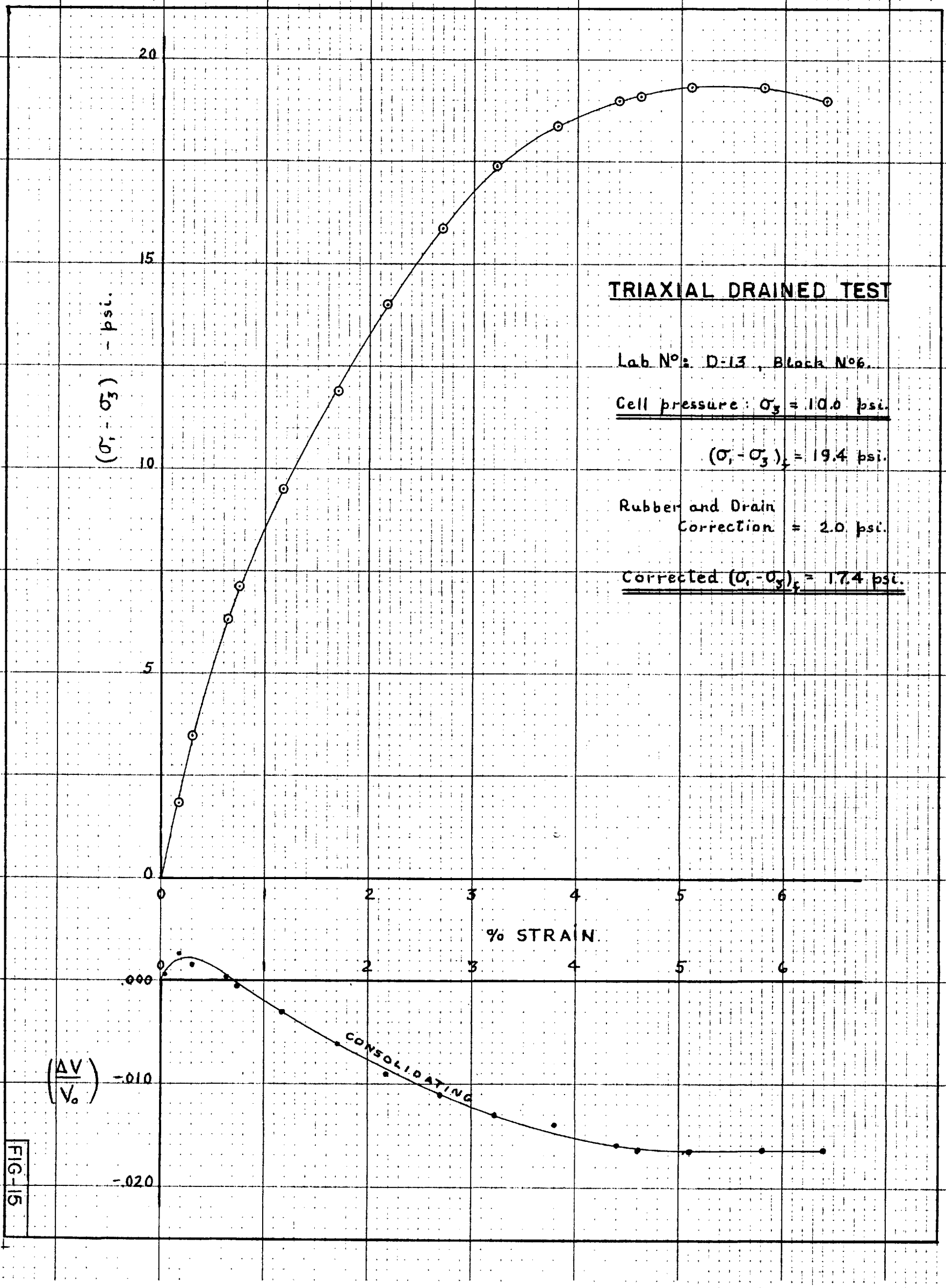
FIG-14

TABLE 6

Sample	Depth below top of London Clay	Consistency			c' lb/ft.^{2}	ø'	% Strain at Failure	Number of Tests
		LL	PL	w				
Block 1	12.5'	93	30	32.3	340	21.3°	5.2	7
Blocks 5 and 6	8.5'	95	31	32.7	365	19.5°	6.5	7
Block 7	18.5'	95	33	32.3	490	20.7°	4.8	4
Block 5 Tube 5	8.5'	95	31	33.7	375	19.0°	-	10
Weighted Mean	-	94	31	32.9	380	20.0	-	-

Mohr circles and failure envelopes are plotted in Fig. 18 to 21. The failure envelopes were fitted by means of the least square method; modified, very slightly, where necessary to allow for a circle which seemed to be rather atypical.

Another set of average values for c' and ø', for the triaxial tests, has been obtained by plotting all



TRIAXIAL DRAINED TEST

Lab N°: D-13 , Block N°6.

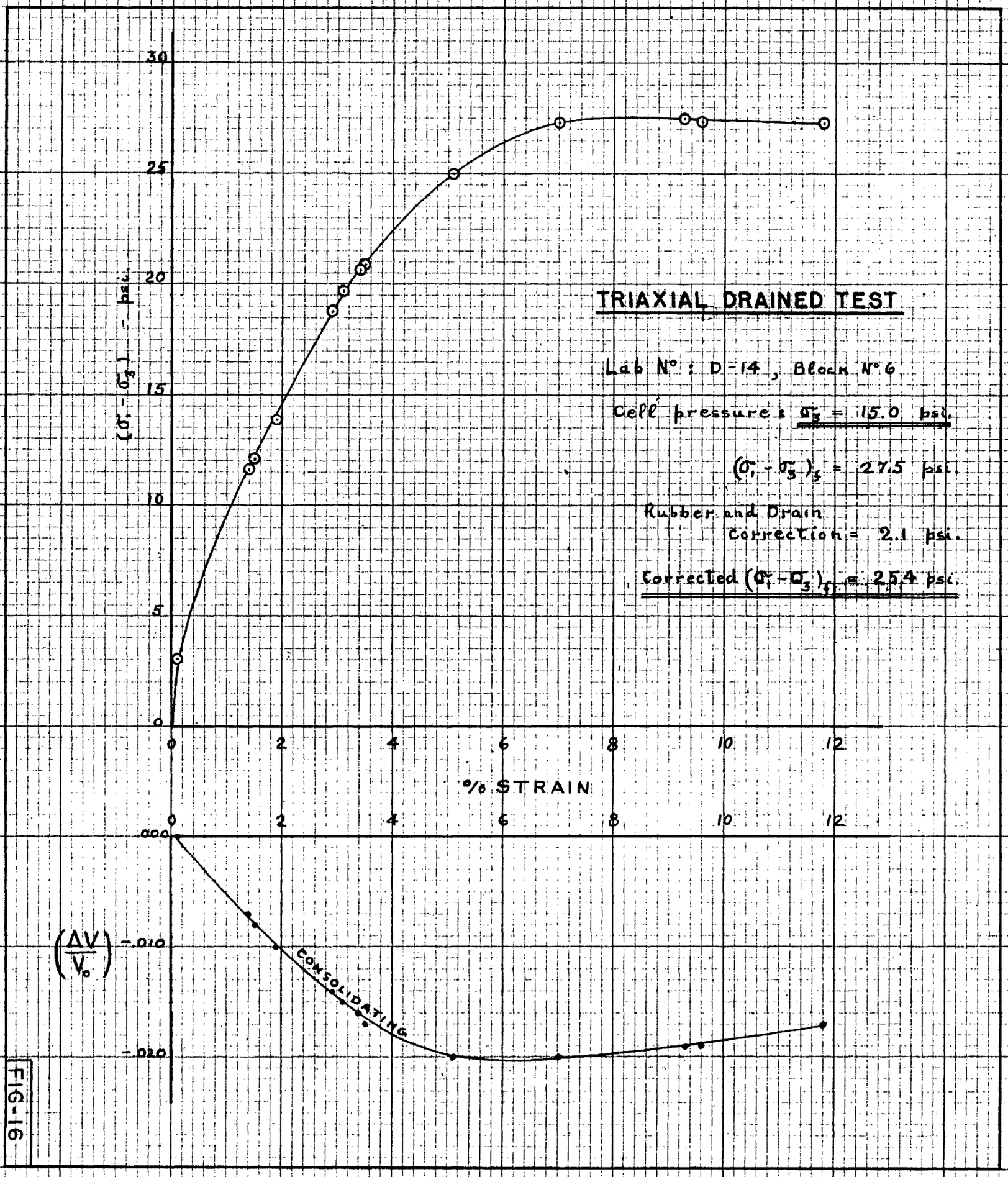
Cell pressure : σ_3 = 10.0 psi.

$(\sigma_1 - \sigma_3)_f$ = 19.4 psi.

Rubber and Drain Correction = 2.0 psi.

Corrected $(\sigma_1 - \sigma_3)_f$ = 17.4 psi.

FIG-15



TRIAXIAL DRAINED TEST

Lab N° : D-14 , Block N° 6

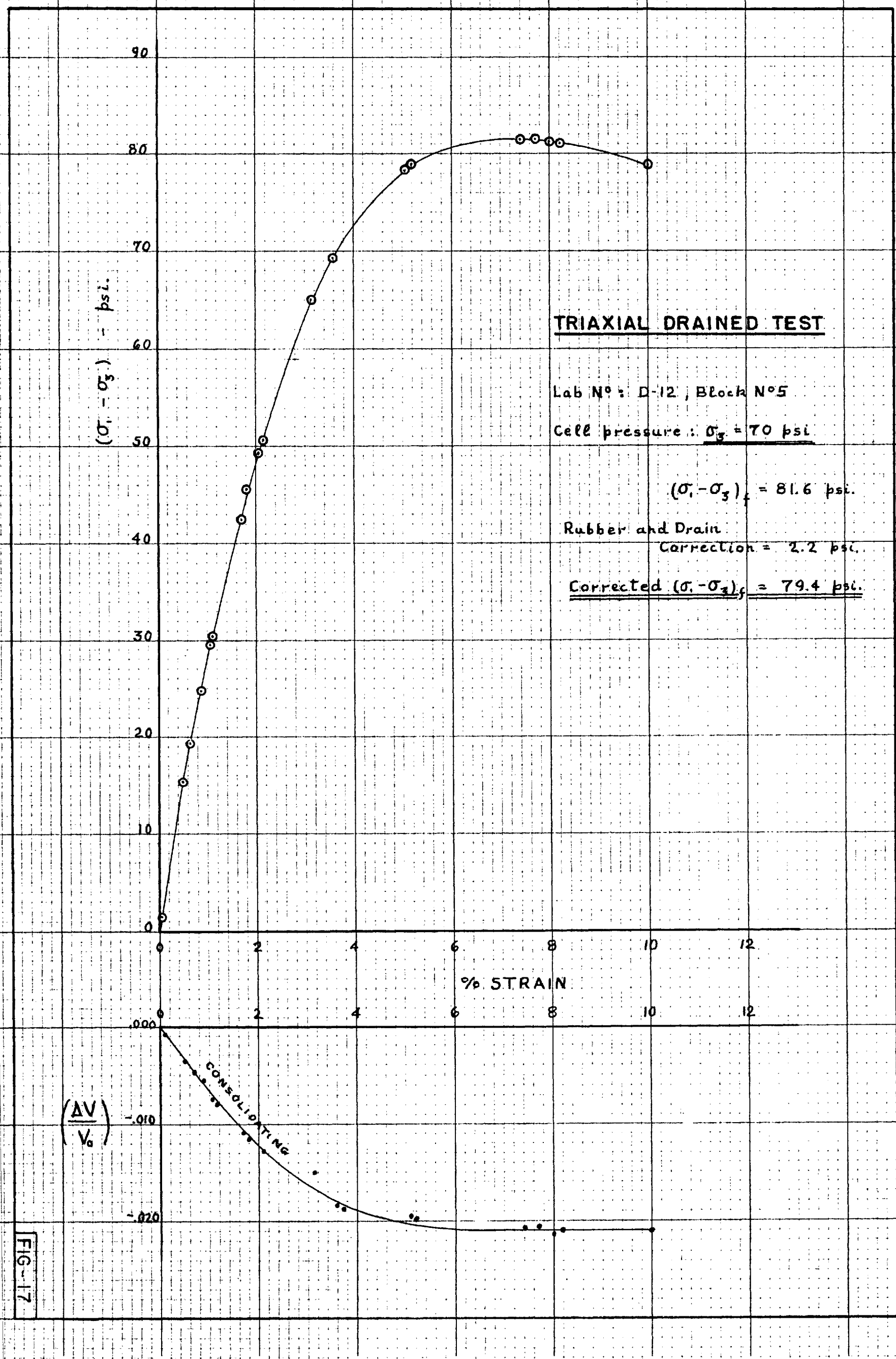
Cell pressure : σ_3 = 15.0 psi.

$(\sigma_1 - \sigma_3)_f$ = 27.5 psi.

Rubber and Drain correction = 2.1 psi.

Corrected $(\sigma_1 - \sigma_3)_f$ = 25.4 psi.

FIG-16



TRIAXIAL DRAINED TEST

Lab N° : D-12 , Block N°5

Cell pressure : σ_3 = 70 psi

$(\sigma_1 - \sigma_3)_f$ = 81.6 psi.

Rubber and Drain Correction = 2.2 psi.

Corrected $(\sigma_1 - \sigma_3)_f$ = 79.4 psi.

FIG-17

TRIAXIAL DRAINED TESTS

BLOCK Nº 1

$$\begin{cases} C' = 2.36 \text{ psi} = 340 \text{ lbs/ft}^2 \\ \phi' = 21.3^\circ \end{cases}$$

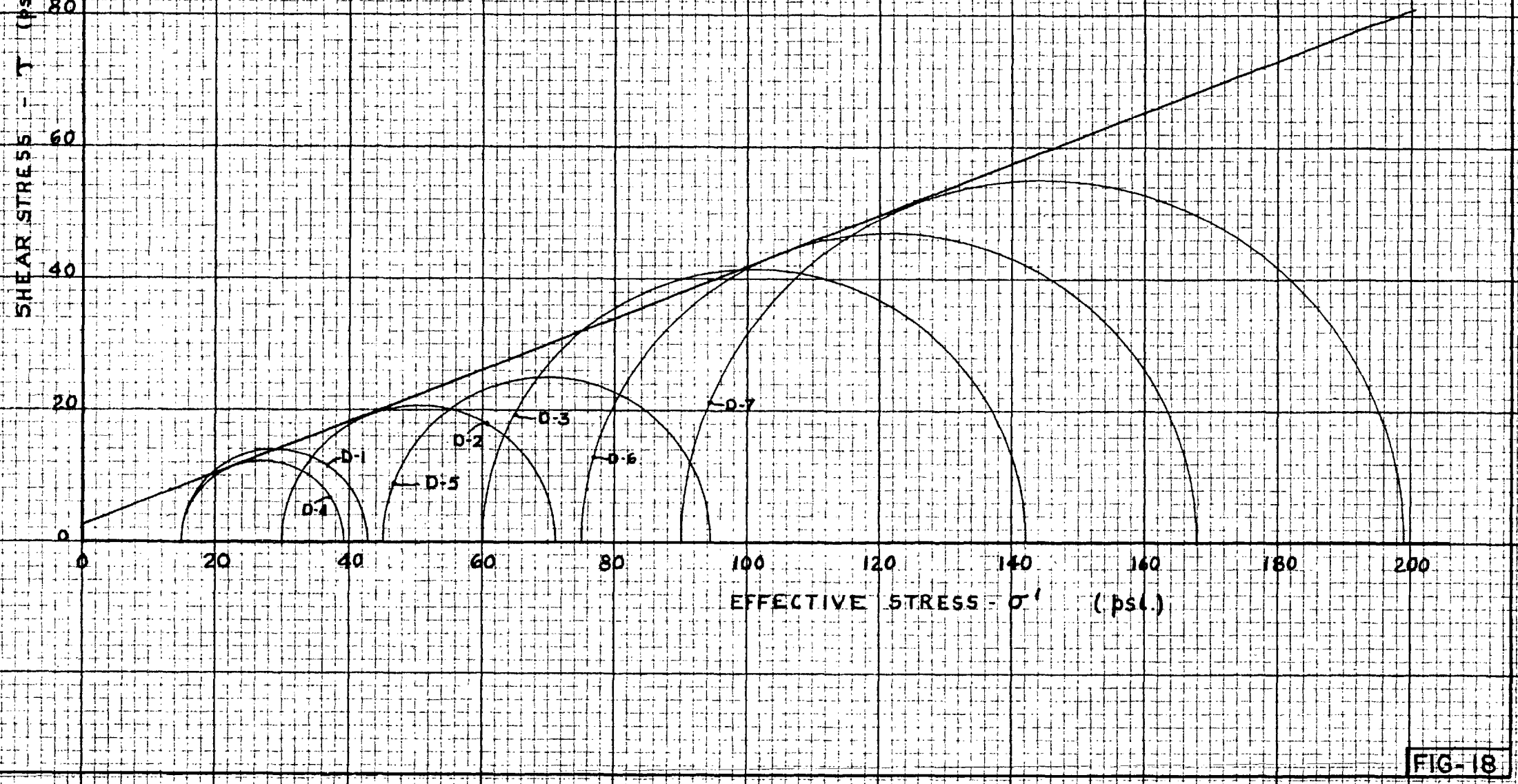


FIG-18

TRIAXIAL DRAINED TESTS.

BLOCKS Nº 5 and Nº 6

$$\begin{cases} c' = 2.55 \text{ psi} = 365 \text{ lbs/ft}^2 \\ \phi' = 19.5° \end{cases}$$

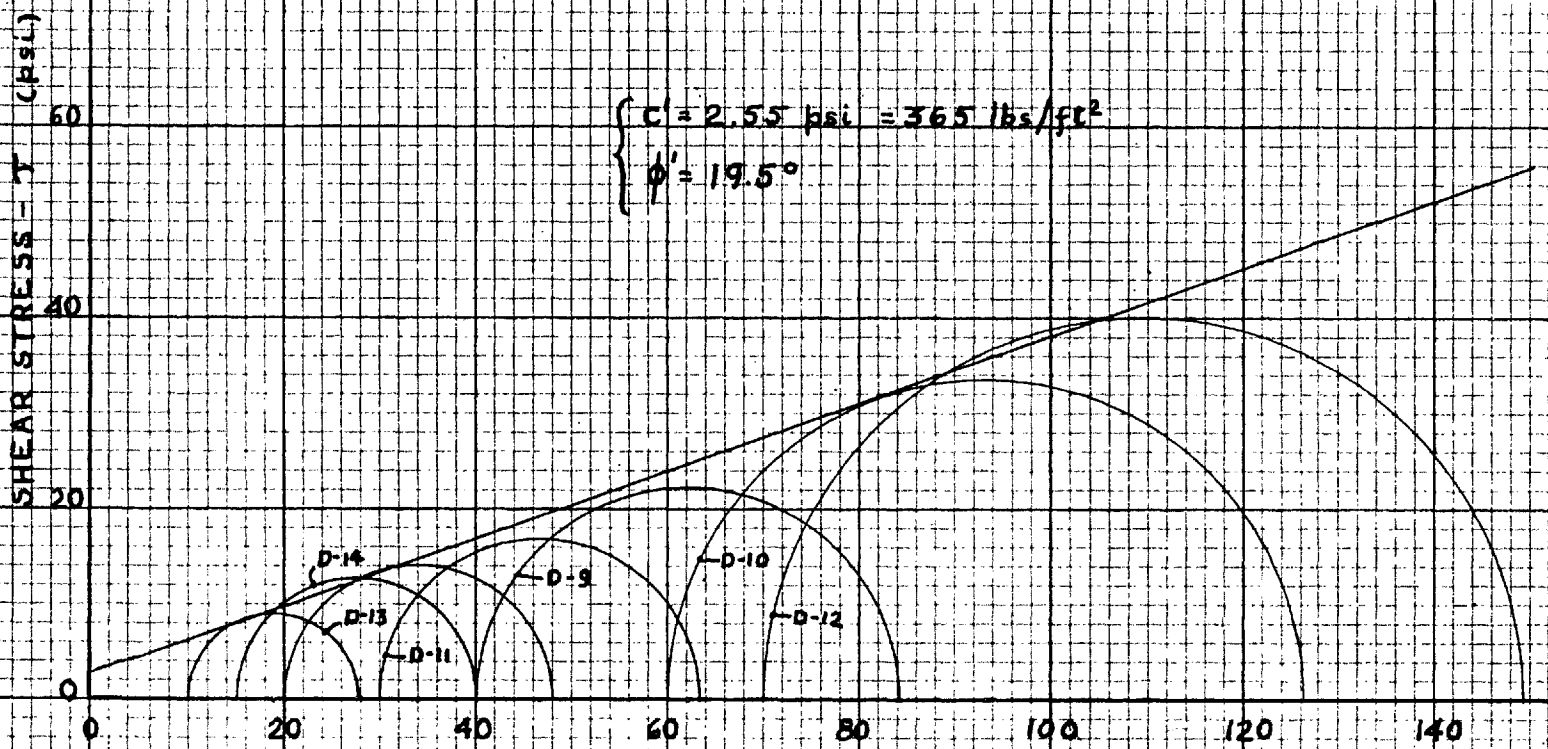


FIG-19

DRAINED TESTS (TRIAXIAL)

BLOCK Nº 7

$$\begin{cases} C' = 3.40 \text{ psi} = 490 \text{ lbs/ft}^2 \\ \phi' = 20.7° \end{cases}$$

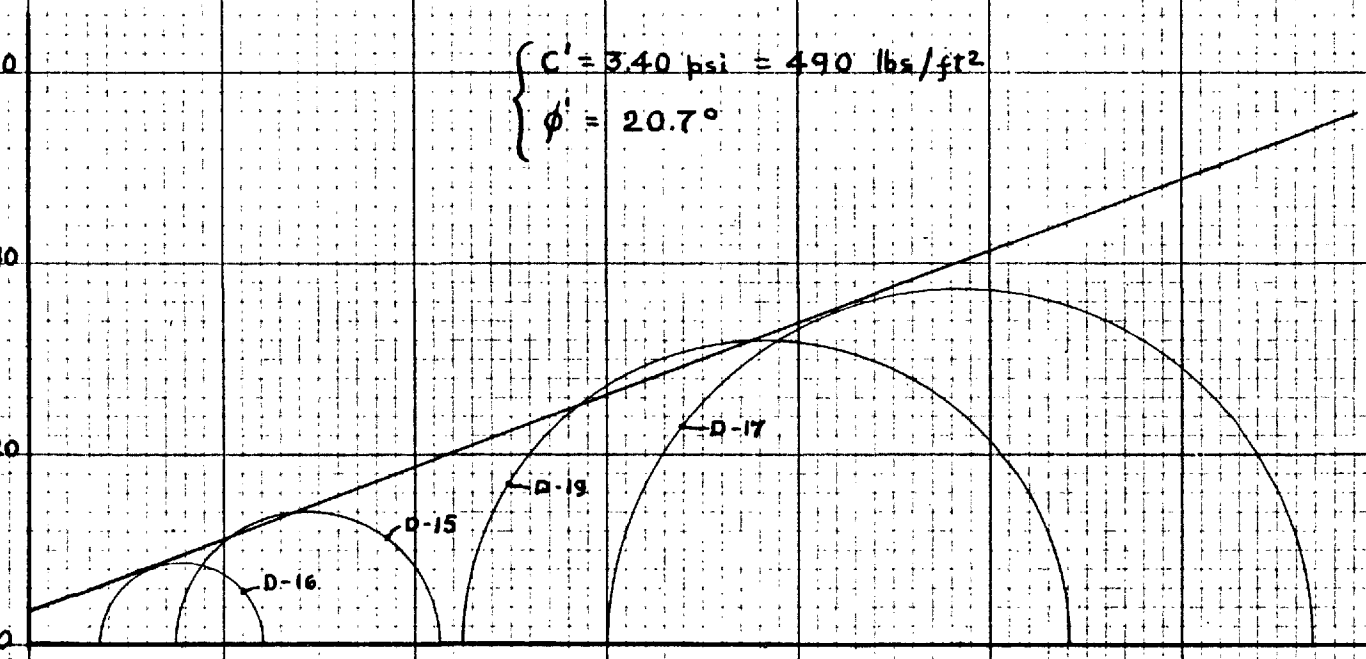


FIG-20

SHEAR BOX DRAINED TESTS

● — TUBE N°5

■ — BLOCK N°5

$C' = 2.61$ psi. $= 375$ lbs/ft^2

$\phi' = 19.0°$

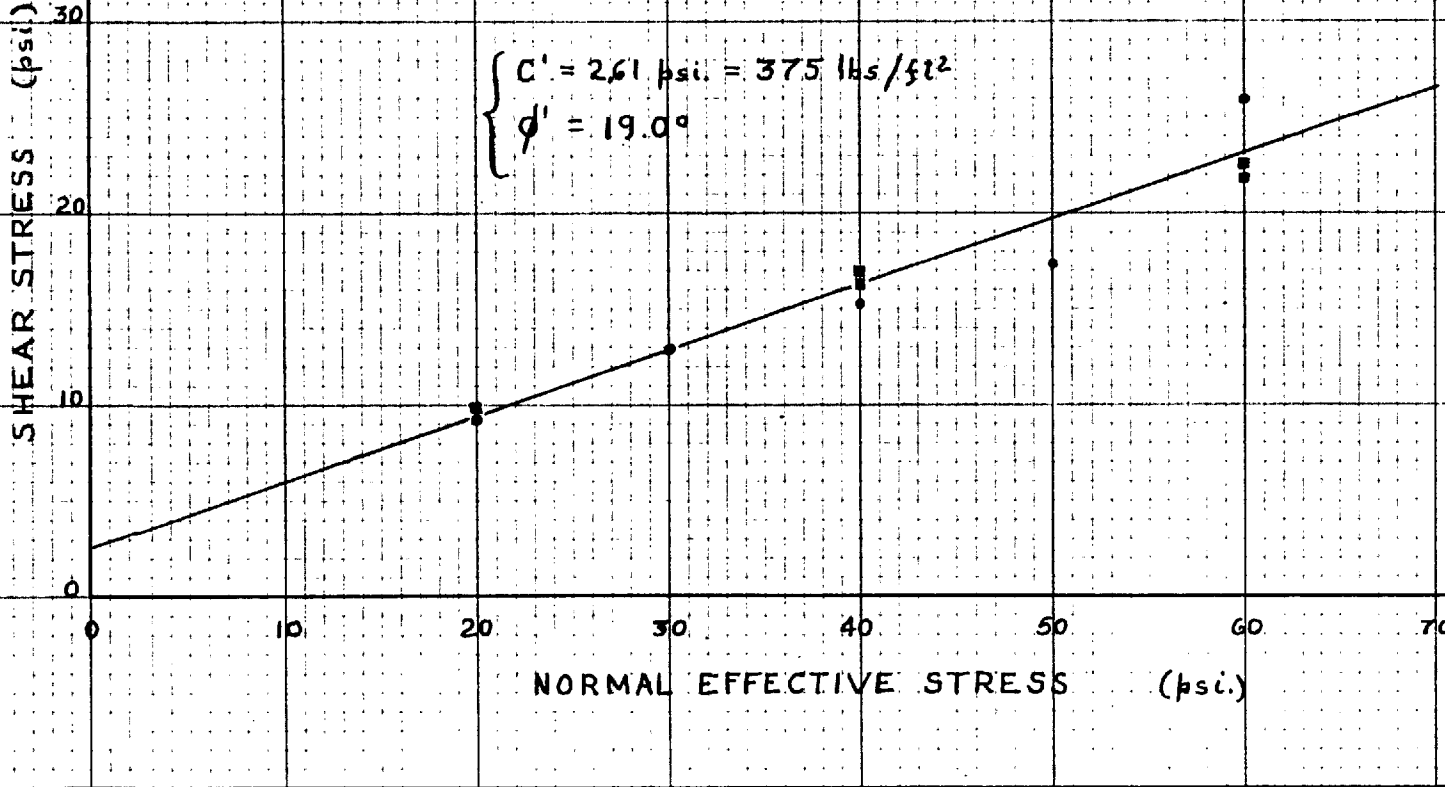


FIG-21

the Mohr circles and finding the best failure envelope (Fig.22). This gives $c' = 350$ lb./sq.ft. and $\phi' = 20.8^{\circ}$. Using these figures, together with the shear box tests, the weighted mean values are $c' = 360$ lb./sq.ft. and $\phi' = 20.3^{\circ}$. Within the limits of experimental accuracy it is sufficient to take

$$c' = 370 \text{ lb./sq.ft.} \qquad \phi' = 20.0^{\circ}$$

It is interesting to note that if Hill's (Hill 1956) interpretation of the shear box tests is used the parameters are $c' = 400$ lb./sq.ft. and $\phi' = 20^{\circ}$. The triaxial tests on the same material give $c' = 365$ and $\phi' = 19.5^{\circ}$ and these are close to the values given by the usually accepted shear box interpretation ($c' = 375$ $\phi' = 19.0^{\circ}$).

Volume changes during shear are shown in Fig.23. The consolidation tends to be rather less under small cell pressures, but when the cell pressure is 20 lb./sq.in. or over there is no significant variation in the volume changes.

Volume changes during consolidation are plotted in Fig.24. The swelling pressure (pressure at which no volume change occurs) is definitely higher than

TRIAXIAL DRAINED TESTS

from BLOCKS N° 1,5,6,7

$$\begin{cases} C' = 2.44 \text{ psi.} = 350 \text{ lbs/ft}^2 \\ \phi' = 20.8° \end{cases}$$

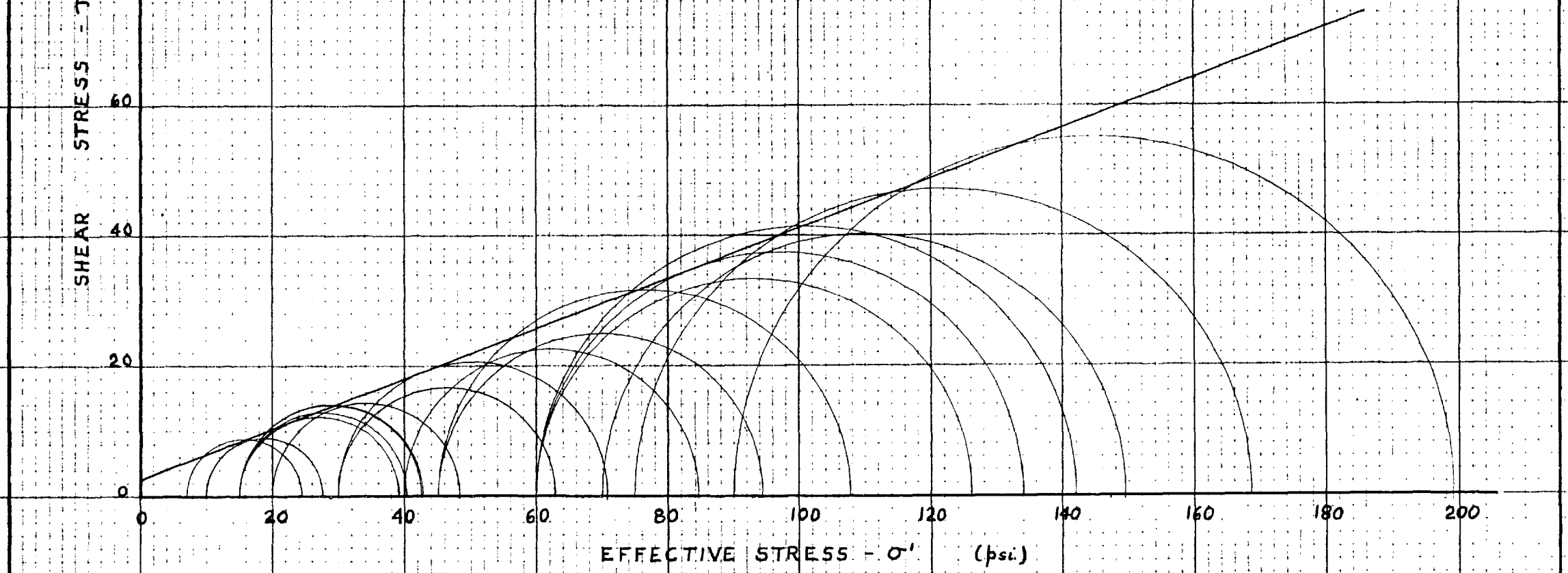


FIG-22

VOLUME CHANGE DURING SHEARING

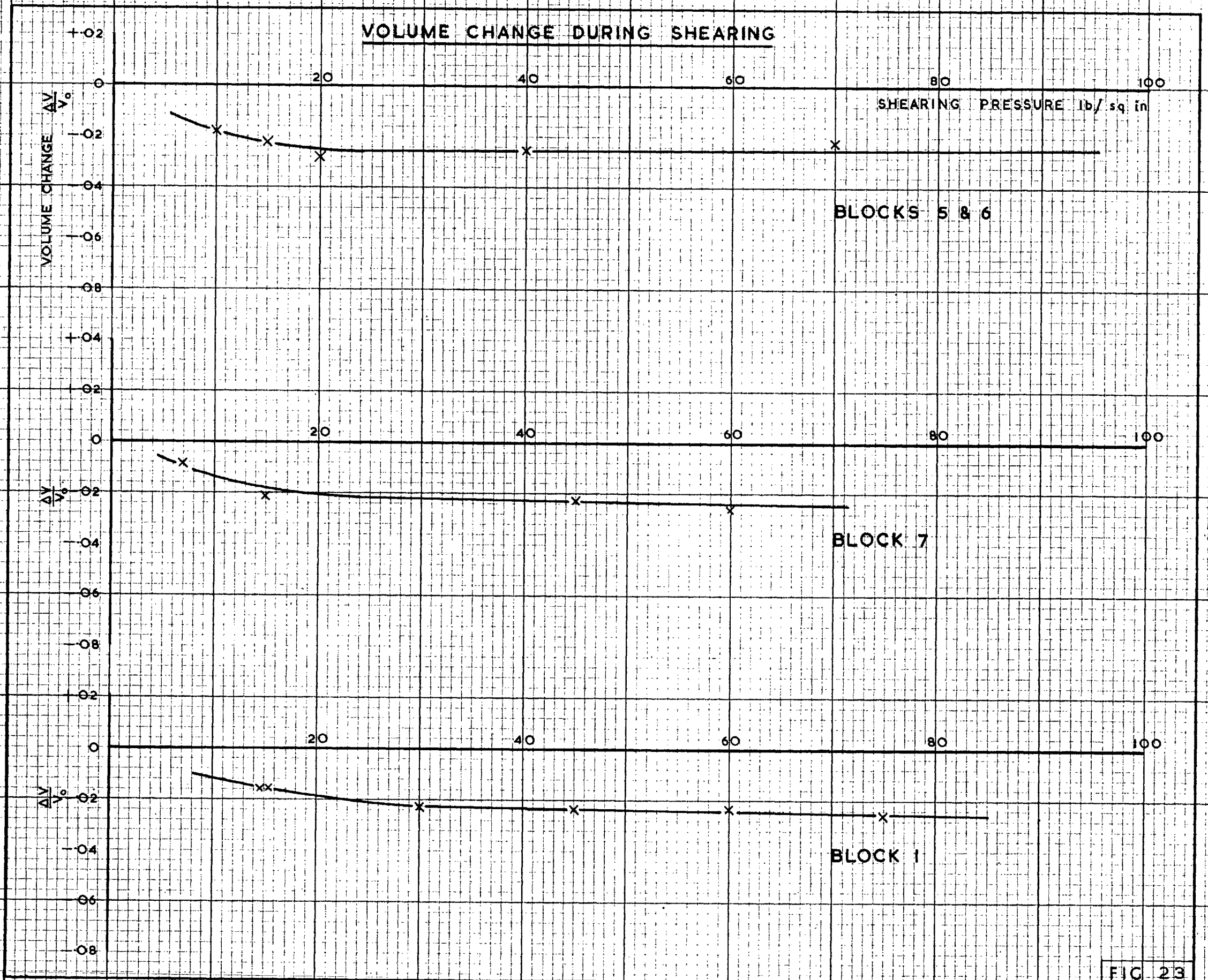


FIG 23

VOLUME CHANGE DURING CONSOLIDATION

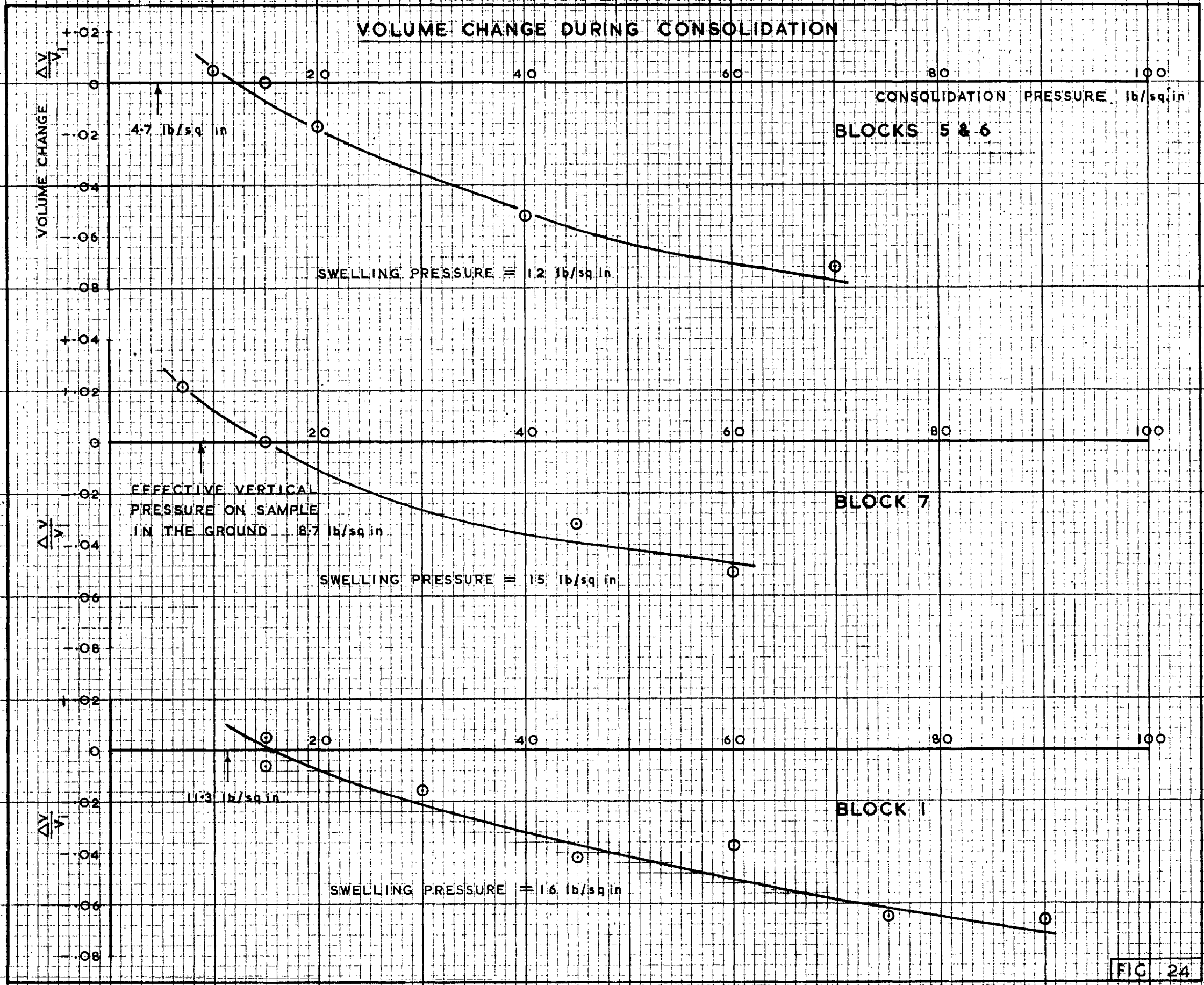


FIG 24

the effective vertical pressure which was acting on the sample in the ground, for all three depths of sampling. This may indicate that the maximum effective pressure in the ground is greater than the vertical pressure or, in other words, K_o is greater than unity. Or there may be negative pore pressure changes on sampling greater than those due simply to the release of total stresses*.

The swelling pressure has also been measured in the oedometer, by finding the load which just prevents a volume change when the specimen is immersed under water. From Tube 6 the critical pressure was a little less than 10 lb./sq.in. whilst on a specimen from Block 6 the pressure was about 15 lb./sq.in. These samples both came from the same depth, where the effective overburden pressure was 4.7 lb./sq.in. And, from the previously mentioned triaxial tests, the swelling pressure for Blocks 5 and 6 was 12 lb./sq.in. The oedometer tests therefore give closely similar results.

---

* The converse effect for normally-consolidated clays has been shown experimentally (Bishop and Henkel 1953).

(c) Consolidated-Undrained Tests

Consolidated-undrained tests have been made on Blocks 6, 7 and 8, using filter paper drains in all cases and a back-pressure when pore water pressures were measured*.

On Block 6 all specimens were consolidated under 30 lb./sq.in. but the rate of shearing was different. The cell pressure was actually 60 lb./sq.in. with a back pressure of 30 lb./sq.in. in the specimen. This helps in getting full saturation and prevents cavitation if any negative changes in pore pressure occur. The principal results are given in Table 7.

For times to failure of 2 days or more there is no effect on strength or pore pressure changes, but for more rapid tests the strength rises appreciably (Fig.25) and so does the pore pressure. Pore pressure was measured at the base of the specimen. Probably in the quick tests the pore pressure on the failure plane is lower than that measured. In the slow tests the pore pressures have time

---

* see Bishop, A. W. and Henkel, D. J. (1957) for a description of the apparatus and techniques used in this laboratory investigation.

TABLE 7

Block 6

w = 33.0 LL = 95 PL = 31

Consolidation pressure = 30 lb./in.^{2}

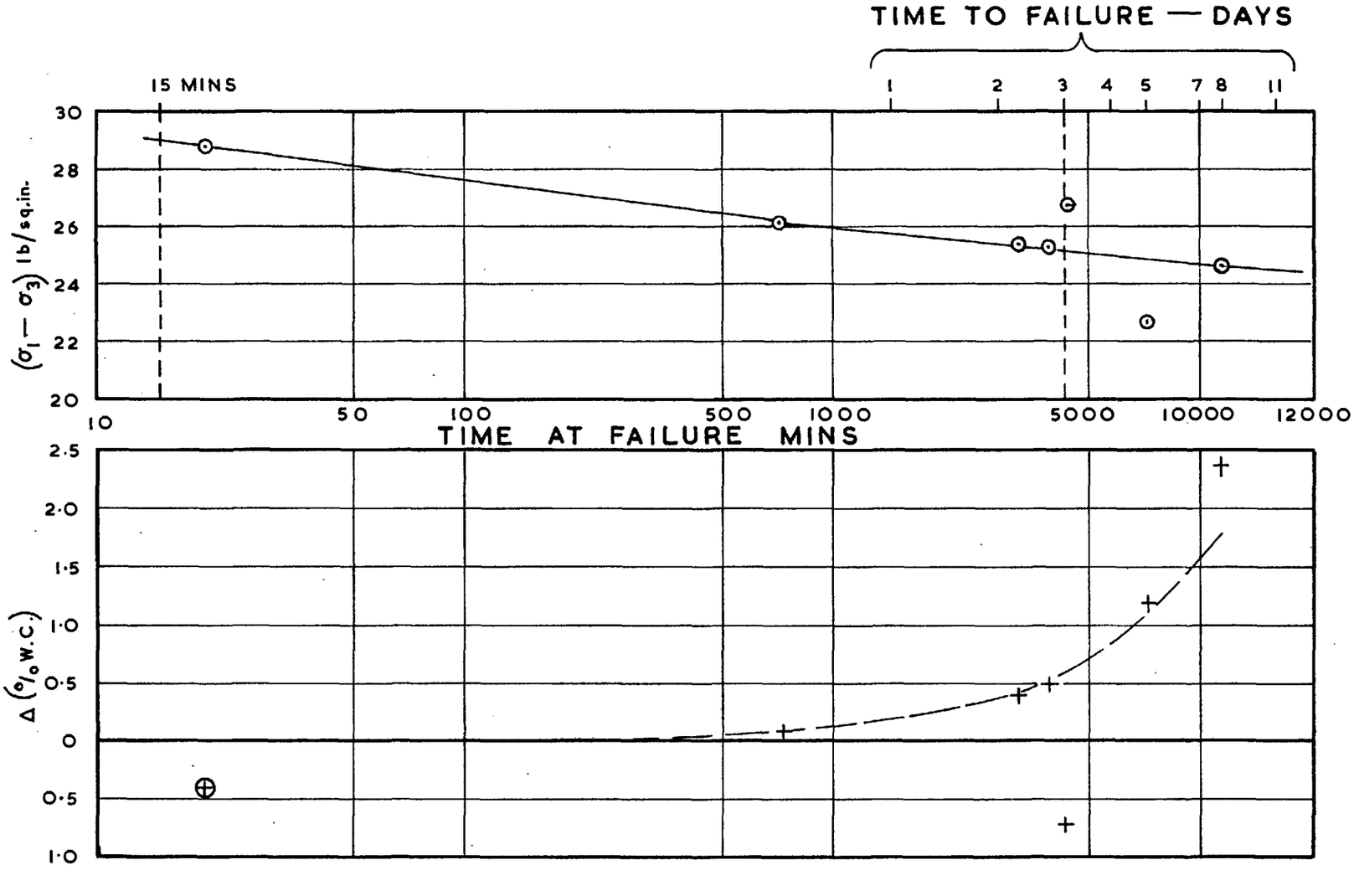
Rate of Strain per cent/min.	Time to Failure	$(\sigma_1 - \sigma_3)$ at failure lb/sq.in.	Pore Pressure at Failure u lb/sq.in.	$A = \frac{\Delta u}{\Delta(\sigma_1 - \sigma_3)}$ at failure	Strain at Failure per cent
0.5000	20 mins	28.9	16.9	0.59	4.7
0.0080	12 hrs	26.2	16.1	0.61	5.2
0.0017	2.7 days	25.3	12.5	0.49	5.3
0.0017	2.2 days	25.4	12.9	0.51	4.0
0.0017	3.0 days	26.7	12.4	0.46	6.0
0.0004	8.0days	24.6	12.5	0.51	7.8

to equalise throughout the specimen. The slow tests will therefore give genuine values for the effective stresses. There is also a tendency for the water content, after failure, to be higher on the shear plane in the slow tests. Theoretically the water contents in these tests should also be slightly lower at the ends, but the differences are too small to measure.

VARIATION IN UNDRAINED STRENGTH WITH TIME TO FAILURE

CONSOLIDATED-UNDRAINED TESTS

BLOCK 6



CONSOLIDATION PRESSURE 30 lb/sq.in.

NOTE: Δ (% W.C.) = Change of water content on the plane during shear,
= % W.C. on the plane − average % W.C. at both ends

FIG 25

In an effort to discover more about the pore pressure three tests were run on Block 7 using a horizontal probe at the centre of the specimen. A porous bronze probe ⅜" diameter and ¾" long (Plate 1) was connected to a polythene tube which ran along the sample, inside the rubber membrane, to the top perspex cap. From this point a lead was provided by a nylon tube which passed through the base of the cell and was connected to the null indicator of the pore pressure apparatus. A lay-out of the arrangement is shown on Plate 2. The results are given in Table 8, but it is doubtful whether any firm conclusion

TABLE 8

Block 7

Consolidation pressure = 30 lb./sq.in.

Time to Failure	$(\sigma_1 - \sigma_3)$ at Failure lb/sq.in.	Change of Pore Pressure (Δu) lb./sq.in.	
		Base	Centre
5 hrs.	30.2	17.2	17.2
5 hrs.	26.0	18.3	16.8
3 days	28.0	17.8	17.0

can be drawn. However, in the second test in the above Table the probe was very close to the failure plane, and

TABLE 9

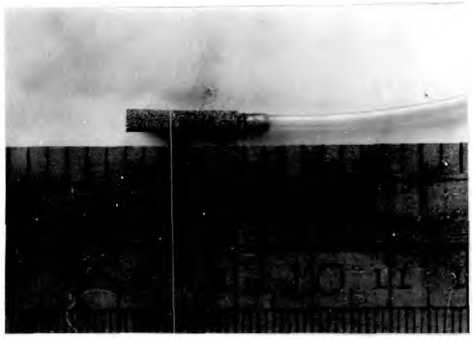
Block 7

w = 33 LL = 95 PL = 33

Consolidation Pressure lb./sq.in.	Time to Failure	$(\sigma_1 - \sigma_3)$ at Failure lb./sq.in.	Pore Pressure at Failure u lb/sq.in.	$A = \frac{\Delta u}{\Delta(\sigma_1 - \sigma_3)}$	Strain at Failure per cent	$(\sigma_1 - \sigma_3)$ corrected for 3 days at failure lb./sq.in.
15	1 day	15.8	10.0	0.63	1.7	15.3
30	5 hrs.	30.2	17.2*	0.57*	3.1	28.2
30	5 hrs.	26.0	16.8*	0.65*	2.8	24.3
30	1 day	27.2	18.7	0.69	2.5	26.4
30	3 days	28.0	17.0*	0.61*	2.4	28.0
45	7 hrs.	42.8	26.6	0.62	2.8	40.4
60	7 hrs.	52.3	33.3	0.64	2.4	49.2

* measured by probe

PLATE I

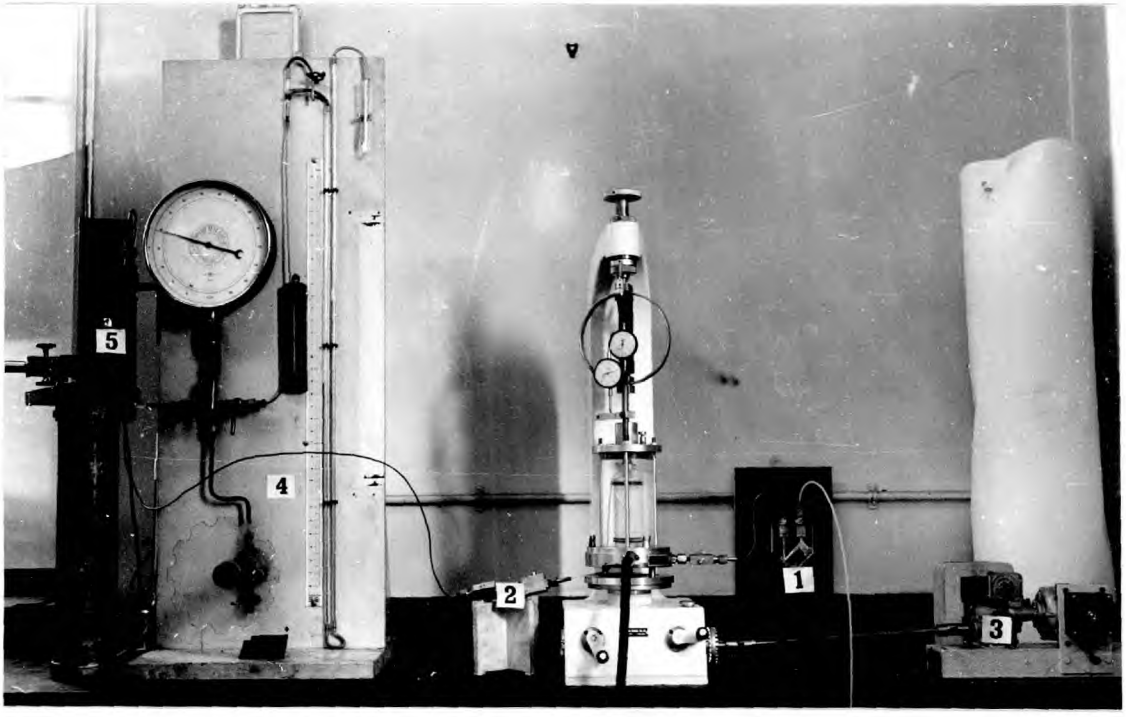


Detail of the Probe



Sample mounted in the cell with the probe in place

PLATE II



Triaxial Set-up for Consolidated-Undrained Tests

1. Null Indicator for pore pressure readings at the base of the sample.
2. Lead to the null indicator connected to the probe.
3. Motor-drive.
4. Pore pressure board.
5. Null indicator read through a microscope to decrease the time of reading.

there seems to be a fairly definite indication that the pore pressure was lower on the plane than at the end of the specimen (Fig.26).

The full set of results for Block 7 are given in Table 9. The total stress envelope at failure is shown in Fig.27, where each test has been corrected, by means of Fig.25, to a 3 day time to failure. These corrections are very small. The parameters are

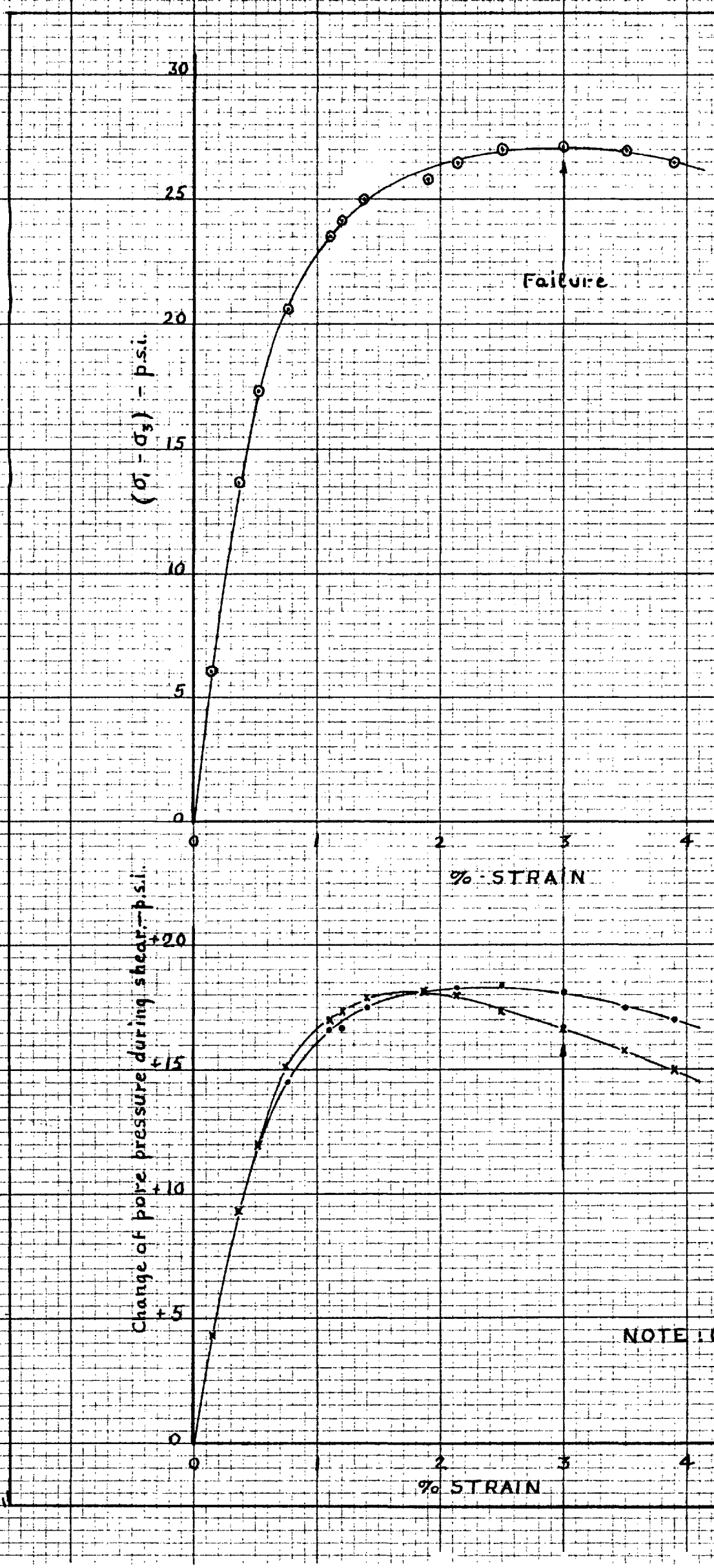
$$c_{cu} = 245 \text{ lb./sq.ft.}$$
$$\phi_{cu} = 16.0^{\circ}$$

Tests on Block 8 were all carried out in 15 minutes to failure, in order to obtain results comparable with those in the routine undrained tests. The results are:-

TABLE 10
Block 8

w = 33.0 LL = 95 PL = 33
Time to failure = 15 minutes

Consolidation Pressure lb./sq.in.	$(\sigma_1 - \sigma_3)$ at Failure lb./sq.in.	Strain at Failure per cent
15	20.8	2.4
30	34.1	3.8
45	44.4	3.3
60	49.8	6.4
60	63.4	3.0



CONSOLIDATED-UNDRAINED TEST

TEST N° - CU-15

$(\sigma_1 - \sigma_3)_f$ = 27.1 p.s.i.

Rubber membrane and drain correction = -1.1 p.s.i.

Corrected $(\sigma_1 - \sigma_3)_f$ = 26.0 p.s.i.

Time to failure = 5 hrs.

• - pore pressure at the base

x - " " at the probe

NOTE : At failure, the probe was partly on the shear plane.

FIG-26

TRIAXIAL CONSOLIDATED-UNDRAINED TESTS.

BLOCK Nº 7

Tests corrected for 3 days to failure

$$\begin{cases} C_{cu} = 1.70 \text{ psi} = 245 \text{ lbs/ft}^2 \\ \phi_{cu} = 16.0^\circ \end{cases}$$

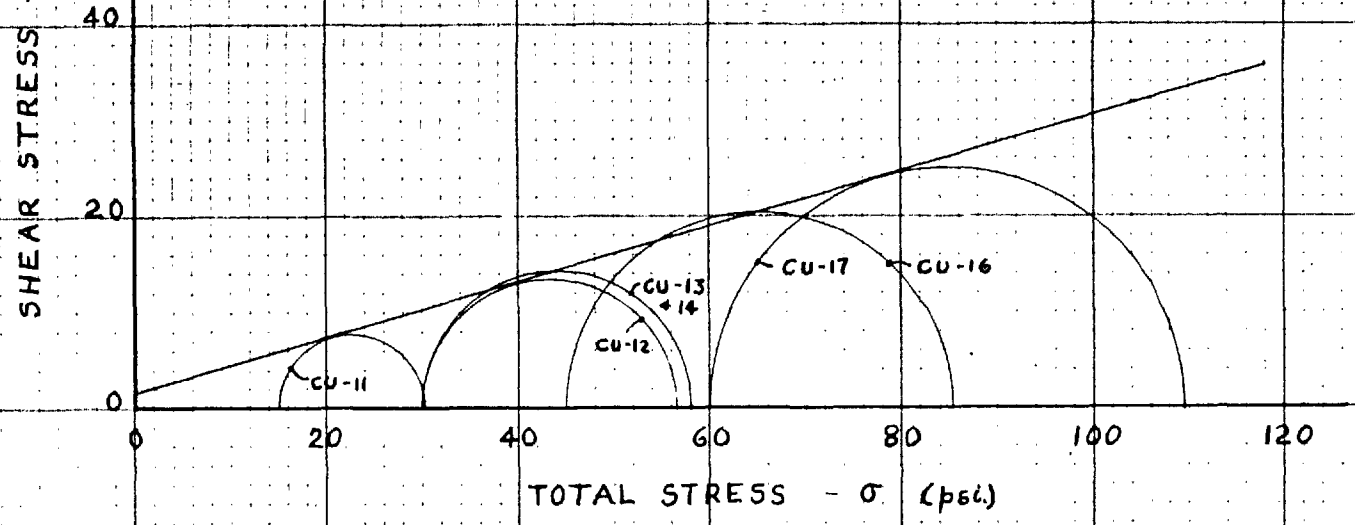


FIG-27

The parameters are (Fig.28):

$$c_{cu} = 460 \text{ lb./sq.ft.} \qquad \phi_{cu} = 16.7^{\circ}$$

(d) Comparison of Drained and Undrained Tests

The most convenient comparison of the effective stress failure envelopes in the drained and undrained tests is by means of the $J/3 - (\sigma_1 - \sigma_3)_f$ plot. In Fig.29 and 30 this comparison is made and it is seen that there is little difference in the case where a slow rate of strain hasbeen adopted for the undrained tests. It is especially to be noted that the test in which the pore pressure probe was located on the failure plane is in close agreement with the drained tests.

The pore pressure coefficient A can be found by relating the total stress circle, in the undrained test, and the effective stress envelope (which can be taken from the drained tests). For that purpose, the following formula can be used:

$$\tfrac{1}{2}(\sigma_1 - \sigma_3)_f = \frac{c' \cos \phi' + p' \sin \phi'}{1 + (2A - 1) \sin \phi'}$$

where c' and ϕ' are the effective stress parameters given

TRIAXIAL CONSOLIDATED-UNDRAINED TESTS.

BLOCK Nº 8

15 minutes to failure

$$\begin{cases} C_{cu} = 321 \text{ psi} = 460 \text{ lbs/ft}^2 \\ \phi_{cu} = 16.7^\circ \end{cases}$$

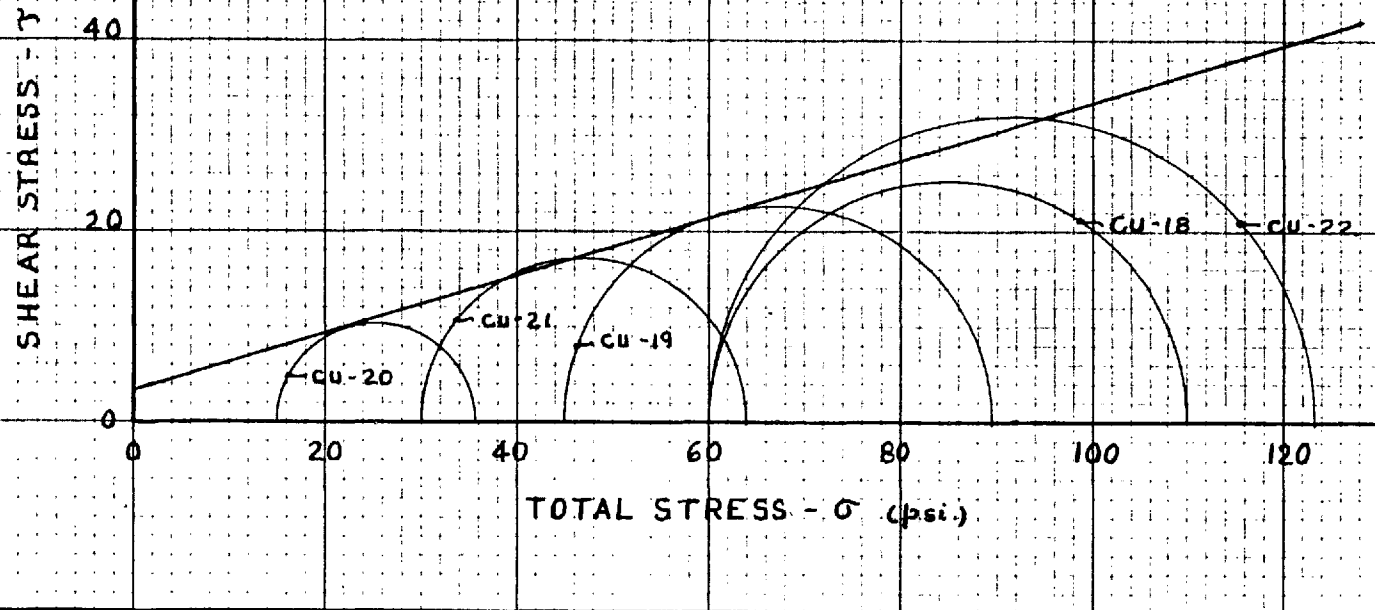
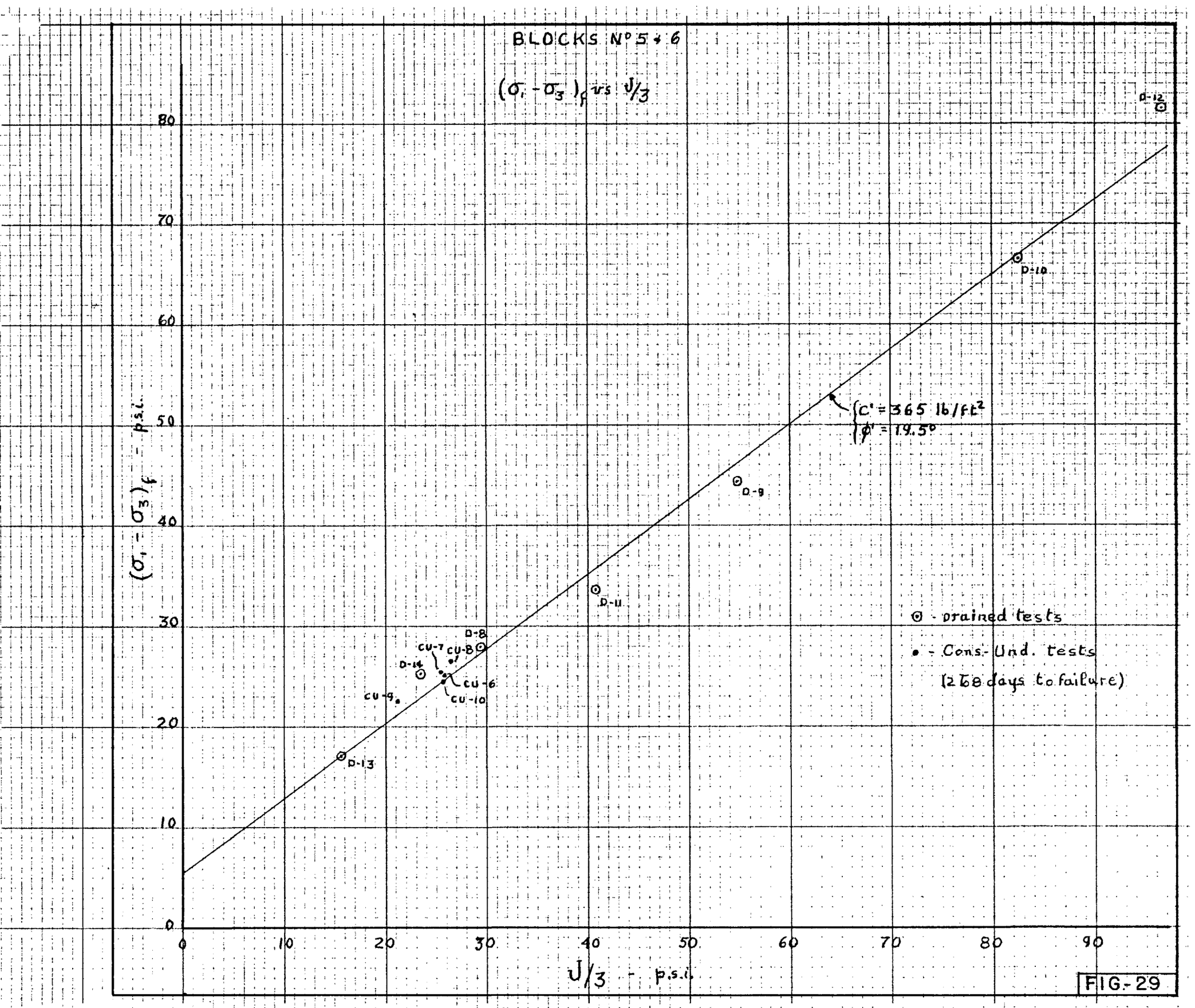
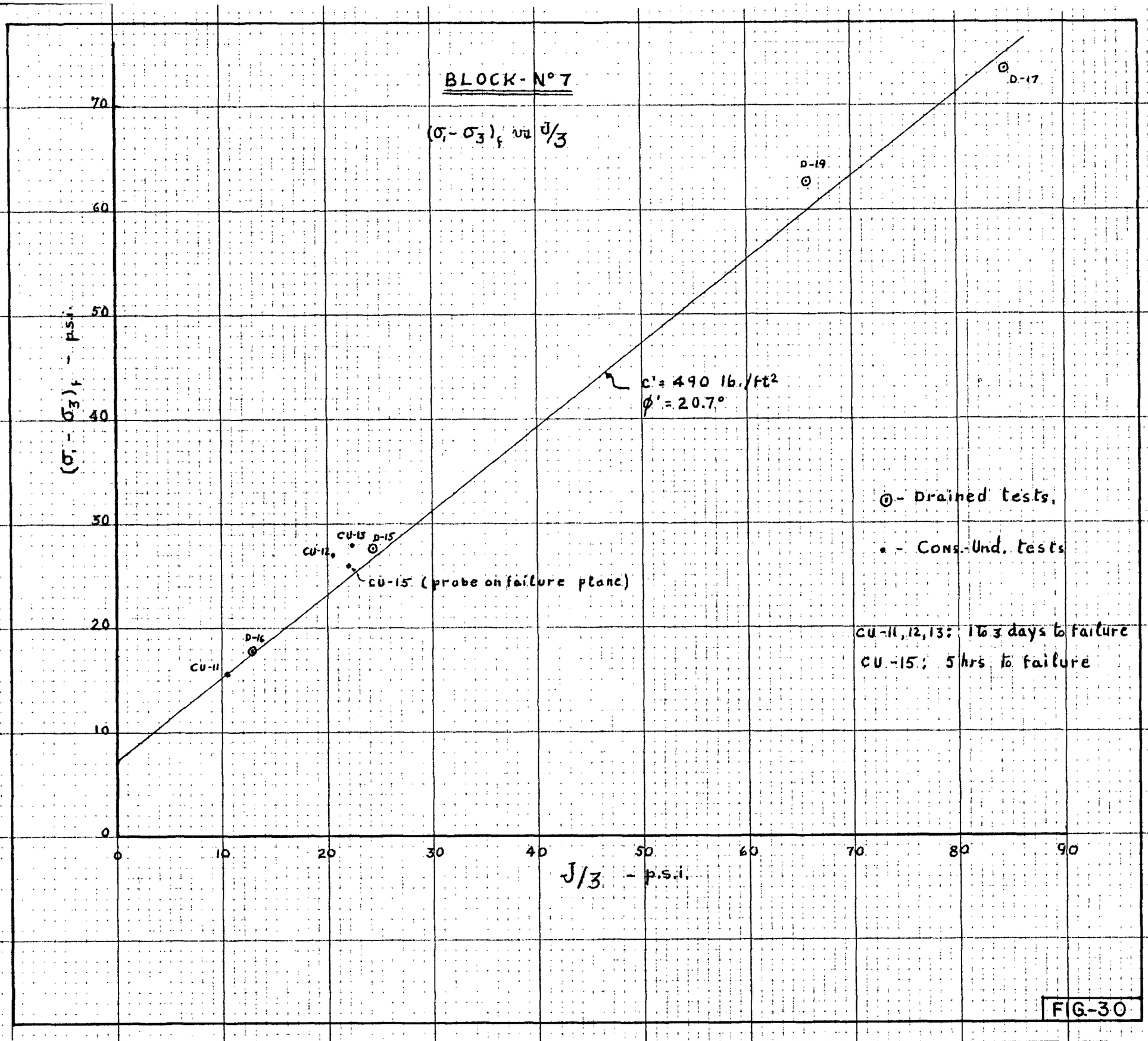


FIG-28


BLOCKS N° 5 + 6
$(\sigma_1 - \sigma_3)_f$ vrs $J/3$
$(\sigma_1 - \sigma_3)_f$ - p.s.i.
$J/3$ - p.s.i.
0
10
20
30
40
50
60
70
80
90
D-12
D-10
D-9
D-11
D-8
D-14
CU-7
CU-8
CU-6
CU-10
CU-9
D-13
$C' = 365$ lb/ft^2
$\phi' = 19.5°$
⊙ - drained tests
• - Cons.-Und. tests
(268 days to failure)
FIG-29


BLOCK - N° 7
$(\sigma_1 - \sigma_3)_f$ vs $J/3$
$(\sigma_1 - \sigma_3)_f$ - p.s.i.
$J/3$ - p.s.i.
0
10
20
30
40
50
60
70
80
90
D-17
D-19
D-15
CU-13
CU-12
CU-15 (probe on failure plane)
D-16
CU-11
c' = 490 lb./ft²
φ' = 20.7°
⊙ - Drained tests,
• - Cons.-Und. tests
CU-11, 12, 13: 1 to 3 days to failure
CU-15; 5 hrs to failure
FIG-30

by the drained tests and $\frac{1}{2}(\sigma_1 - \sigma_3)_f$ is the undrained strength corresponding to a consolidation pressure p'.

Table 11 gives a comparison between the measured values of A and the values calculated using the effective stress envelopes of the individual blocks (Table 6) or the average envelope for the site (c' = 370 lb./sq.ft. and $\emptyset'$ = 20°). For block 8 where the undrained tests were carried out at 15 minutes to failure, the effective stress envelopes were also corrected for a time to failure of 15 minutes to allow for the creep effects (Bishop and Henkel, 1957). This correction which amounts to 4% per log cycle to be applied to the deviator stress has little effect on the calculated value of A.

First of all, taking the slow tests (1 day or more) the values of A as measured and as deduced from the effective stress envelope, are similar. For the more rapid tests (5-7 hours) the measured values of A are decidedly higher than those deduced from the envelope. It is probable that the deduced values are more representative of the conditions on the failure plane in these relative quick tests, since the actual pore pressures on the failure plane will be lower than those measured at

TABLE 11

Comparison of "A" measured and calculated

Sample	σ_3 lb/sq.in.	Time to Failure	A at failure				
			Measured	From effective stress envelope			
				Individual Block		Average	
				3 days to failure	15 mins to failure	3 days to failure	15 mins to failure
Block 6	30	2-8 days	0.49	0.46	-	0.49	
Block 7	15	1 day	0.63	0.61	-	0.43	-
"	30	5 hrs.	0.61	0.48	-	0.31	-
"	30	1-3 days	(0.65)	0.50	-	0.38	-
"	45	7 hrs.	0.62	0.35	-	0.26	-
"	60	7 hrs.	0.64	0.40	-	0.32	-
Block 8	15	15 mins	-	0.24	0.31	0.10	0.17
"	30	15 mins	-	0.23	0.31	0.12	0.20
"	45	15 mins	-	0.30	0.38	0.21	0.29
"	60	15 mins	-	0.32	0.40	0.24	0.31

the base. Also in the slower tests the pore pressure on the failure plane will increase by migration of water from the rest of the specimen; and this leads to a lower strength.

Finally the values of A may be calculated by a comparison of the average drained envelope (c' = 370 lb./sq.ft. ϕ' = 20°) or the envelope corrected for 15 minutes to failure (c' = 395 lb./sq.ft., ϕ' = 21.1°) and the consolidated undrained envelope for 15 minute tests (c_{cu} = 460 lb./sq.ft., ϕ_{cu} = 16.7°) and for 3 days (c_{cu} = 245 lb./sq.ft., ϕ_{cu} = 16.0°). The results are given in Table 12.

TABLE 12

Deduced values of "A"

Consolidation pressure lb./sq.in.	Values of A		
	15 minutes		3 days
	average c', ϕ'	corrected average c', ϕ'	
σ_3 = 5	0.00	0.07	0.48
10	0.07	0.14	0.44
15	0.11	0.19	0.42
30	0.18	0.25	0.39
45	0.21	0.28	0.38
60	0.22	0.30	0.38

The 15 minute values probably represent little if any migration of pore water and therefore give approximately lower limits for A. Conversely, since the pore pressures measured at the base in 3 day tests give effective stress circles lying close to the drained envelope, these values may probably be representative of fairly complete migration and may be upper limits.

(c) Summary of "A" Values

If it is assumed that $K_o = 1$ then the average consolidation pressure $\bar{\sigma}'$, along the critical slip surface*, before excavation took place is about 10 lb./sq.in. But there is some indication that K_o is higher than unity, as already mentioned. Taking $K_o = 2$ the average consolidation pressure is about 20 lb./sq.in. (The actual computed values are 11.2 and 18.5 lb./sq.in. for the two cases).

Considering, first, the 15 minute tests which will give a lower limit for A, we have the values given in Table 13.

Thus for the $K_o = 2$ case ($\bar{\sigma}' = 15$ lb./sq.in.) the relevant value of A probably lies between 0.15 and 0.25,

---

* for this slip surface see the section of effective stress analysis.

TABLE 13

	Uncorrected c' Ø' envelope		Corrected c' Ø' envelope	
	$\bar{\sigma}'$ = 10	$\bar{\sigma}'$ = 20	$\bar{\sigma}'$ = 10	$\bar{\sigma}'$ = 20
Individual block	-	0.24	-	0.31
Average envelope	-	0.10	-	0.18
Comparison of envelopes	0.07	0.12	0.14	0.20
Mean		0.15		0.23

and 0.20 could be taken as a reasonable average. For $\bar{\sigma}'$ = 10 lb./sq.in. the value of A appears to be about 0.05 less than for $\bar{\sigma}'$ = 20 lb./sq.in., and an average of A = 0.15 is unlikely to be greatly in error.

For the 1 to 3 day tests, which may correspond to fairly complete migration of pore water into the slip zone the A values are seen to depend hardly at all on the consolidation pressure, and from various methods of estimating A the following values are obtained:

measured pore pressures	0.49, 0.63
individual block	0.46, 0.61, 0.50
average envelope	0.49, 0.43, 0.38
comparison of envelope	0.42, 0.44
Average	0.48

(f) Field Permeability Measurement

In the hope of gaining more information about ground water level behind a slope, a Casagrande type piezometer was established on 18 March 1958 near the Pump House excavation (Fig.31). Unfortunately when the site was next visited in May the excavation had already been backfilled (on 18 April 1958) and the piezometer was already reading a level almost equal to normal ground water level.

The opportunity was taken, however, of emptying the piezometer, and observing the rate of rise of water in the standpipe, from which the permeability of the clay can be calculated. The results are plotted in Fig.32. Observations were continued for about 6 weeks and during this time ground water level rose about 7 inches. This will have little effect on the calculations and ground water level is taken as constant at final position.

The theory is as follows (Hvorslev 1951); assuming an isotropic material, the coefficient of permeability is given by:

$$k = \frac{d^2 . \ln\left[2\frac{L}{D}\right]}{8L(t_2 - t_1)} \ln \frac{H_1}{H_2} \quad \text{for } \frac{L}{D} > 4$$

where D and L are respectively the diameter and length of the piezometer tip, d is the internal diameter of the tube (Fig.31), H_1 and H_2 are the differences in level of ordinary ground water and water in the pipe at times t_1 and t_2.

The calculated value of K is 3.7×10^{-9} cm./sec. Laboratory consolidation tests give the average value of $K = 2 \times 10^{-9}$ cm./sec.

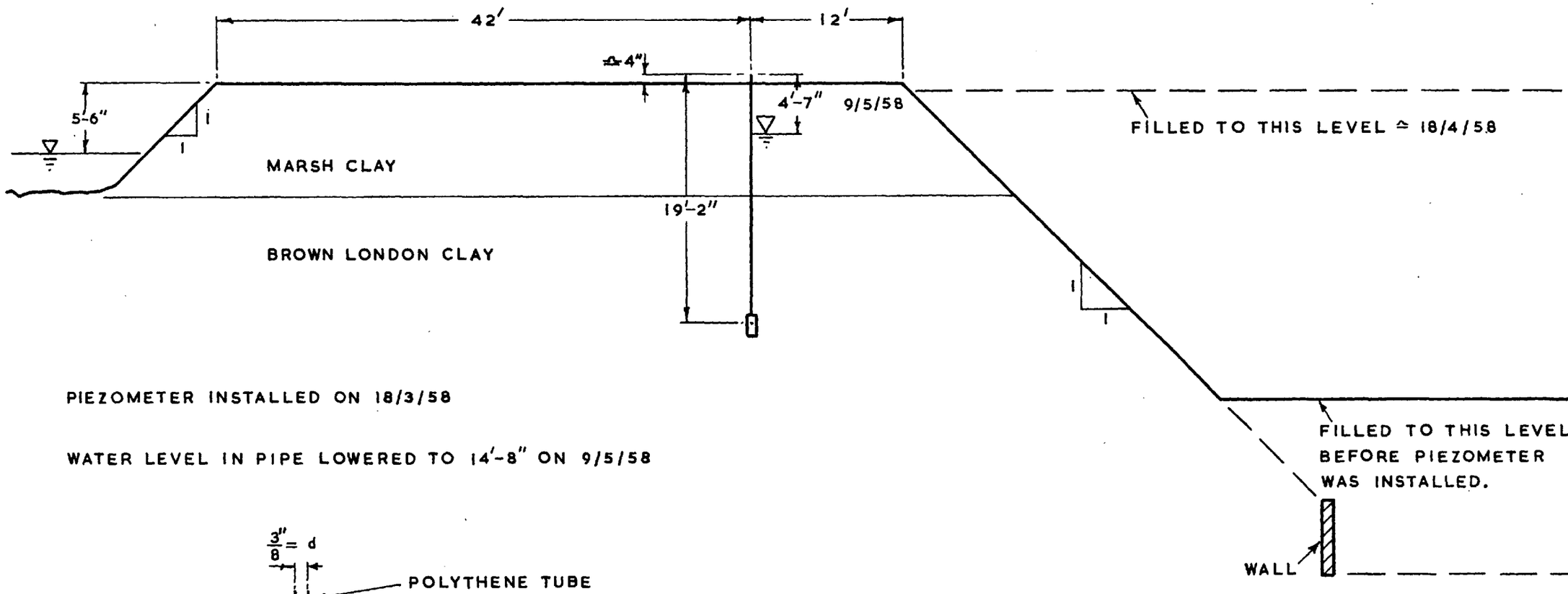
The theoretical curve in Fig.32 has been obtained by feeding the value of $K = 3.7 \times 10^{-9}$ cm./sec. into the above formula.

The field permeability is thus very similar to that measured in the laboratory: and it is concluded that the fissures could not have been open in the ground. The piezometer was, however, probably sufficiently far behind the slope to be out of the zone of severe shear stresses.

LOCATION OF PIEZOMETER

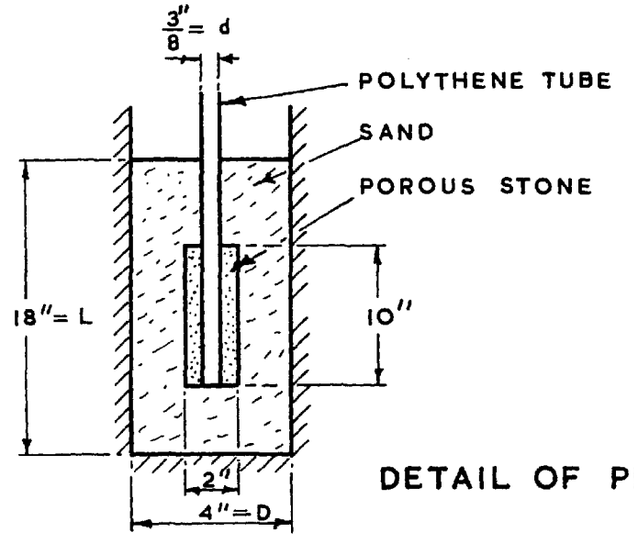
N. SIDE OF PUMP HOUSE EXCAVATION

SCALE 1"=10'



PIEZOMETER INSTALLED ON 18/3/58

WATER LEVEL IN PIPE LOWERED TO 14'-8" ON 9/5/58



DETAIL OF PIEZOMETER

FIG 31

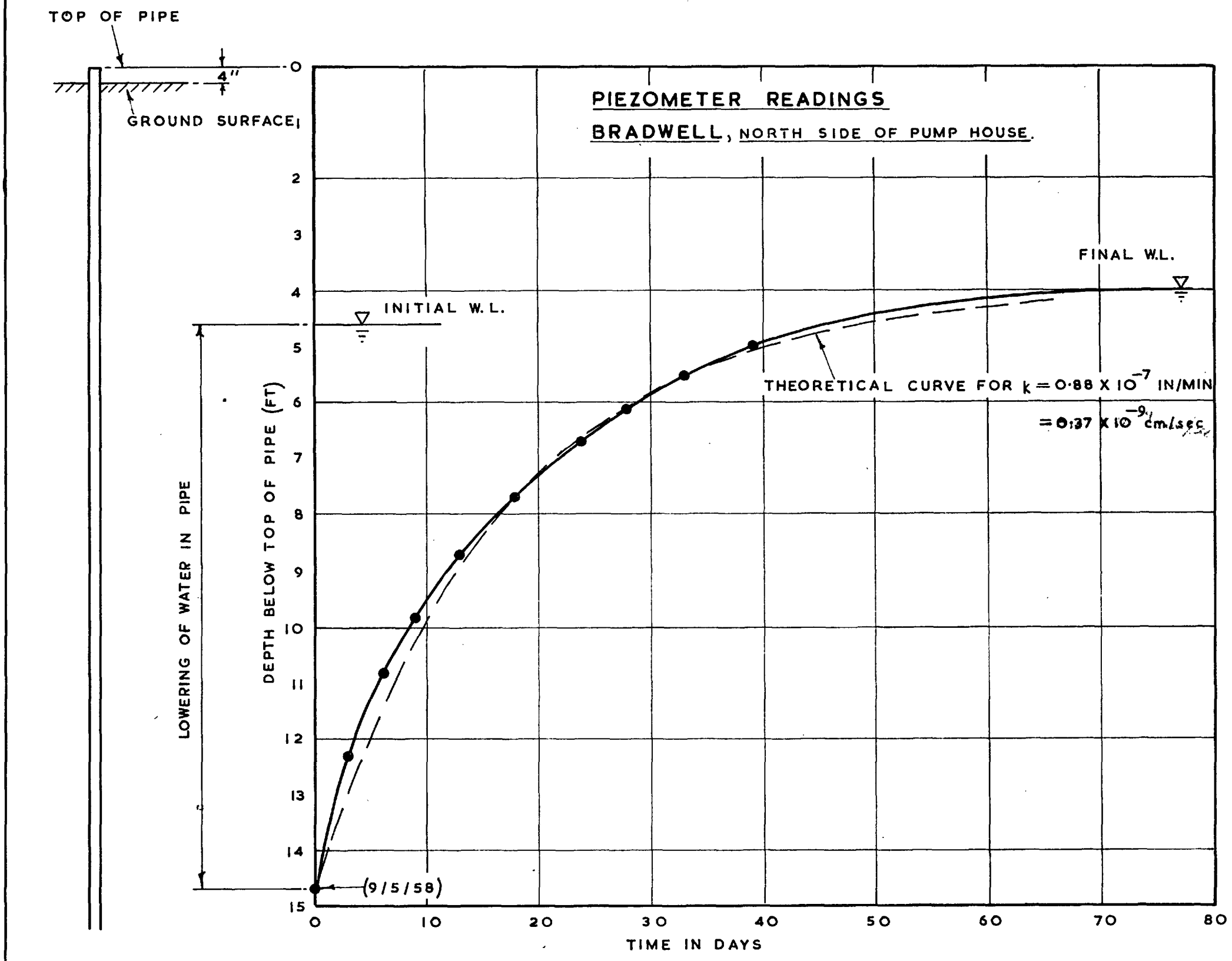

TOP OF PIPE
4"
GROUND SURFACE
PIEZOMETER READINGS
BRADWELL, NORTH SIDE OF PUMP HOUSE.
INITIAL W.L.
FINAL W.L.
THEORETICAL CURVE FOR k = 0·88 X 10⁻⁷ IN/MIN
= 0·37 X 10⁻⁹ cm/sec
LOWERING OF WATER IN PIPE
DEPTH BELOW TOP OF PIPE (FT)
(9/5/58)
0
10
20
30
40
50
60
70
80
TIME IN DAYS
0
2
3
4
5
6
7
8
9
10
11
12
13
14
15

FIG 32

CHAPTER III

TOTAL STRESS ANALYSIS

For saturated clays stressed under conditions of no volume change (i.e. at constant water content) the strength is independent of changes in total stress. Or, in other words, in this condition $\phi = 0$. During excavation the opportunities for water content change would be very slight and the $\phi = 0$ assumption must be a close approximation to reality.

1. REACTOR EXCAVATION, SLIP I

In a steep-sided slope the assumptions concerning depth of tension crack are of decided importance. Therefore a wide range of such assumptions has been made, to ensure that all possibilities are covered.

The assumptions may be summarised as follows (see also Fig.33).

(1) Tension crack through the fill, with no cracks in the marsh clay or London Clay. With this assumption, two cases have been investigated, 1(a) the slip circle continuous through the London Clay and marsh clay, 1(b) the slip circle stops at the junction of the London Clay and marsh clay, there being a zone of active pressure in the marsh clay, equivalent to a slip plane inclined at 45° to the horizontal. Clearly, on this assumption, the most critical slip surfaces extend back far enough to include the fill.

(2) A tension crack extending to a depth equal to 0.3 H where H is the height of the London Clay slope (i.e. a depth of 8.4 ft.).

(3) As in case (2) but a crack extending to 0.5 H.

(4) As before but cracks to a depth 0.7 H.

In cases (2), (3) and (4) the tension crack extends up through the marsh clay, in front of the toe of the fill. It should be noted that tension cracks cannot extend into the London Clay where this underlies the fill since, even at the top of the London Clay, under the fill, the overburden

pressure is about $3c/\gamma$. On the other hand, where there is only marsh clay above the London Clay, tension cracks can theoretically extend even deeper than those used in cases (2), (3) and (4) since, as will be seen from Fig.33, the depths are less than $1.5\ c/\gamma$.

(5) Tension crack down to the junction of the brown and blue London Clay.

(6) Tension crack down to a level equal to the bottom of the excavation.

In cases (5) and (6) the most critical surface includes a tension crack rising to the top edge of the slope.

In all cases, where appropriate, water pressure has been taken as acting in the crack, up to ground water level.

Details of the analyses are set out in Appendix C, but the critical surfaces for each tension crack assumption are shown in Fig.33 together with the values of shear strength required in the London Clay for a factor of safety equal to 1.0. Assumption 1(a) and 1(b) lead to almost identical results, and the required strength is 1090 lb./sq.ft. This is equal to $0.54\ \bar{c}$ where $\bar{c}$ is the

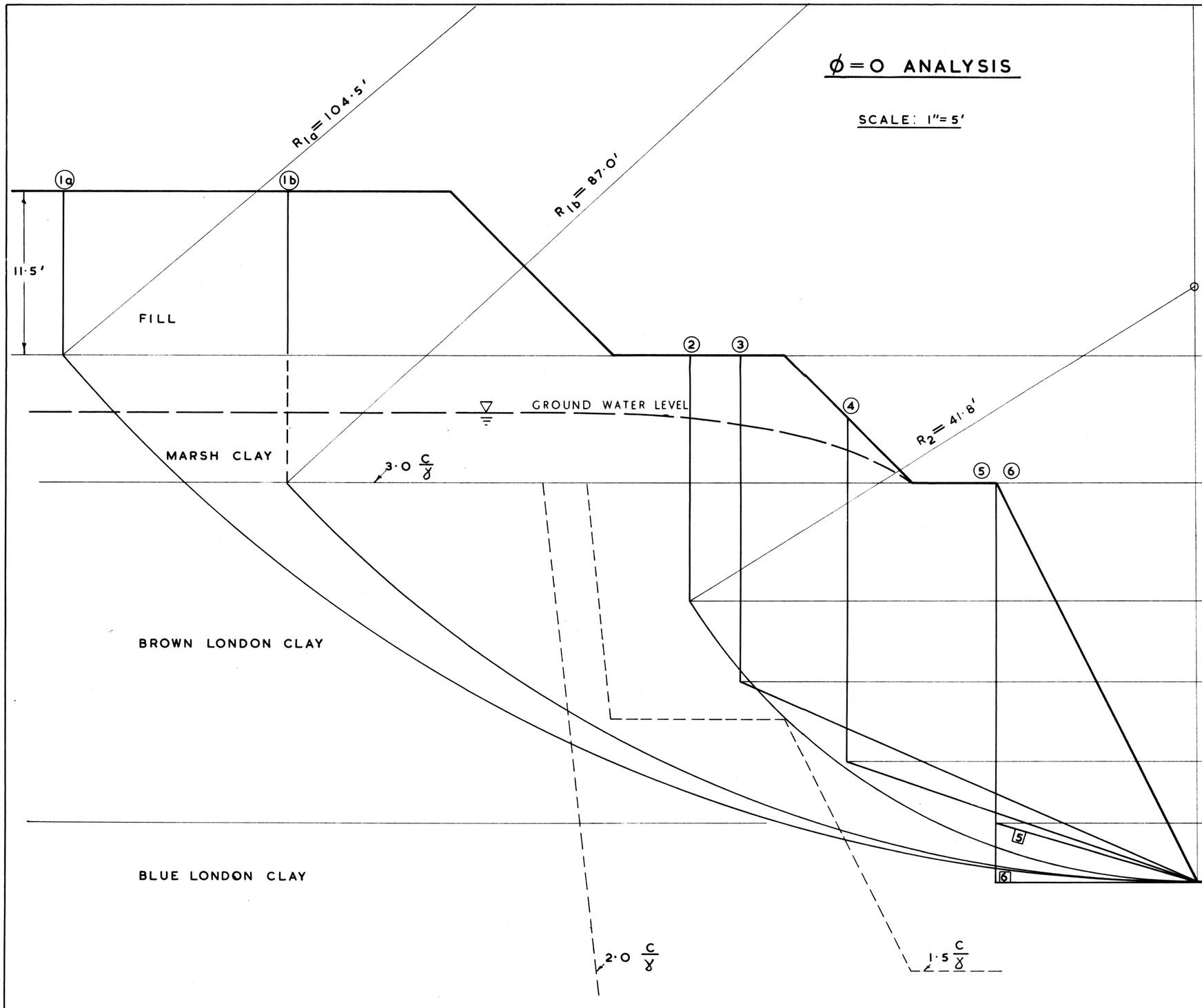
averaged measured shear strength of the London Clay, along the slip surface. For cases (2) and (3) the required strength is less than in case (1), and as the slip surfaces are deeper, the measured strength is higher, and the ratio is about 0.46. For case (4) the required strength is slightly more than in case (1), but the ratio of required to measured strength is hardly different from cases (2) and (3).

Cases (5) and (6) however, require considerably higher strengths and the ratio rises to 0.6 or 0.7. But these are rather extreme conditions, since they not only assume that the tension crack extends to a great depth (compared with the depth of the excavation) but also assume that the crack is filled with water for its entire height. If the water level was assumed to meet the surface of the slope in London Clay at ⅔ of its height (18.6' from the bottom of the excavation), the case (6) would then require a strength of 1160 lb./sq.ft., which is only 0.46 of the measured strength.

There can be little doubt that the failure would not have occurred, or at least would have been long delayed, had the fill not been in position. Therefore the

$\phi = 0$ ANALYSIS

SCALE: 1"= 5'



CASE	C REQ LB/SQFT	$\bar{C}$ MEAS LB/SQ FT	C REQ / $\bar{C}$ MEAS
1a	1090	2020	0.54
1b	1095	2020	0.54
2	1000	2190	0.40
3	1015	2200	0.47
4	1140	2320	0.49
5	1440	2420	0.59
6	1750	2500	0.70

REACTOR HOUSE EXCAVATION SLIP 1

FIG 33

most reasonable slip surfaces correspond to Case (1). Moreover the actual slip was not dissimilar from this case. Admittedly the first movement seemed to be confined to the clay just behind the slope, but this was probably due to overstressing caused by the weight of the fill, and it is likely that even before this first visible movement occurred there had been some strain in the body of the clay.

Consequently a ratio of required to measured strength equal to 0.54 is considered to be the best approximation.

2. REACTOR EXCAVATIONS, SLIP II

The preceding type of analysis, with assumption (1a) has been carried out for the second slip in the Reactor excavation, where the fill was 8 ft. thick, instead of 11½ ft. The required shear strength in London Clay was 1010 lb./sq.ft. as compared with an average measured value of 2020 lb./sq.ft. The ratio of required to measured shear strength is therefore 0.50.

This value is slightly lower than for slip I, which is consistent with the fact that the second slip occurred about 19 days after excavation, whilst the first slip occurred 5 days after excavation.

3. TURBINE HOUSE EXCAVATION

The 23 ft. deep excavation for the Turbine House remained stable for several months and, even then, there was no failure, but the excavation was backfilled against the walls of the completed structures.

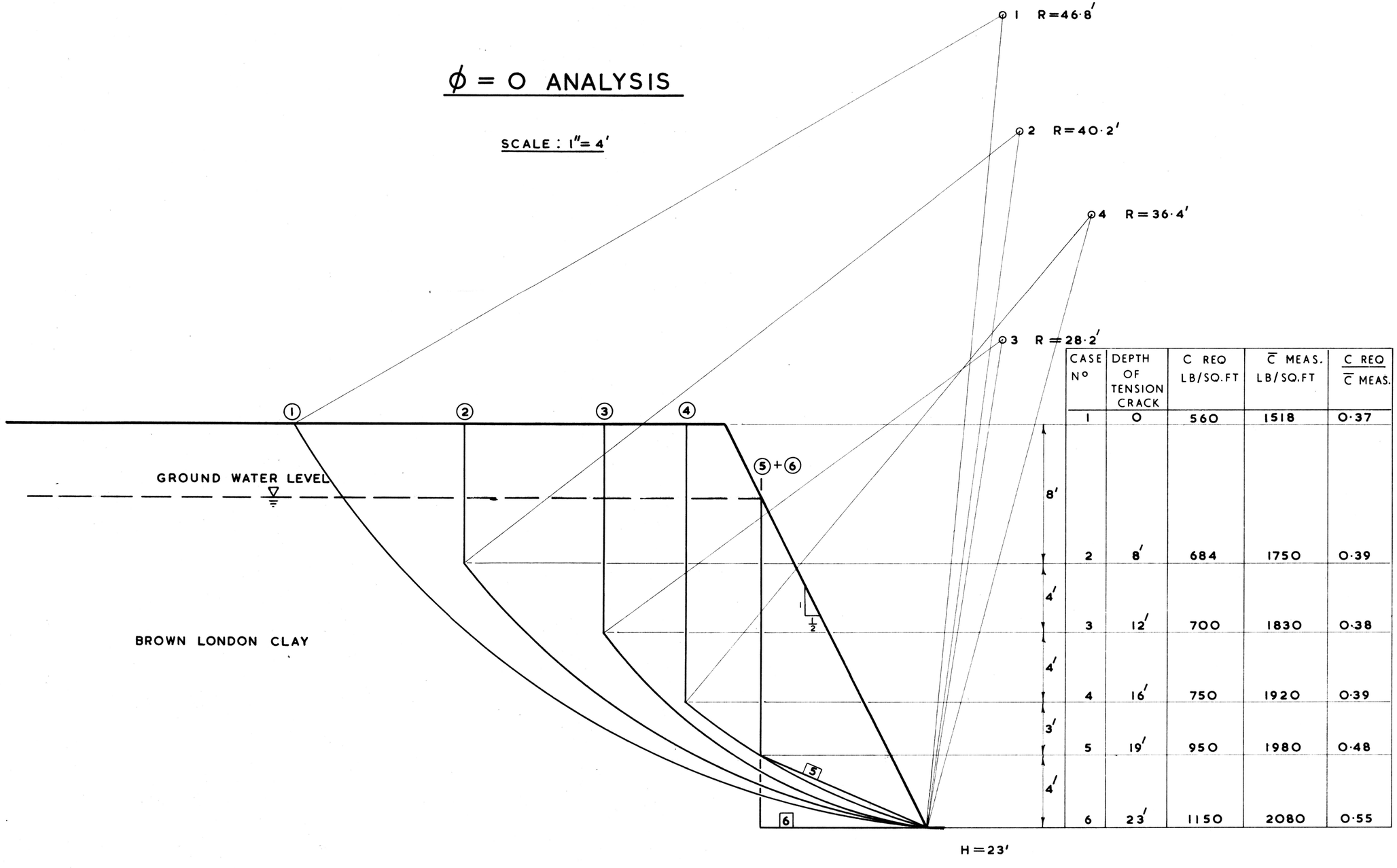
Six different depths of tension crack have been assumed (Fig.34), and the ratios of the strength required for stability to the measured strength range between 0.37 and 0.55. The latter case is rather extreme since it corresponds to a tension crack extending to a level equal to the bottom of the cut and the ground water level is assumed to be at the surface of the slope. A deep slip, corresponding to case (1) in the Reactor analysis, gave a ratio 0.39. Moreover, the average of all four analyses, excepting the two cases (5) and (6)* in Fig.34, is 0.38. The value 0.39 is probably sufficiently representative. It is, of course, a lower limit since the factor of safety was more than 1.0, as the slope was stable.

---

* It should be noted that as for the Reactor House Excavation, the ratio given by case (6) is very sensitive to the height of the water level at the surface of the slope. If the water level is assumed to meet the surface at half the height of the slope, the value of this ratio becomes 0.35.

$\phi = 0$ ANALYSIS

SCALE : 1"= 4'



CASE N°	DEPTH OF TENSION CRACK	C REQ LB/SQ.FT	$\bar{C}$ MEAS. LB/SQ.FT	C REQ / $\bar{C}$ MEAS.
1	0	560	1518	0·37
2	8'	684	1750	0·39
3	12'	700	1830	0·38
4	16'	750	1920	0·39
5	19'	950	1980	0·48
6	23'	1150	2080	0·55

TURBINE HOUSE EXCAVATION

$1{\cdot}5\ \frac{C}{\gamma}$

FIG 34

It may be noted that a depth corresponding to 1.5 c/γ is considerably deeper than the excavation.

4. PUMP HOUSE EXCAVATION

This excavation was 39 ft. deep, with a uniform slope of 1:1, and with 9 ft. of marsh clay overlying the London Clay. The slope remained stable for at least 4 months. Analysis of a deep slip, with tension crack extending through the marsh clay, showed a ratio of required strength (840 lb./sq.ft.) to measured strength (2120 lb./sq.ft.) of 0.40. This is practically the same as that for the Turbine House, but in the Pump House the slope, with the maximum height of 39 ft., exists only in two short lengths of 32 ft. (Fig.8) and it may receive some support from the adjoining slopes. The Pump House excavation is therefore perhaps not quite a clear cut case.

Summary of Total Stress Analysis

The results of the foregoing analyses may be summarised in Table 14.

TABLE 14

	Average depth of slip surface	Time to slip after completion of excavation	Stable for at least	Strength required / Strength measured
Reactor No.1 Slip I	29'	5 days	-	0.54
Reactor No.1 Slip II	28'	19 days	-	0.50
Pump House	20'	-	4 months	>0.40
Turbine House	14'	-	4½ months	>0.39

5. COMPARISON WITH LONG-TERM FAILURES

Ten slips in London Clay, occurring at intervals of between 13 and 81 years after excavation, have been analysed at Imperial College. The results are given in Table 15.

These are plotted together with the Bradwell results in Fig.35, and it will be seen that the ratio of required to measured strength decreases with time. But whereas about one-half of the strength is lost almost immediately after excavation a further halving of the strength requires a period of the order 40 years.

TABLE 12

Location	Time to Failure years	Average depth of slip surface	$\frac{C_{req.}}{C_{meas.}}$
Wembley Hill	13	23'	0.35
Park Village East	19	25'	0.30
Mill Lane	28	24'	0.29
Uxbridge	29	18'	0.31
Northolt	35	15'	0.22
Kensal Green	53	11'	0.26
Sudbury Hill I	54	11'	0.17
Sudbury Hill II	57	19'	0.20
Wood Green	55	20'	0.29
Upper Holloway	81	10'	0.11

The reasons for the long-term decrease in strength lie outside the scope of this Thesis, and the results plotted in Fig.35 have been given merely to show the relation between short-term and long-term failures.

RATE OF SOFTENING OF LONDON CLAY

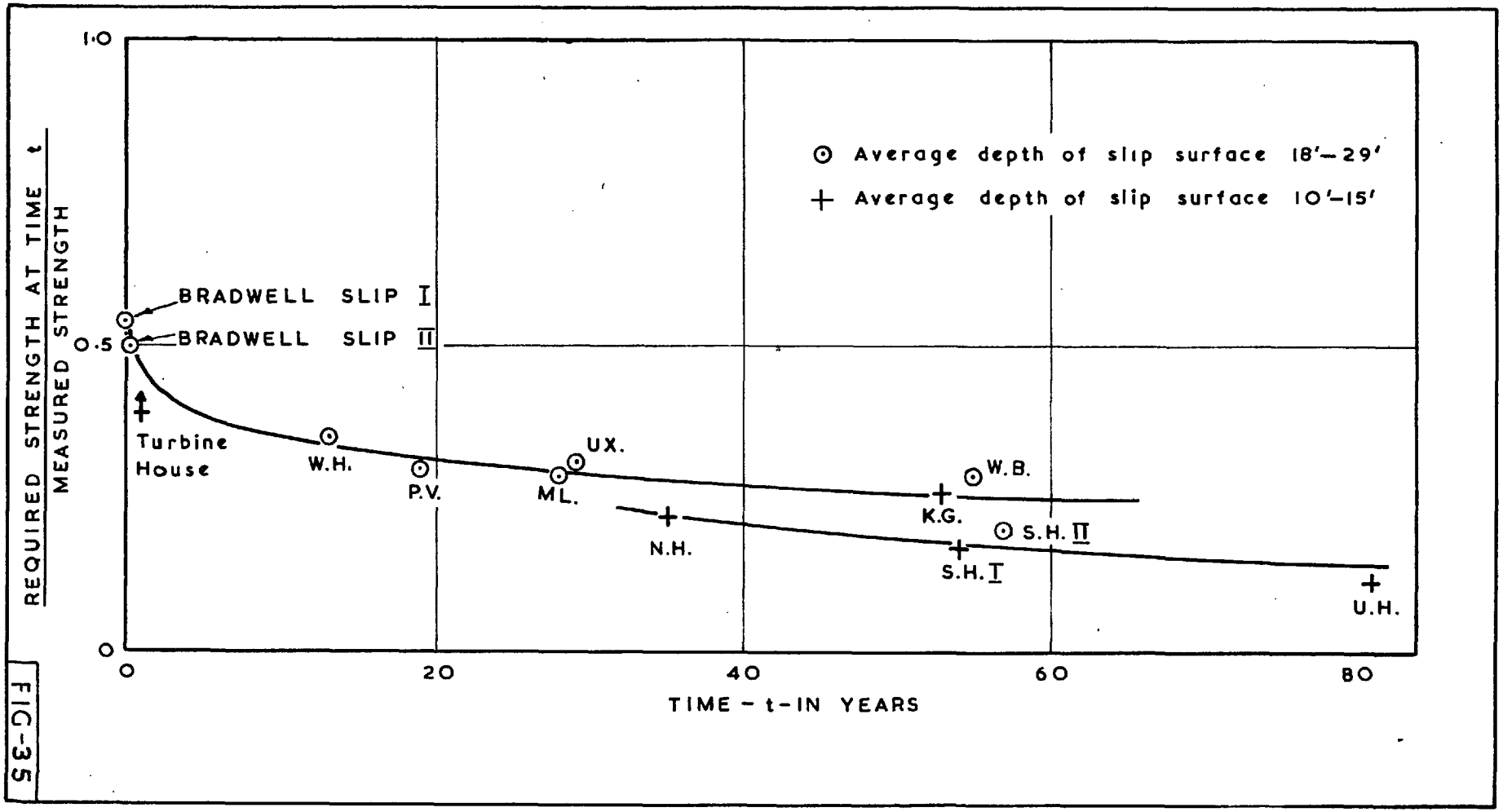


FIG-35

CHAPTER IV

EFFECTIVE STRESS ANALYSIS

In order to gain a further understanding of the problem of stability of the Bradwell slopes has been investigated from an effective stress point of view. With long-term stability the pore pressures are known from piezometer observations or from reasonable assumptions concerning ground water levels. With the short term problem, however, it is necessary to calculate the pore pressures unless, of course, one had been so fortunate as to have rapid-response piezometers installed at exactly the section of the slip, just before the slip occurred.

1. USE OF ELASTIC STRESS DISTRIBUTION

An essential requirement for calculating the pore pressures is a knowledge of the stresses in the clay

behind the slope. The stresses have been estimated from elastic theory and also from an approximate "plastic" solution. The elastic solution was obtained by means of photo-elastic tests on gelatine models. The technique of these tests is outlined in Appendix D, and the stress patterns are given in Figs. 36 and 37. The results are only approximate, with errors of perhaps ±10 per cent, but the alternative of using the Airy stress function ϕ and solving the biharmonic equation

$$\frac{\delta^4 \phi}{\delta x^4} + \frac{2\delta^4 \phi}{\delta x^2 \delta y^2} + \frac{\delta^4 \phi}{\delta y^4} = 0$$

by means of the Relaxation method would have been far too lengthy.

From the stress patterns, values of σ_1 and σ_3 can be obtained for a number of points along a slip surface. Then, from the equation (Skempton 1954)

$$\Delta u = \Delta\sigma_3 + A\,(\Delta\sigma_1 - \Delta\sigma_3)$$

the change in pore pressure at any of these points can be calculated for a given value of A, assuming that before excavation both the principal stresses were equal to the

FIG-36

BRADWELL SLOPE

σ_1 AND σ_3

NOTE : Points I to II correspond to the slices from the effective stress circle, FIG 40

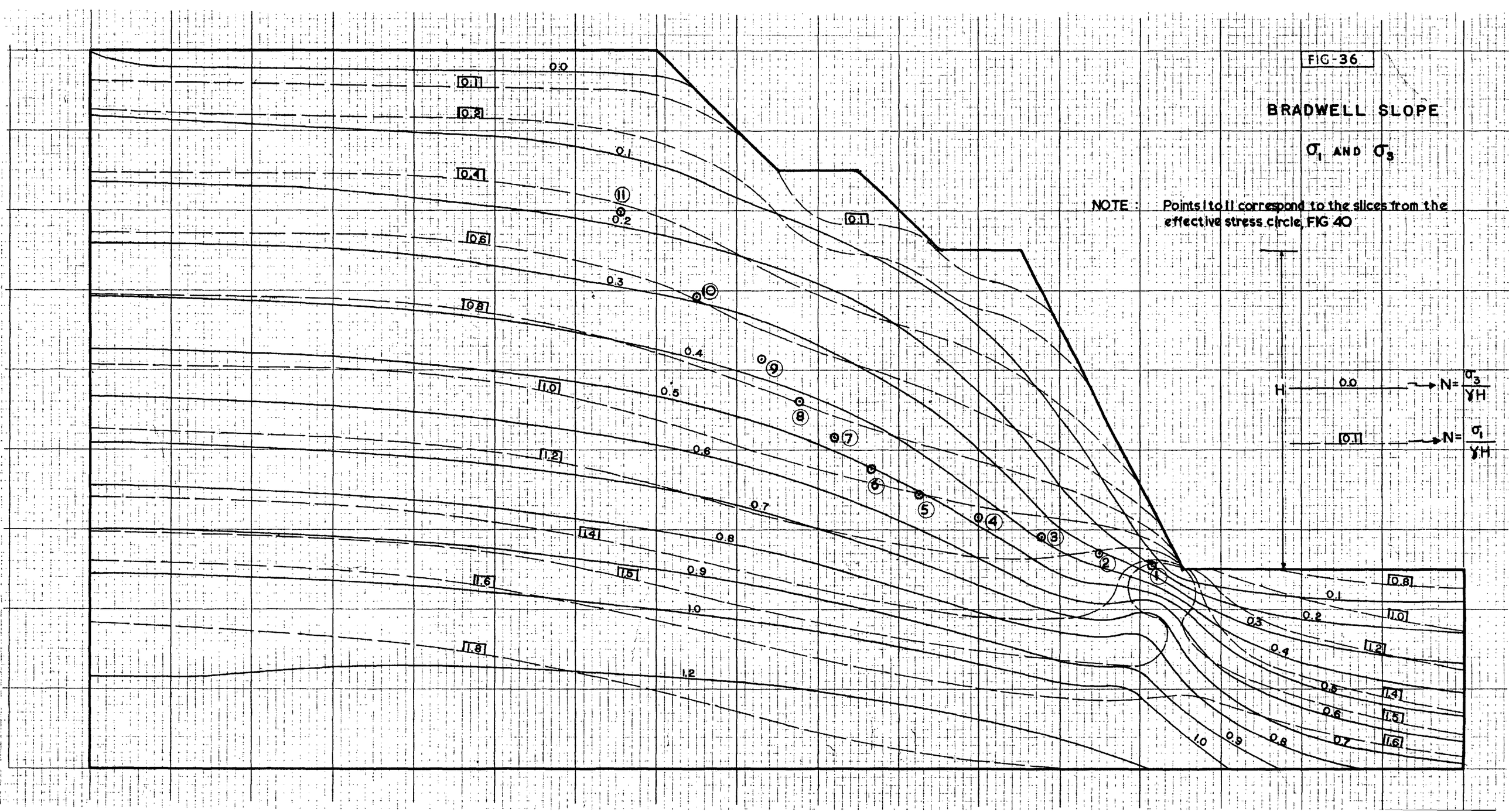
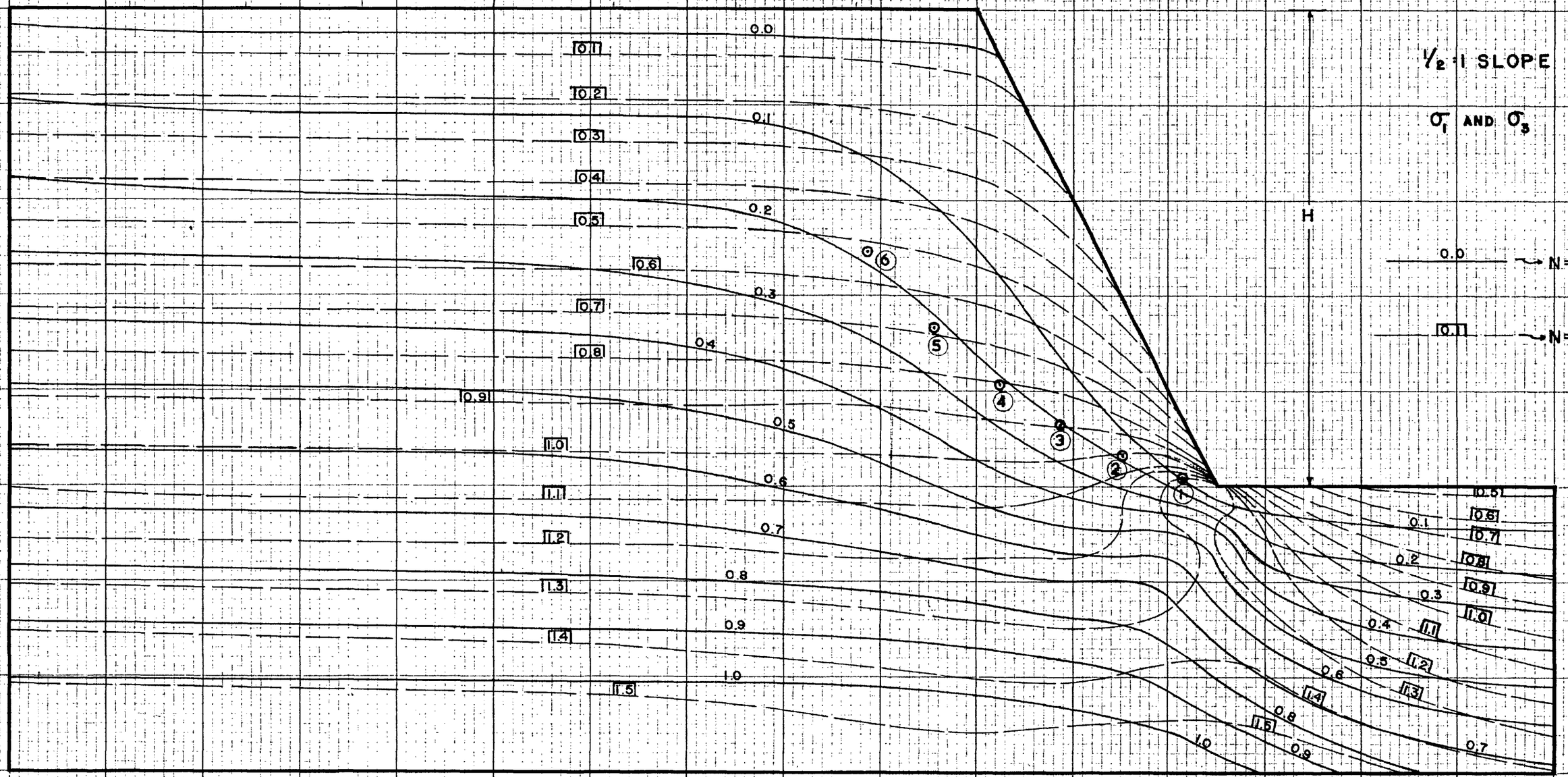


FIG 37



NOTE: Points 1 to 6 correspond to the slices from the effective stress circle, FIG 41.

total overburden pressure: that is, K_o was assumed to be 1.0. The original pore pressure is known, as it is simply $u_o = \gamma_w h_w$ where h_w is the depth of the point below ground water level. Hence, the pore pressure after excavation is

$$u = u_o + \Delta u$$

The effective stress analysis can then be carried out by the usual method (Bishop 1955) and, knowing $\phi' = 20^\circ$ and that the factor of safety is 1.0, the value of c' can be found. Other circles are then analysed until a maximum value of c' for this given value of A is obtained. The entire procedure is then repeated for another value of A. It was found that for all values of A approximately the same critical slip circle is obtained.

In this way a relation is found between c' and A for the Reactor and the Turbine House excavations (Fig.38 and 39)*. The stresses and pore pressures for the critical circles (Fig.40 and 41) are given in Tables 16 and 17.

2. USE OF "PLASTIC" STRESS DISTRIBUTION

To find the stresses by a "plastic" solution, the same critical circle was used and the shear stress

* For the marsh clay A was assumed to be 0.6 and c' = 0.

REACTOR HOUSE EXCAVATION

(PORE PRESSURES FOR THE EFFECTIVE STRESS CIRCLE, FIG 40)

TABLE - 16

Stress & pressure in lbs/in^2 $K_o = 1$

Slice No	Original		After Excavation [$\Delta u = \Delta\sigma_3 + A(\Delta\sigma_1 - \Delta\sigma_3)$]												
	$\sigma_1 = \sigma_3$	u_o	σ_1	σ_3	$\Delta\sigma_1$	$\Delta\sigma_3$	$(\Delta\sigma_1 - \Delta\sigma_3)$	A = ·6		A = ·3		A = 0		A = -·3		
								Δu	u	Δu	u	Δu	u	Δu	u	
11	3·5	0·3	8·1	2·5	4·6	-1·0	5·6	2·4	2·7	-	-	-	-	-	-	Plastic.
			10·0	4·3	6·5	0·8	5·7	4·2	4·5	-	-	-	-	-	-	Elastic.
10	9·9	3·9	12·9	4·6	3·0	-5·3	8·3	-0·3	3·6	-2·8	1·1	-5·3	-1·4	-7·8	-3·9	Plastic
			14·0	6·8	4·1	-3·1	7·2	1·2	5·1	-0·9	3·0	-3·1	0·8	-5·3	-1·4	Elastic.
9	14·5	6·3	16·3	4·8	1·8	-9·7	11·5	-2·8	3·5	-6·2	0·1	-9·7	-3·4	-13·2	-6·9	Plastic.
			16·7	8·6	2·2	-5·9	8·1	-1·0	5·3	-3·5	2·8	-5·9	0·4	-8·3	-2·0	Elastic.
8	17·6	7·9	19·3	6·5	2·2	-11·1	13·3	-3·1	4·8	-7·1	0·8	-11·1	-3·2	-15·1	-7·2	Plastic.
			18·4	9·8	0·8	-7·8	8·6	-2·6	5·3	-5·2	2·7	-7·8	0·1	-10·4	-2·5	Elastic.
7	20·4	9·3	23·8	9·2	3·4	-11·2	14·6	-2·4	6·9	-6·8	2·5	-11·2	-1·9	-15·6	-6·3	Plastic.
			20·3	11·0	-0·1	-9·4	9·3	-3·8	5·5	-6·6	2·7	-9·4	-0·1	-12·2	-2·9	Elastic.
6	22·2	10·5	26·2	10·7	4·0	-11·5	15·5	-2·2	8·3	-6·9	3·6	-11·5	-1·0	-16·1	-5·6	Plastic.
			22·2	11·7	0·0	-10·5	10·5	-4·2	6·3	-7·3	3·2	-10·5	0·0	-13·7	-3·2	Elastic.
5	24·5	11·5	26·2	9·6	1·7	-14·9	16·6	-4·9	6·6	-9·9	1·6	-14·9	-3·4	-19·9	-8·4	Plastic.
			23·4	12·0	-1·1	-12·5	11·4	-5·7	5·8	-9·1	2·4	-12·5	-1·0	-15·9	-4·4	Elastic.
4	26·2	12·3	26·8	9·5	0·6	-16·7	17·3	-6·3	6·0	-11·5	0·8	-16·7	-4·4	-21·9	-9·6	Plastic.
			24·2	11·2	-2·0	-15·0	13·0	-7·2	5·1	-11·1	1·2	-15·0	-2·7	-18·9	-6·6	Elastic.
3	27·5	13·0	26·8	9·0	-0·7	-18·5	17·8	-7·8	5·2	-13·2	-0·2	-18·5	-5·5	-23·8	-10·8	Plastic.
			26·0	9·3	-1·5	-18·2	16·7	-8·2	4·8	-13·2	-0·2	-18·2	-5·2	-23·2	-10·2	Elastic.
2	28·7	13·7	20·6	2·3	-8·1	-26·4	18·3	-15·4	-1·7	-20·9	-7·2	-26·4	-12·7	-31·9	-18·2	Plastic.
			28·4	7·5	-0·3	-21·2	20·9	-8·7	5·0	-14·9	-1·2	-21·2	-7·5	-27·5	-13·8	Elastic.
1	29·5	14·1	13·1	-5·5	-16·4	-35·0	18·6	-23·8	-9·7	-29·4	-15·3	-35·0	-20·9	-40·6	-26·5	Plastic.
			35·0	4·7	5·5	-24·8	30·3	-6·6	7·5	-15·7	-1·6	-24·8	-10·7	-33·9	-19·8	Elastic.
→	20·7	4·8	20·5	6·0					3·5		-1·1		-5·2		-9·4	Plastic.

→ Average along the slip surface for the plastic stress distribution.

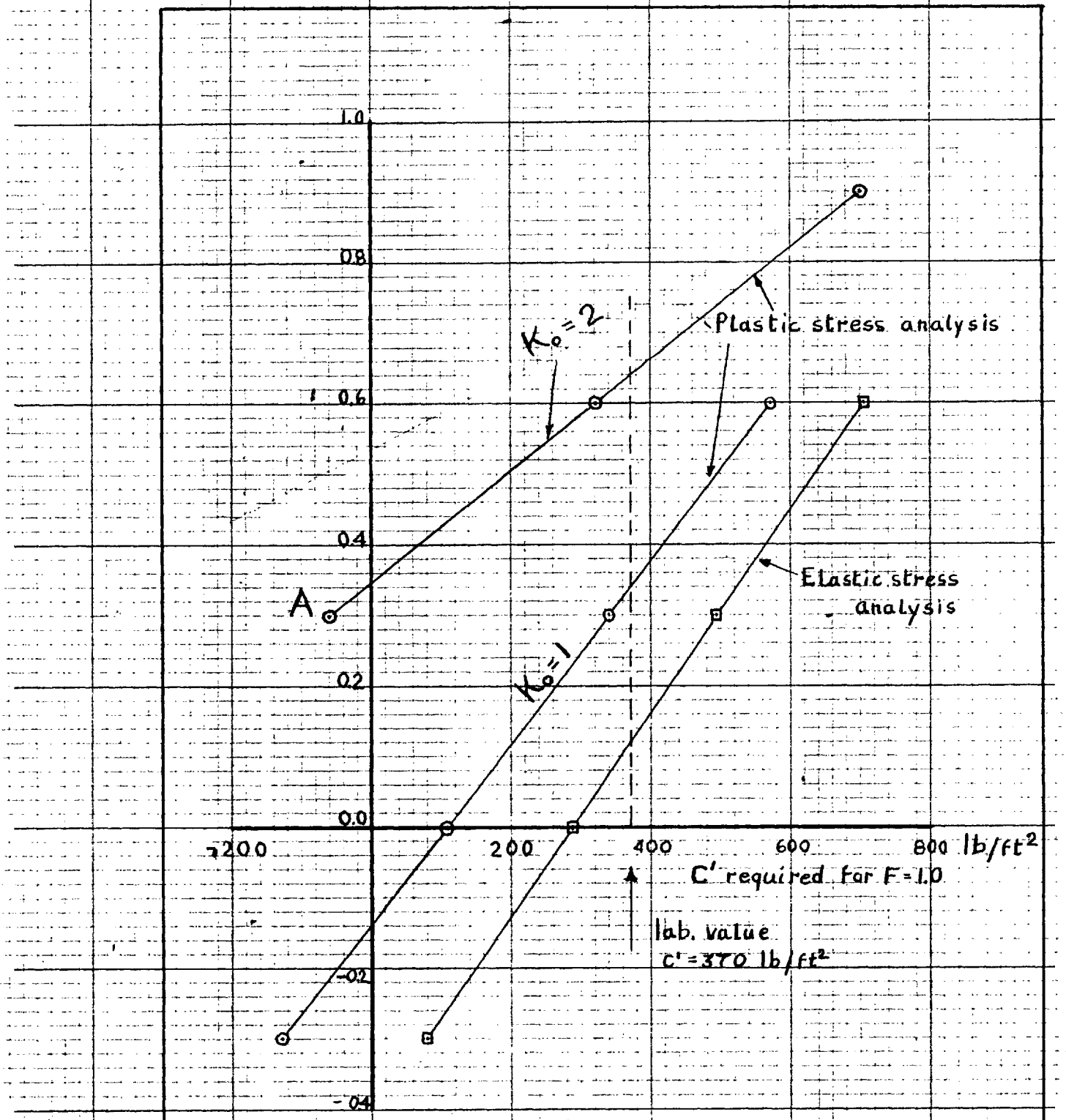
TABLE - 17

TURBINE HOUSE EXCAVATION

(PORE PRESSURES FOR THE EFFECTIVE STRESS CIRCLE, FIG. 41)

Stress & pressure in lbs/in^2. $K_o = 1$

Slice №	Original		After Excavation					$\Delta u = \Delta\sigma_3 + A(\Delta\sigma_1 - \Delta\sigma_3)$								
								A = 0·9		A = 0·6		A = 0·3		A = 0		
	$\sigma_1 = \sigma_3$	u_o	σ_1	σ_3	$\Delta\sigma_1$	$\Delta\sigma_3$	$\Delta\sigma_1 - \Delta\sigma_3$	Δu	u	Δu	u	Δu	u	Δu	u	
6	9·7	3·3	6·4	-·3	-3·3	-10·0	6·7	-4·0	-0.7	-6·0	-2·7	-8·0	-4·7	-10·0	-6·7	Plastic.
			10·1	3·6	+0·4	- 6·1	6·5	-0·2	+3·1	-2·2	+1·1	-4·1	-0·8	- 6·1	-2·8	Elastic.
5	12·8	4·9	10·7	2·6	-2·1	- 10·2	8·1	- 2·9	+2·0	-5·3	-0·4	-7·8	-2·9	-10·2	-5·3	Plastic.
			13·0	4·2	+0·2	- 8·6	8·8	-0·7	+4·2	-3·3	+1·6	-6·0	-1·1	-8·6	-3·7	Elastic
4	15·1	6·1	13·6	4·8	-1·5	- 10·3	8·8	- 2·4	+3·7	-5·0	+1·1	-7·7	-1·6	-10·3	-4·2	Plastic.
			15·3	4·2	+0·2	- 10·9	11·1	-0·9	+5·2	-4·2	+1·9	-7·6	-1·5	-10·9	-4·8	Elastic.
3	16·7	7·0	13·1	3·7	-3·6	- 13·0	9·4	-4·5	+2·5	-7·4	-0·4	-10·2	-3·2	-13·0	-6·0	Plastic.
			17·2	4·0	+0·5	- 12·7	13·2	-0·8	+ 6·2	-4·8	+2·2	- 8·7	-1·7	-12·7	-5·7	Elastic.
2	18·0	7·6	10·9	1·2	-7·1	- 16·8	9·7	- 8·1	-0·5	-11·0	-3.4	-13·9	-6.3	-16·8	-9·2	Plastic.
			19·6	3·5	+1·6	- 14·5	16·1	0·0	+7·6	-4·8	+2·8	- 9·7	-2·1	-14·5	-6·9	Elastic.
1	18·8	8·1	7·3	-2·7	-11·5	- 21·5	10·0	- 12·5	-4·4	-15·5	- 7·4	-18·5	-10·4	-21·5	-13·4	Plastic
			25·0	1·9	+6·2	- 16·9	23·1	+ 3·9	+12·0	-3·0	+5·1	-10·0	-1·9	-16·9	-8·8	Elastic.

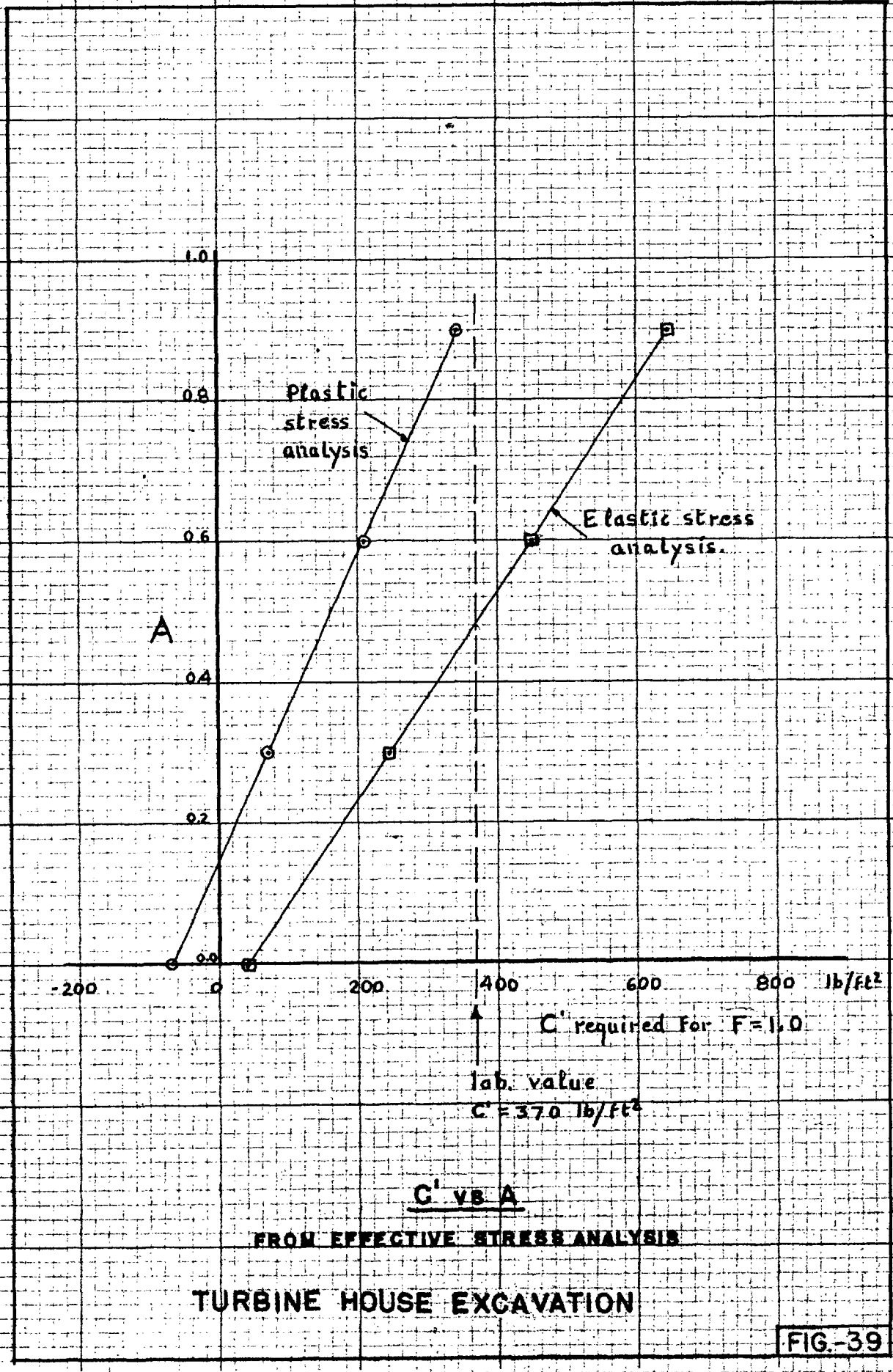


C' vs A

FROM EFFECTIVE STRESS ANLYSIS

REACTOR HOUSE EXCAVATION (SLIP-1)

FIG.- 38



C' VS A

FROM EFFECTIVE STRESS ANALYSIS

TURBINE HOUSE EXCAVATION

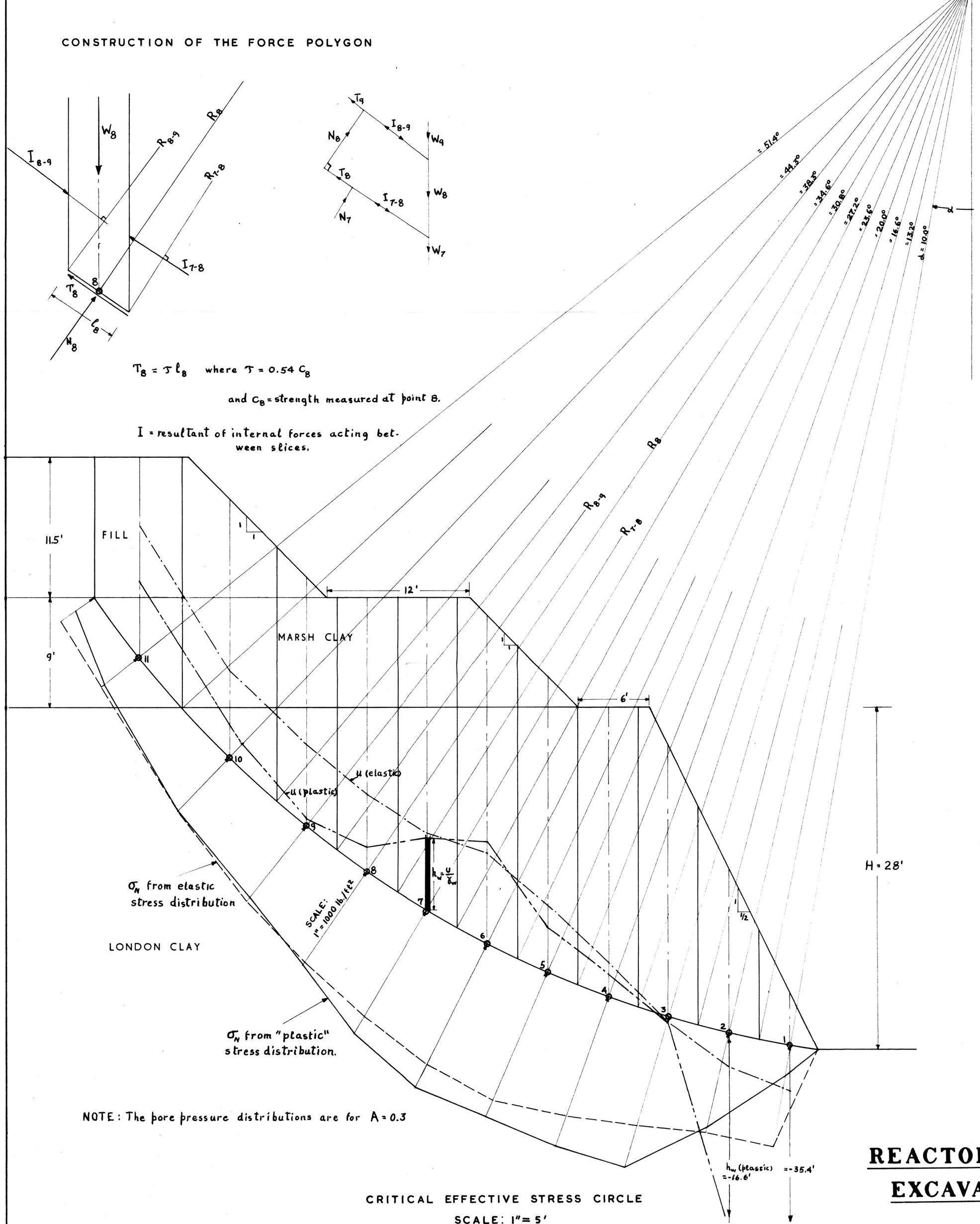
FIG.-39

CONSTRUCTION OF THE FORCE POLYGON

$T_8 = \tau l_8$ where $\tau = 0.54\ C_8$

and C_8 = strength measured at point 8.

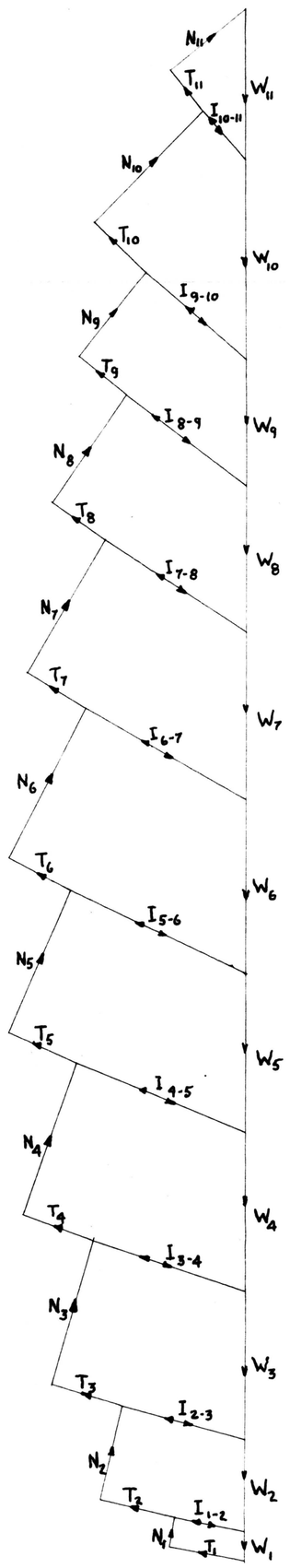
I = resultant of internal forces acting between slices.



NOTE: The pore pressure distributions are for A = 0.3

CRITICAL EFFECTIVE STRESS CIRCLE

SCALE: 1" = 5'



SCALE: 1" = 10,000 lb.

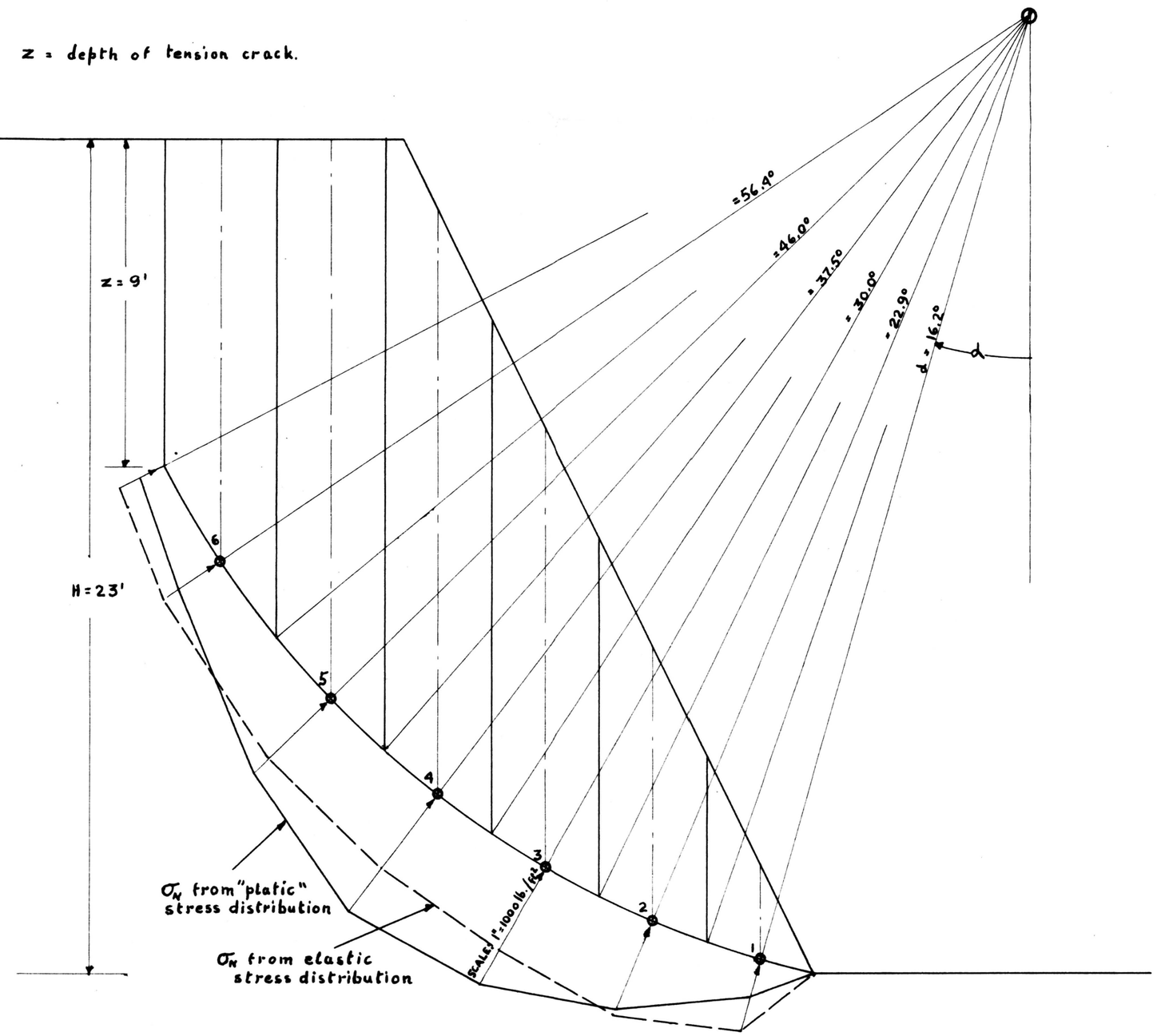
REACTOR HOUSE EXCAVATION

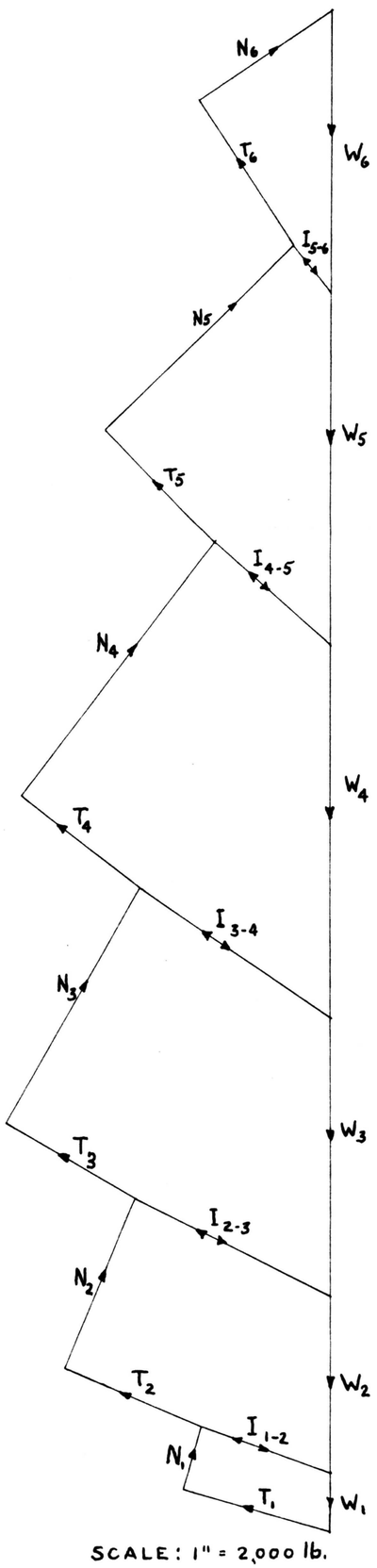
FIG 40

NOTE: The force polygon was constructed as in Fig. 40, with $\tau = 0.35\,c$.

SCALE: 1" = 3'

z = depth of tension crack.





CRITICAL EFFECTIVE STRESS CIRCLE

TURBINE HOUSE EXCAVATION

FIG-41

at any point on this circle for the Reactor House excavation was assumed to be $\tau = 0.54c$ where c is the undrained shear strength of the clay at that point and 0.54 is the reduction factor required for $F = 1.0$ on the particular critical circle used in the effective stress analysis*. This is obviously no more than a rough approximation to the shear stresses since it implies that (0.54 x strength) is developed simultaneously at all points around the slip surface which will only hold good if the strength remains constant after failure.

To find the normal stress at any point on the slip surface, a reasonable assumption is made concerning the direction of internal forces acting across the vertical faces between the slices, and a polygon of forces can then be drawn. In general this will not close, and the internal force has then to be altered in direction until the polygon does close. In fact, it was found that the polygon closed when the internal forces were taken to be parallel to the slip surface at the interface between the slices (Fig.40). Having obtained the normal stresses σ_n in this way, the principal stresses were assumed to be

---

* required shear strength 1060 lb./sq.ft., averaged measured strength 1950 lb./sq.ft., ratio = 0.54.

$$\sigma_1 = \sigma_n + \tau$$

$$\sigma_3 = \sigma_n - \tau$$

The calculation of pore pressures then follows exactly as before, and the results are also given in Table 16. The distribution of the normal stresses around the slip surface as derived by the two methods is plotted in Fig.40 and it will be seen that, except near the toe of the slope, there is remarkably little difference. The distribution of pore pressures, however, does show quite considerable differences, especially near the toe.

The same analysis was carried out for the Turbine House excavation. In this case the shear stress at any point was $\tau = 0.35c$ for the critical circle (Fig.41) and the stresses and pore water pressures are given in Table 17.

Neither method is free from objection. Clearly the stress state at failure must be appreciably different from the elastic theory assumptions, whilst the "plastic" solution is admittedly very approximate. Nevertheless, this method allows an analysis to be made with the assumption that before excavation $\sigma_3' = K_o \sigma_1'$ where $K_o \neq 1$, since the stresses at failure will presumably be

uninfluenced by the initial stresses in this form of calculation.

The results of a "plastic" analysis with $K_o = 2$ are given in Table 18 and they lead to the relation between c' and A given in Fig.38.

3. CONSIDERATIONS ON THE VALUE OF c'

Before considering the significance of these analyses, we must also investigate the Turbine House excavation. As this slope did not fail, the stresses may be at least indicated by the elastic analysis. And there can be little doubt that during the 4½ months in which this slope remained stable there must have been ample opportunity for migration of pore water to the more highly stressed zones. Thus we could take A = 0.5 (as in the slow laboratory tests). The corresponding pore pressures are plotted in Fig.42 and the value of c' must be more than 370 lb./sq.ft. - as found from Fig.39 which has been obtained in exactly the same way as the analogous graphs for the Reactor excavations. But the elastic analysis is based on $K_o = 1$, and if K_o is higher than 1.0 then the required minimum value of c' will be lower, as will be seen by analogy with Fig.38. Perhaps as an

TABLE - 18 -

REACTOR HOUSE EXCAVATION

Pore pressures for the effective stress circle, FIG-40, from plastic stress distribution.

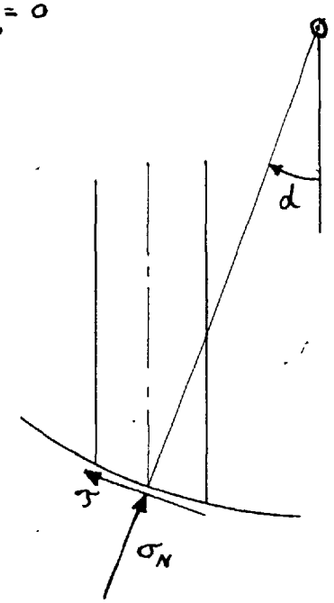
Stresses & pressures in lb./in.² $K_o = 2$

Slice N°	Original			After excavation : $u = u_o + \Delta u$ where $\Delta u = \Delta\sigma_3 + A(\Delta\sigma_1 - \Delta\sigma_3)$								A=.3	A=.6	A=.9
	σ_{v_o}	σ_{h_o}	u_o	σ_v	σ_h	τ_{hv}	$\Delta\sigma_v$	$\Delta\sigma_h$	$\Delta\sigma_1$	$\Delta\sigma_3$	$\Delta\sigma_1 - \Delta\sigma_3$	u	u	u
1	29.5	44.9	14.1	6.9	0.6	8.7	-22.6	-44.5	-19.5	-47.3	27.8	-24.9	-16.4	-8.1
2	28.7	43.6	13.7	15.5	7.4	8.2	-13.2	-36.2	-10.6	-39.0	28.4	-16.7	-8.2	+0.3
3	27.5	42.2	13.0	22.7	13.0	7.4	-4.8	-29.2	-2.8	-31.2	28.4	-9.6	-1.1	+7.5
4	26.2	40.0	12.3	23.7	12.6	6.6	-2.5	-27.4	-0.9	-29.0	28.1	-8.2	+0.3	+8.8
5	24.5	37.6	11.5	24.0	11.8	5.6	-0.5	-25.8	+0.7	-27.0	27.7	-7.1	+1.2	+9.5
6	22.2	34.4	10.5	24.8	12.1	4.5	+2.6	-22.3	+3.2	-23.0	26.2	-4.8	+3.1	+10.8
7	20.4	31.3	9.3	22.8	10.0	3.5	+2.4	-21.3	+3.0	-21.7	24.7	-5.0	+2.4	+9.9
8	17.6	27.2	7.9	19.3	6.9	2.4	+1.7	-20.3	+2.0	-20.6	22.6	-5.9	+0.9	+7.7
9	14.5	22.7	6.3	16.2	4.9	1.2	+1.7	-17.6	+1.8	-17.8	19.6	-5.7	+0.2	+6.1
10	9.9	15.9	3.9	12.8	4.6	0.1	+2.9	-11.3	+2.9	-11.2	14.1	-3.1	+1.2	+5.5
11	3.5	3.5	0.3	8.0	2.6	-0.6	+4.5	-0.9	+4.6	-0.9	5.3	—	+2.7	—
											Average $\bar{u}$ along slip surface	-8.3	-1.2	+6.0

Originally, for K_o condition:

$$\sigma_{h_o} = K_o \sigma'_{v_o} + u_o$$

$$\tau_{hv_o} = 0$$



At failure;

$$\sigma_v = \sigma_N + \tau \cos(90° - 2\alpha)$$

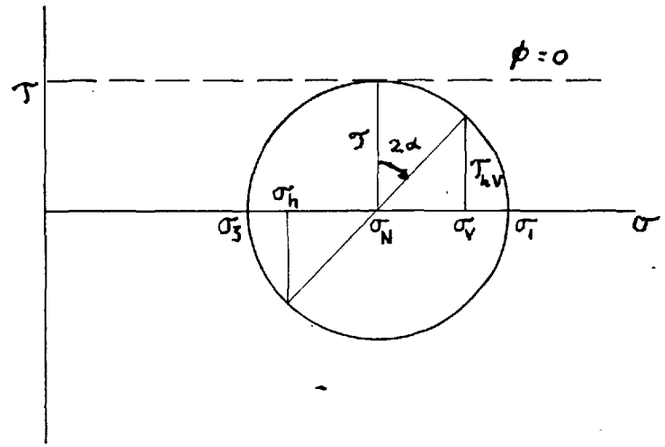
$$\sigma_h = \sigma_N - \tau \cos(90° - 2\alpha)$$

$$\tau_{hv} = \tau \sin(90° - 2\alpha)$$

$$\Delta\sigma_v = \sigma_v - \sigma_{v_o}$$

$$\Delta\sigma_h = \sigma_h - \sigma_{h_o}$$

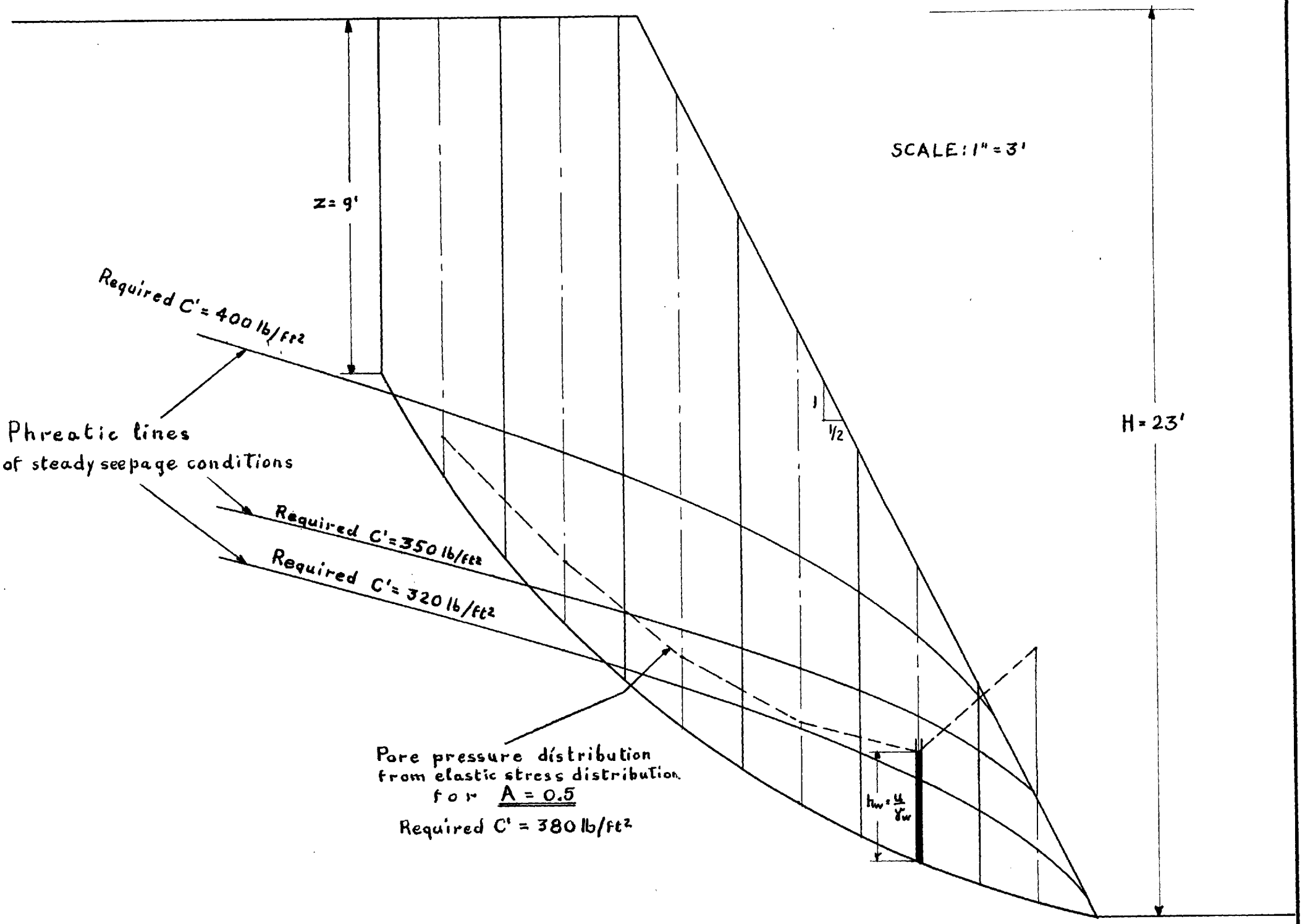
$$\Delta\tau_{hv} = \tau_{hv} - \tau_{hv_o} = \tau_{hv}$$



Hence:

$$\Delta\sigma_1 = \frac{\Delta\sigma_v + \Delta\sigma_h}{2} + \sqrt{\left(\frac{\Delta\sigma_v - \Delta\sigma_h}{2}\right)^2 + \Delta\tau_{hv}}$$

$$\Delta\sigma_3 = \frac{\Delta\sigma_v + \Delta\sigma_h}{2} - \sqrt{\left(\frac{\Delta\sigma_v - \Delta\sigma_h}{2}\right)^2 + \Delta\tau_{hv}}$$



TURBINE HOUSE EXCAVATION

STEADY SEEPAGE

FIG.- 42

extreme case the plastic analysis may give some indication of the lower limit of c', which is about 180 lb./sq.ft. (Fig.39). It is, however, quite possible that the pore pressures after 4½ months would be beginning to approximate to those given by the steady seepage condition. Consequently a "long-term" analysis has been made with various assumptions as to the ground water levels for this condition. These water levels are shown in Fig.42 and for the three different assumptions, which represent a considerable range, the required minimum values of c' are 320, 350 and 400 lb./sq.ft.

It is clearly not possible to give an accurate value for the lower limit of c', but probably this lies closer to the value obtained from the steady seepage case than to the result from the plastic analysis. And, as we have seen, the elastic analysis with $K_o = 1$ also gives a result quite close to the steady seepage case. Possibly c' = 300 is about as close as one could get to a fair estimate of the minimum value. And, obviously, it cannot be greater than the laboratory value of 370 lb./sq.ft.

Now the work on really long-term failures in London Clay indicates that c' decreases with time.

Consequently, if it is correct to say that in the Turbine House excavation c' is unlikely to be less than 300 lb./sq.ft. its value certainly could not be less than this for the Reactor excavation slips, which occurred within a few days or weeks of the cutting being made.

4. PRELIMINARY CONCLUSIONS

It is therefore possible to take 300 and 370 lb./sq.ft. as the probable limits for c' and, for the Reactor slip, the corresponding values of the pore pressure coefficient A, as found from Fig.38, are given in Table 19.

TABLE 19

c'	$K_o = 1$		$K_o = 2$
lb./sq.ft.	Elastic	Plastic	Plastic
370	0.12	0.34	0.64
300	0.02	0.25	0.58
Approximate Mean	0.1	0.3	0.6

Dealing with the elastic case, this could be imagined to apply immediately after an instantaneous

excavation. But the shear strength at the base of Slice No.1, corresponding to A = 0.1*, is about 1400 lb./sq.ft. (and the actual undrained strength is 1340 lb./sq.ft.) whereas the shear stress on the elastic analysis is 2200 lb./sq.ft. Thus the clay in this region is heavily overstressed and a shear failure would at once develop, working progressively back into the slope. This would cause an important redistribution of stresses and the plastic condition would soon be developed. Thus at failure the plastic analysis is appropriate and it is seen that the required value of A lies between 0.3 and 0.6 as K_o varies from 1.0 to 2.0.

Now, in the time interval of several days before the slip occurred some migration of pore water almost certainly would occur, and this would correspond roughly to the 1 to 3 day test value of A = 0.5. Hence, since K_o probably lies between the limits mentioned above, and since the value of A also lies between the corresponding limits of 0.3 and 0.6, it may be concluded that the Reactor slip is consistent with the following conditions,

c' between 300 and 370 lb./sq.ft.

A between 0.3 and 0.6

K_o between 1.0 and 2.0

---

* at this point, u = -1110 lb./sq.ft. and σ_n = 1700 lb./sq.ft.

MORE DETAILED CONCLUSIONS

The problem can be investigated in more detail, by taking into account the actual strength of the clay around the slip surface. From a total stress analysis of the Reactor House excavation (Slip I) it has been found that the average strength of the London Clay along the effective stress slip circle is 1060 lb./sq.ft. And this must, in fact, be the actual shear stress, or strength along this circle.

Now, in the plastic analysis, the average normal total stress $\bar{\sigma}_n$ on the slip at failure, in the London Clay, is 1900 lb./sq.ft. This is independent of K_o and is obtained simply by summing the normal forces and dividing by the length of the area in the London Clay. Similarly the average pore pressure $\bar{u}$ acting on this arc can be found, although this will depend on K_o and A.

The relations between $\bar{u}$ and A for the two cases $K_o = 1$ and $K_o = 2$ are plotted in Fig.43.

However, for F = 1, there is only one value of A for a particular value of c' and K_o, as shown in Table 19. Hence the average strength in the London Clay can be calculated as follows.

(i) c' = 370 lb./sq.ft. $K_o = 1$ A = 0.34

from Fig.43 $\bar{u}$ = - 0.03 lb./sq.in. = -40 lb./sq.ft.

But $S = c' + (\bar{\sigma}_n - \bar{u}) \tan \phi'$

$\therefore S = 370 + (1900 + 40) \times 0.364 =$ 1075 lb./sq.ft.

(ii) c' = 300 $K_o = 1$ A = 0.25

$\bar{u}$ = -1.6 lb./sq.in. = - 230 lb./sq.ft.

S = 300 + (1900 + 230) x 0.364 = 1075 lb./sq.ft.

(iii) c' = 370 $K_o = 2$ A = 0.64

$\bar{u}$ = - 0.02 lb./sq.in. = -30 lb./sq.ft.

S = 370 + (1900 + 30) x 0.364 = 1070 lb./sq.ft.

(iv) c' = 300 $K_o = 2$ A = 0.58

$\bar{u}$ = - 1.7 lb./sq.in. = -240 lb./sq.ft.

S = 300 + (1900 + 240) x 0.364 = 1080 lb./sq.ft.

These are all in agreement with each other, and with the known strength of 1060 lb./sq.ft. - thus providing a good check on the calculations.

The strength of 1060 lb./sq.ft. is 54% of the measured (15 minute) undrained test strength of 1950 lb./sq.ft. Part of this loss of strength will be due to fissures. As an indication of this effect the well known difference between unconfined and triaxial strengths of London Clay may be quoted. The best sets of such tests are from Chingford (Glossop 1948, 50 tests) and from Walton (Golder and Skempton 1948, 200 tests). The results are summarised in Table 20.

TABLE 20

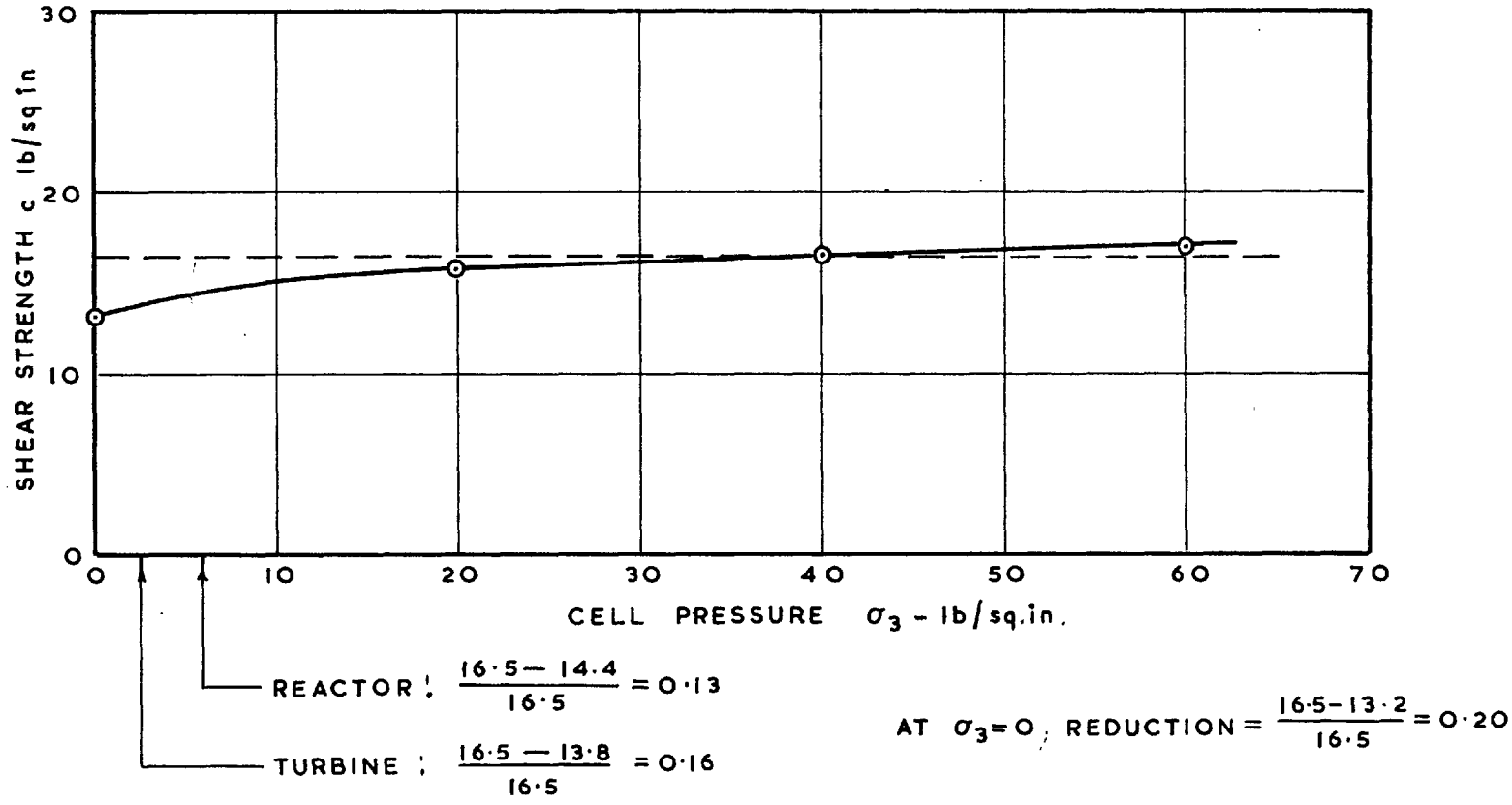
Cell pressure lb./sq.in.	$\frac{1}{2}(\sigma_1-\sigma_3)$ - lb./sq.in.	
	Chingford	Walton
0	13.2	13.2
20	15.8	15.9
40	16.5	16.5
60	17.1	17.0

These are plotted in Fig.44. For the Reactor slope the average value of σ_3 after excavation is about 6 lb./sq.in. and for the Turbine House the figure is 2.4 lb./sq.in. These correspond to a reduction in strength of about 15 per cent below the average of the triaxial test results. This is not an accurate means of assessing the mechanical weakening due to fissures, but may be, for lack of anything better, taken as measure of this effect.

Thus, the strength of the fissured clay can be assumed to be about 0.85 x 1950 = 1650 lb./sq.ft. But the actual strength on the slip surface is 1060 lb./sq.ft., which is 64 per cent of the "fissured strength". This further reduction of 36 per cent is probably due to migration of water into the narrow slip zone.

If no migration had occurred the strength would be 1650 lb./sq.ft. and the pore pressures would correspond to those deduced from the 15 minute laboratory tests, for which we know that $A = 0.2$. But an average strength of 1650 lb./sq.ft. must be associated with a definite average pore pressure $\bar{u}$ on the slip surface, as given by the equation

$$S = \eta c' + (\bar{\sigma}_n - \bar{u}) \tan \phi'$$



RELATION BETWEEN c & σ_3 IN UNDRAINED TESTS ON LONDON CLAY FROM CHINGFORD & WALTON

(TOTAL OF 250 SAMPLES)

FIG 44

where η = the reduction coefficient for fissure (=0.85)

$\therefore$ 1650 = 0.85 x 370 + (1900 - $\bar{u}$) 0.364

$\therefore$ (1900 - u) x 364 = 1650 - 315

$\therefore$ $\bar{u}$ = -1770 lb./sq.ft. = <u>-12.3 lb./sq.in.</u>

Thus we have A = 0.2 and $\bar{u}$ = -12.3 lb./sq.in., and these values give a point in Fig.43 which has been plotted as a double circle. The corresponding value of K_o is roughly 2.2 (which is not inconsistent with the swelling tests). The two lines for K_o = 1 and K_o = 2, Fig.43, converge to a point. Another line has then been drawn through the A = 0.2, $\bar{u}$ = -12.3 lb./sq.in. point to converge to the same point as K_o = 1 and K_o = 2 lines. This new line gives the relation for K_o = 2.2.

But for c' = 315 lb./sq.ft. the average pore pressure, for a strength of 1060 lb./sq.ft. must be given by the equation

$$1060 = 315 + (1900 - \bar{u}) \times 0.364$$

or $\bar{u}$ = -150 lb./sq.ft. = -1.0 lb./sq.in.

Hence from the $K_o \approx 2.2$ line the value of A = 0.64. This is only slightly higher than the value of A determined from the 1 to 3 day tests where, as previously mentioned, considerable migration of pore water is known to have occurred.

CONCLUSIONS

The foregoing deductions may be summarised as follows.

(i) The average shear strength as measured in undrained triaxial tests without open fissures is 1950 lb./sq.ft.

(ii) With very small values of σ_3 after the excavation has been made, some fissures will open up, and the average strength will fall to 1650 lb./sq.ft. At this stage A = 0.2 and the average pore pressure is - 12.3 lb./sq.in.

(iii) Migration of pore water will at once commence, and at the time of failure, the average pore pressure will be - 1.0 lb./sq.in. with a corresponding average shear strength of 1060 lb./sq.ft. and A = 0.64. And this strength is 54% of the triaxial strength, as found in the total stress analysis.

Finally, it may be added that, in the course

of time, had a slip not occurred, the pore pressure would become equal to the steady seepage value and a further reduction in strength would take place. Moreover, there is evidence that on a long time scale c' decreases still further.

The most striking point revealed by the analyses is the rapid drop in strength of the clay, and this seems to be due to a rapid decrease in negative pore pressures in the slip zone, associated with a migration of pore water into this zone. The speed of this process is probably increased by the presence of fissures, and the fissures themselves also lead to a mechanical weakening of the clay. But it is at least an open question as to whether the decrease in negative pore pressures may not occur quite rapidly in a non-fissured over-consolidated clay. No field case of end-of-construction failure in such a clay has been investigated. Yet there seems to be no reason why a considerable reduction in strength should not occur within a few days or weeks.

If this is correct then a reduction factor will have to be applied to the $\emptyset = 0$ analysis of short-term stability in all over-consolidated clays, although this

will almost certainly be a bigger reduction for fissured than for intact clays of this category.

APPENDIX A

All the test results used in the present research problem are tabulated as follows:

Table A-1: Undrained tests (Series I)

(i) London clay at surface (Wimpey)

(ii) Marsh clay at surface (Wimpey)

(iii) London clay at surface (Simon-Carves)

Table A-2: Sampling Data.

Table A-3: Undrained tests (Series II).

Table A-4: Undrained tests (Series III).

Table A-5: Undrained tests (Series IV and V).

Table A-6: Drained triaxial tests.

Table A-7: Drained shear box tests.

Table A-8: Consolidated-undrained tests.

TABLE - A1

UNDRAINED TESTS

SERIES 1

i) London Clay at Surface (Wimpey)

Bore Hole	Depth of Sample ft.	Consistency			Strength lbs/sq.ft.	
		W	LL	PL	4" specimen	1.5" specimen
F-14/2.	10-11.5	35	94	31	1250	1000
	20-21.5	32	96	32	1950	"
	30-31.5	32	98	32	1800	3100
	40-41.5	31	93	34	2700	"
	70-71.5	30	84	27	3400	"
F-16	15-16.5	35	99	30	1350	"
G-13	15-16.5	34	101	33	1600	"
	25-26.5	33	95	32	1900	"
G-16	10-11.5	35	95	31	900	1400
	15-16.5	34	"	"	1550	"
	25-26.5	33	"	"	2200	"
	30-31.5	32	95	32	2300	2500
	52-53.5	31	95	31	2000	"
	72-73.5	33	95	29	2750	"
H-12	15-16.5	34	"	"	1700	"
	25-26.5	33	"	"	2600	"
J-11	4.5-6	36	95	30	900	"
	15-16.5	32	96	29	1700	"
	20-21.5	32	96	29	1900	"
	25-26.5	33	95	30	2250	"
J-13	6-7.5	34	93	31	950	"
	16-17.5	32	97	28	1650	"
	26-27.5	32	104	27	2900	"
	30-31.5	32	97	27	2650	"
	40-41.5	31	"	"	2700	"

TABLE - A1 (continued)

Bore Hole	Depth of Sample ft.	Consistency			Strength lbs/sq.ft.	
		W	LL	PL	4" specimen	1.5" specimen
J-15	15-16.5	34	-	-	1650	-
	25-26.5	32	-	-	1950	-
	40-41.5	31	-	-	3500	-
	60-61.5	28	91	28	3000	-
	78.5-80	30	96	30	4000	-
J-17	9-10.5	35	97	31	950	-
	30-31.5	32	-	-	1700	-
K-9	6-7.5	33	89	29	1250	-
	20-21.5	32	95	32	2150	-
K-13	15-16.5	33	94	29	1850	-
	20-21.5	32	-	-	1900	-
	25-26.5	32	94	34	3350	-
K-17	10-11.5	34	-	-	1400	-
	20-21.5	33	-	-	1650	-
L-15	15-16.5	33	-	-	2100	-

ii) Marsh Clay at Surface. (Wimpey)

Bore Hole	Thickness of Marsh Clay ft.	Depth beneath Marsh Clay ft.	Consistency			Strength lbs/sq.ft.	
			W	LL	PL	4" specimen	1.5" specimen
B-10	10	0-1.5	35	-	-	950	-
		15-16.5	31	95	29	1850	-
B-12	10	1-2.5	37	93	31	950	-
		10-11.5	-	107	29	1600	-
		19-20.5	33	100	32	2000	-
B-14	9.5	9.5-11	34	93	29	1350	-
		29.5-31	33	95	26	1700	-

TABLE - A1 (continued)

Bore Hole	Thickness of Marsh Clay ft.	Depth beneath Marsh Clay ft.	Consistency			Strength lbs/sq.ft.	
			W	LL	PL	4" specimen	1.5" specimen
B-16	8.5	11.5-13	32	92	27	2500	-
		31-32.5	31	100	27	3000	-
C-11	8.5	6.5-8	31	-	-	1400	-
C-15	7	8-9.5	34	93	29	1550	-
D-8	7.5	2.5-4	36	-	-	1050	-
		12.5-14	34	99	31	1800	-
		22.5-24	31	100	32	2300	-
D-10	7.5	2.5-4	36	96	31	950	-
D-13	8	8-9	34	92	29	1250	-
		9-10.5	34	92	30	1450	-
		16.5-18	34	91	30	1350	-
		27-28.5	31	98	30	2200	-
		37-38	32	-	-	2300	-
		57-58	29	-	-	2800	-
		67-68.5	30	-	-	3650	-
D-14	7	8-9.5	33	95	31	1650	-
D-16	7	8-9.5	34	96	26	1500	-
D-12	10.5	0.5-2	36	95	23	-	1500
		4.5-6	33	-	-	-	2150
		9.5-11	33	98	29	-	2600
		19.5-21	32	98	29	-	2900
		29.5-31	31	-	-	-	3300
		39.5-41	30	90	27	-	3750
		49.5-51	29	-	-	-	4000
		59.5-61	29	89	26	-	4400
E-11	7.5	0.5-2	36	93	27	700	-
E-13	6	19-20.5	34	100	32	2200	-

TABLE - A1 (continued)

Bore Hole	Thickness of Marsh Clay ft.	Depth beneath Marsh Clay ft.	Consistency			Strength lbs/sq.ft.	
			W	LL	PL	4" specimen	1.5" specimen
F-8	6.5	2.5-4	36	90	31	850	-
		8.5-10	33	-	-	1650	-
		13.5-15	33	94	29	1650	-
		23.5-25	32	-	-	2400	-
F-10	8	1-2.5	37	92	30	850	-
		17-18.5	32	101	30	1900	-
F-12	7.5	12.5-14	33	95	31	1900	-
		22.5-24	33	-	-	2000	-
		32.5-34	31	95	28	2750	-

iii.) London Clay at Surface (Simon-Carves)
(Tests on 1.5" specimen)

Bore Hole	Depth below Surface ft.	Consistency			Cell Pressure lb/sq.in.	Strength lb/sq.ft.	Strength at over-burden pressure lb/sq.ft.
		W	LL	PL			
K-9/2	32-32.5	30	95	31	0	2497	
					30	2595	2580
					60	2693	
	42-43.5	30	102	35	0	3035	
					30	2693	2800
					60	2644	
	52-53.5	30	100	35	20	2790	
					40	1725	2300
					60	2387	
	62-63.5	30	98	35	20	3231	
					40	2693	3300
					60	3734	
	72-73.5	29	100	34	20	2693	
					40	3244	3700
					60	3611	

TABLE - A1 (continued)

Bore Hole	Depth below Surface ft.	Consistency			Cell Pressure lb/sq.in.	Strength lb/sq.ft.	Strength at over-burden pressure lb/sq.ft.
		W	LL	PL			
K-9/2	82-83.5	29	94	34	20 40 60	4847 5509 6120	6350
	92-93.5	28.5	100	33	20 40 60	3977 4529 3402	4000
K-13/2	22-23.5	33	98	31	0 30 60	1792 2179 2520	2020
	32-32.5	33	105	34	0 30 60	2700 3060 3770	3120
	42-43.5	32	98	32	0 30 60	1564 3716 2399	2800
	52-53.5	30	105	34	0 30 60	1898 2153 2986	2600
	62-63.5	30	98	31	0 30 60	2962 3281 3158	3500
	72-73.5	29	88	29	0 30 60	4774 5019 5164	5150
	82-83.5	29	102	30	0 30 60	4344 4308 4946	4800

TABLE A-2

Sampling Data

Type of Sample	Nº	Date of Sampling	Site	Grid Reference	Elev O. D.	Depth below surface ft	Thickness of Marsh clay ft	Depth beneath marsh-clay ft.	Total over-burden pressure p.s.i	Consistency		
										W	LL	PL
TUBE	(A)	3/10/57	Pump house	C-9	-7·51	12·5	10·4	2·1	9·8	35·5	93	31
"	(B)	"	"	"	-12·03	17·0	"	6·6	13·6	33·5	91	32
"	(C)	"	"	"	-13·77	18·8	"	8·4	15·1	33·5	94	32
"	(D)	"	"	"	-16·55	21·5	"	11·1	17·3	33·0	95	33
TUBE	1	28/11/57	"	D-10	-18·0	23·0	10·5	12·5	17·9	32·0	93	30
BLOCK	1	"	"	"	"	"	"	"	"	"	"	"
TUBE	2	"	"	"	-14·5	19·5	"	9·0	15·0	33·0	93	30
BLOCK	2	"	"	"	"	"	"	"	"	"	92	30
BLOCK	3	18/3/58	"	"	-19·0	24·0	10·5	13·5	19·2	33·0	-	-
BLOCK	4	"	"	"	-20·0	25·0	"	14·5	20·0	33·0	-	-
BLOCK	5	7/4/59	Cooling Pond	G-15	-1·5	8·5	0·0	—	7·1	33·0	95	31
BLOCK	6	"	"	"	"	"	"	—	"	33·0	"	"
TUBE	5	"	"	"	"	"	"	—	"	35·0	95	31
TUBE	6	"	"	"	"	"	"	—	"	36·0	"	"
TUBE	7	"	"	"	"	"	"	—	"			
BLOCK	7	22/4/59	"	"	-12·0	18·5	0·0	—	15·4	33·0	95	33
BLOCK	8	"	"	"	"	"	"	—	"	"	"	"

TABLE A-3

Undrained tests SERIES II

Tube Nº	Test Nº	Method of preparation of sample	Depth below surface	Consistency W	Consistency LL	Consistency PL	% W.C. after test	γ lbs/ft^3	% strain at failure	E lbs/in^2	σ_3 p.s.i.	$(\sigma_1-\sigma_3)$ at failure p.s.i.	Rubber membrane correction p.s.i	$(\sigma_1-\sigma_3)$ corrected p.s.i	Average $(\sigma_1-\sigma_3)$ corrected p.s.i	Average Cu lbs/ft^2
A	U-1	Jacked	12·5'	35·5	93	31	34·1	119·8	4·7	1140	10·0	18·8	1·1	17·7		
A	U-2	"	"	"	"	"	35·0	122·5	6·8	1050	"	16·6	1·2	15·4	16·0	1150
A	U-3	"	"	"	"	"	34·4	118·0	7·4	680	"	16·2	1·2	15·0		
A	U-4	Trimmed	"	"	"	"	34·6	119·0	3·3	830	"	12·2	1·0	11·2	11·5	830
A	U-5	"	"	"	"	"	34·6	119·0	3·1	880	"	12·8	1·0	11·8		
B	U-6	Jacked	17·0'	33·5	91	32	33·1	121·0	4·8	1420	14·0	22·8	1·2	21·6		
B	U-7	"	"	"	"	"	33·2	120·2	4·8	1200	"	20·6	1·2	19·4	19·3	1390
B	U-8	"	"	"	"	"	33·0	121·2	6·7	1220	"	18·1	1·3	16·8		
B	U-9	Trimmed	"	"	"	"	33·1	119·3	3·5	1500	"	17·0	1·1	15·9	15·8	1140
B	U-10	"	"	"	"	"	32·1	119·8	2·6	1160	"	16·7	1·0	15·7		
C	U-11	Jacked	18·8	33·4	94	32	32·9	120·2	4·2	1640	15·0	17·8	1·1	16·7		
C	U-12	"	"	"	"	"	33·6	121·8	7·0	920	30·0	27·7	1·4	26·3	21·2	1530
C	U-13	"	"	"	"	"	33·4	120·0	5·5	960	60·0	22·0	1·3	20·7		
C	U-14	Trimmed	"	"	"	"	33·2	119·8	4·2	2000	60·0	22·1	1·2	20·9	18·9	1360
C	U-15	"	"	"	"	"	33·3	120·0	3·0	2200	15·0	18·0	1·1	16·9		
D	U-16	Jacked	21·5'	33·0	95	33	32·5	123·6	5·0	1180	17·0	25·6	1·2	24·4		
D	U-17	"	"	"	"	"	32·4	121·0	5·5	1000	"	26·0	1·3	24·7	23·1	1660
D	U-18	"	"	"	"	"	32·4	122·0	2·7	1480	"	21·3	1·1	20·2		
D	U-19	Trimmed	"	"	"	"	31·1	121·0	4·0	1640	"	25·0	1·2	23·8	22·6	1630
D	U-20	"	"	"	"	"	32·1	120·5	3·3	1260	"	22·6	1·1	21·5		

TABLE A -4

Undrained tests SERIES III

Sample Nº	Test Nº	Consistency.			% W.C after test.	γ lbs/ft^3	% strain at failure	E lbs/in^2	σ_3 p.s.i	$(\sigma_1 - \sigma_3)_f$ p.s.i.	R.M. Correction p.s.i	$(\sigma_1 - \sigma_3)$ correction p.s.i
		W	L L	P L								
BLOCK-3	U - 59	33	—	—	33·1	120·0	4·5	2170	8·0	20·4	1·0	19·4
"	U - 60	"	—	—	33·3	120·0	3·2	3100	8·0	24·5	0·9	23·6
"	U - 61	"	—	—	32·3	119·5	3·8	2750	8·0	23·7	1·0	22·7
"	U - 62	"	—	—	33·9	119·5	4·0	2900	8·0	24·5	1·0	28·5
"	U - 63	"	—	—	33·1	—	7·0	2400	8·0	23·7	1·2	22·5
"	U - 64	"	—	—	33·1	119·5	7·0	2130	8·0	23·4	1·2	22·2
"	U - 65	"	—	—	32·4	120·0	5·0	2300	8·0	23·6	0·9	22·7
"	U - 66	"	—	—	32·4	120·5	4·6	2180	8·0	18·4	1·0	17·4
"	U - 67	"	—	—	34·6	—	·9	3600	4·0	18·0	0·7	17·3
"	U - 68	"	—	—	33·2	—	1·7	2600	4·0	20·2	0·8	19·4
"	U - 69	"	—	—	35·0	—	1·7	1800	4·0	26·2	0·8	25·4
"	U - 70	"	—	—	31·0	120·5	1·5	2500	2·0	22·5	0·7	21·8
"	U - 71	"	—	—	31·0	120·5	2·3	1750	2·0	26·8	0·8	26·0
"	U - 72	"	—	—	31·4	—	4·0	1800	2·0	26·2	0·9	25·3

TABLE A-5

Undrained tests (TUBE No.6) SERIES IV

Test Nº	Size of Sample	Preparation of Sample	W	LL	PL	% W.C. after test	γ lbs/in²	% ϵ at failure	E lbs/in²	σ_3 p.s.i	$(\sigma_1-\sigma_3)_f$ p.s.i	R.M. correction p.s.i	$(\sigma_1-\sigma_3)_{cr}$ p.s.i
U-73	4"	from tube	36·0	95	31	36·5	—	12·5	3000	7·0	15·6	0·2	15·4
U-74	1½"	Trimmed from U-73	"	"	"	35·3	120·0	6·7	2400	—	15·2	1·1	14·1
U-75	"	"	"	"	"	36·6	120·0	10·0	1640	—	15·9	1·3	14·6
U-76	"	"	"	"	"	35·7	120·0	9·0	2000	—	17·0	1·3	15·7
U-77	"	Trimmed from tube	"	"	"	34·2	120·0	10·0	2560	—	19·5	1·3	18·2
U-78	"	"	"	"	"	33·0	—	10·0	2320	—	21·0	1·3	19·7

Undrained tests (BLOCK No 7) SERIES V

Test Nº	Consistency			Ends	Plane	γ lbs/ft³	E lbs/in²	% ϵ at failure	σ_3 p.s.i	$(\sigma_1-\sigma_3)_f$ p.s.i	R.M. correction	$(\sigma_1-\sigma_3)$ correction p.s.i.
	W	LL	PL									
U-79	33	95	33	32·8	32·8	121·5	1800	3·7	15·0	19·9	1·1	18·8
U-80	"	"	"	34·0	32·8	—	2750	3·8	"	26·4	1·1	25·3
U-81	"	"	"	32·4	32·9	121·5	2580	4·8	"	26·4	1·2	25·2
U-82	"	"	"	33·0	33·0	121·5	2250	3·6	"	21·2	1·1	20·1

TABLE A-6
DRAINED TRIAXIAL TESTS

Test No	Sample No	Consolidation C. pressure	MOISTURE CONTENT before test	MOISTURE CONTENT after test: Base	Top	Plane	% ϵ_f	$(\sigma_1-\sigma_3)_f$ p.s.i	Rate of Testing in/min.	Time at Failure. DAYS.	Correction D+R.M. p.s.i	$(\sigma_1-\sigma_3)_{cor}$ p.s.i	$\left(\frac{\Delta V}{V_1}\right)$ during consolidation	$\left(\frac{\Delta V}{V_0}\right)$ during shear.
D-1	BLOCK-1	15	32·0	32·2	32·7	32·3	5·6	29·5	·000025	4·0	2·1	27·4	+·005	-·014
D-2	"	30	33·4	31·3	31·6	30·9	3·5	42·8	·00005	3·0	2·1	40·7	-·015	-·021
D-3	"	60	32·7	29·9	29·7	31·1	5·0	84·2	"	3·0	2·2	82·0	-·037	-·022
D-4	"	15	32·0	32·3	32·0	32·4	3·0	26·3	"	2·0	2·0	24·3	-·006	-·015
D-5	"	45	31·7	31·0	31·0	30·2	7·0	52·0	"	3·2	2·2	49·8	-·042	-·021
D-6	"	75	32·0	29·3	29·4	29·0	7·0	95·5	"	3·2	2·2	93·3	-·065	-·025
D-7	"	90	32·0	29·0	28·7	29·7	5·6	111·0	"	3·1	2·2	108·8	-·067	-·027
Blocks-No 5 + No 6														
D-8	BLOCK-5	20	32·6	31·6	30·6	30·6	7·0	30·3	·00005	3·4	2·2	28·1	-·017	-·028
D-9	"	40	32·9	—	—	—	7·0	46·5	"	3·0	2·2	44·3	-·052	-·026
D-10	"	60	32·7	28·1	27·7	27·1	6·1	68·8	"	3·2	2·2	66·6	—	—
D-11	"	30	33·2	30·0	29·7	29·6	5·2	35·0	"	4·0	2·2	32·8	—	—
D-12	"	70	33·0	27·5	27·3	27·2	7·0	81·6	"	4·5	2·2	79·4	-·071	-·021
D-13	BLOCK-6	10	32·1	32·5	32·4	32·9	5·8	19·4	·000013	11·0	2·0	17·4	+·005	-·016
D-14	"	15	32·3	32·2	31·8	32·9	7·0	27·5	·00005	5·0	2·1	25·4	-·001	-·020
Block-No 7														
D-15	BLOCK-7	15	32·4	32·8	32·4	34·4	4·0	29·5	·000025	4·4	2·0	27·5	·000	-·020
D-16	"	7	32·5	33·2	35·3	32·8	3·0	19·5	·000014	6·0	1·8	17·7	+·021	-·007
D-17	"	60	31·4	30·4	29·9	29·0	7·0	75·9	·000050	4·8	2·2	73·7	-·051	-·027
D-19	"	45	33·0	29·9	33·4	28·9	5·2	65·0	·000050	3·3	2·2	62·8	-·032	-·022

TABLE A-7

Drained Shear Box Tests.

(RATE OF STRAIN = ·000038 in/min)

Test Nº	Sample Nº	Normal Pressure p.s.i	WATER CONTENT			Displacement at Failure I N.	Shear Strength p.s.i	Time at failure (days)
			Before test.	after test.				
				Ends	Plane			
1	Tube 5	20·0	35·4	33·8	35·1	·037	9·5	1·5
2	"	40·0	33·6	31·2	31·3	·050	15·3	2·2
3	"	60·0	32·0	31·7	31·0	·055	26·0	3·0
4	"	30	35·0	33·3	33·3	·043	13·0	1·7
5	"	50	36·6	33·7	33·6	·050	17·3	2·2
7	Block 5	40	33·7	30·9	30·4	·061	16·5	2·5
8	"	60	33·0	29·5	29·3	·062	22·6	3·0
10	" (vertical)	20	32·6	33·0	33·0	·030	9·6	1·5
11	" (")	40	32·5	32·4	31·6	·048	16·8	2·5
12	" (")	60	32·3	30·3	29·8	·070	21·9	3·2

TABLE A -8

Consolidated-undrained tests

Test No	Sample No	Moisture Content before test	Moisture Content after test base	Moisture Content after test top	Moisture Content after test plane	consolidation pressure. p.s.i.	cell pressure. σ_3 p.s.i.	back pressure. p_6 p.s.i.	U_f p.s.i. base	U_f p.s.i. probe	$(\sigma_1-\sigma_3)_f$ p.s.i.	% strain at failure	Rate of strain in/min	Time of failure	Drainage & rubber membrane corr. p.s.i.	$(\sigma_1-\sigma_3)$ corrected p.s.i.	σ'_3 measured base	σ'_3 measured probe	σ'_1 measured base	σ'_1 measured probe	A_f measured base	A_f measured probe	A_{f_1}	A_{f_2}
CU-4	Block-6	31·3	31·1	31·0	30·6	30	60	30	469	-	31·3	4·7	·015	20min	-2·4	28·9	13·1	-	42·0	-	·59	-	·29	·28
CU-5	"	31·4	31·4	30·9	31·3	"	"	"	461	-	28·5	5·2	·00025	12hrs	-2·3	26·2	13·9	-	40·1	-	·61	-	·42	·45
CU-6	"	31·6	31·3	30·8	31·4	"	"	"	425	-	27·6	5·3	·00005	2·7days	-2·3	25·3	17·5	-	42·8	-	·49	-	·47	·50
CU-7	"	32·7	32·3	29·9	31·6	"	"	"	429	-	27·6	4·0	"	2·2 "	-2·2	25·4	17·1	-	42·5	-	·51	-	·47	·50
CU-8	"	33·4	31·6	31·6	30·9	"	"	"	424	-	29·0	6·0	"	3·0 "	-2·3	26·7	17·6	-	44·3	-	·46	-	·40	·43
CU-9	"	32·6	31·7	29·8	32·0	"	"	"	463	-	24·8	4·6	·000025	5·0 "	-2·2	22·6	13·7	-	36·3	-	(·72)	-	-	-
CU-10	"	31·8	31·5	29·8	33·0	"	"	"	425	-	27·0	7·8	dead loading ·0000125	8·0 "	-2·4	24·6	17·5	-	42·1	-	·51	-	·52	·54
CU-11	Block 7	32·7	32·6	33·1	33·9	15	30	15	260	-	17·6	1·7	·00005	1day	-1·8	15·8	5·0	-	20·8	-	·63	-	·61	·43
CU-12	"	32·3	31·4	31·0	31·0	30	45	15	337	-	29·2	2·5	·00008	1 "	-2·0	27·2	11·3	-	38·5	-	·69	-	·52	·40
CU-13	"	32·4	32·5	32·8	36·4	30	45·2	15·2	330	322	30·0	2·4	dead load	3 "	-2·0	28·0	12·2	13·0	40·0	41·0	·64	·61	·48	·36
CU-14	"	32·2	32·4	32·4	33·3	30	45	15	322	322	32·2	3·1	·0005	5hrs	-2·0	30·2	12·8	12·8	43·0	43·0	·57	·57	·38	·27
CU-15	"	33·5	34·8	32·9	33·9	30	60	30	483	468	27·1	2·8	"	"	-1·1	26·0	11·7	13·2	37·7	39·2	·70	·65	·58	·46
CU-16	"	32·8	31·2	31·3	31·5	45	75	30	566	-	44·9	2·8	"	7hrs	-2·1	42·8	18·4	-	61·2	-	·62	-	·35	·26
CU-17	"	32·8	30·7	29·7	30·1	60	90	30	633	-	54·6	2·4	"	"	-2·3	52·3	26·7	-	79·0	-	·64	-	·40	·32
CU-18	Block 8	33·6	31·0	31·3	30·9	60	60	-	-	-	52·6	6·4	·015	15min	-2·8	49·8	-	-	-	-	-	-	·47	·39
CU-19	"	33·4	31·1	31·6	33·0	45	45	-	-	-	46·7	3·3	"	"	-2·3	44·4	-	-	-	-	-	-	·30	·21
CU-20	"	32·9	33·2	33·8	33·2	15	15	-	-	-	22·5	2·4	"	"	-1·7	20·8	-	-	-	-	-	-	·24	·10
CU-21	"	35·2	33·4	32·5	33·1	30	30	-	-	-	36·1	3·8	"	"	-2·0	34·1	-	-	-	-	-	-	·23	·12
CU-22	"	32·4	30·6	33·8	31·4	60	60	-	-	-	65·7	3·0	"	"	-2·3	63·4	-	-	-	-	-	-	·17	·10

Note (1.) A_{f_1} is obtained by fitting the circles to the drained envelopes of the individual block.
(2.) A_{f_2} is obtained by fitting the circles to the average drained envelope ($c = 370$ lbs/sqft $\phi' = 20°$)

APPENDIX B

RUBBER MEMBRANE, DRAIN AND AREA CORRECTION FOR SHEAR PLANE FAILURE

Failure of a sample of over-consolidated fissured clay tested in the triaxial apparatus usually occurs on a well defined shear plane. Visual observation shows that this mode of failure effects a severe local deformation on the rubber membrane and the filter paper drain. The load taken by the membrane and drain under this condition is difficult to estimate and no satisfactory analysis has yet been proposed, mainly due to the complexity of the problem.

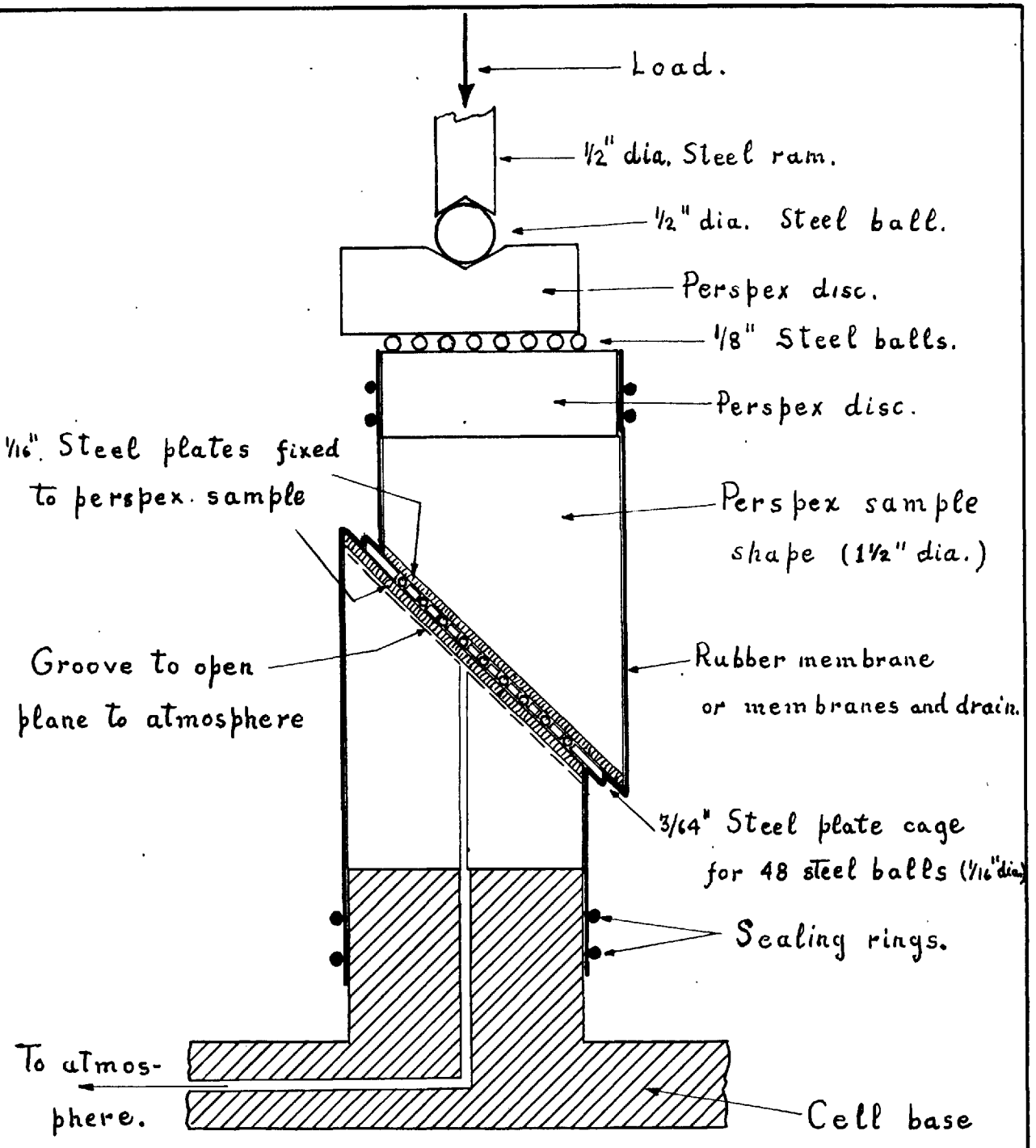
RUBBER MEMBRANE CORRECTION

Some investigations have shown (Triaxial Shear Report, 1947) that a membrane 0.4 mm. thick caused an increase of 2.5 p.s.i. in the deviator stress, irrespective of the cell pressure. This conclusion was based on a comparison between the unconfined and consolidated undrained strengths of samples of a remoulded soft clay which failed on a well defined shear plane. Such an investigation on undisturbed samples of over-consolidated fissured clay is

impracticable due to the scattering of results, especially in the unconfined test.

DeLory (1957) has circumvented the problem of scattering in test results on undisturbed samples by performing tests on a perspex cylinder shaped like a soil sample with a cut across the cylinder, through the centre at an angle of 45° to the horizontal to simulate the shear plane. He lubricated the plane with heavy machine grease to minimize friction and set up the sample in a triaxial cell with one rubber membrane and noted the load required for deformation. The sample was then returned to its original position, enclosed by two membranes, and reloaded. The correction for one membrane was taken as the difference between the two loads. Several runs were made and the results averaged. This process was carried out at cell pressures of 5, 10 and 20 p.s.i.

In the course of the present research, DeLory's tests were repeated using a modified version of the perspex sample (Fig.B-1). Steel balls mounted in a cage were placed on the plane between two steel plates fastened to the perspex sample. Three small holes were drilled in the lower plate to open the plane to the atmosphere. Steel



ARRANGEMENT FOR DETERMINING RUBBER MEMBRANE AND DRAIN CORRECTION FOR FAILURE ON A PLANE

FIG.- B1

balls were used on the top cap to allow a lateral movement of the sample. This arrangement had the advantage of eliminating friction and avoiding the use of grease on the plane.

To ensure that the friction was effectively eliminated, the steel plates were mounted in a shear box apparatus with the steel ball cage between them; normal pressures of 5 to 20 p.s.i. were applied and the shearing stress along the plane was measured. This stress was very small; a maximum of 0.1 p.s.i. was registered for a normal pressure of 20 p.s.i.

A series of tests was then carried out with the perspex sample at a cell pressure of 5 p.s.i., using 1, 2, 3 and 4 membranes superimposed upon each other. The membranes had a standard thickness of 0.2 mm. For each case the stress-strain curves are plotted in Fig.B-2. It can be seen from this figure that the load builds up rapidly and from 1% to 15% strain, the stress-strain curves can be approximated to a straight line. The difference of load between two consecutive curves is fairly constant at a given strain and the average difference for each strain is given by curve 5, Fig.B-2. Curve 5 can

TESTS WITH PERSPEX SAMPLE SHAPE

CELL PRESSURE = 5.0 PSI.

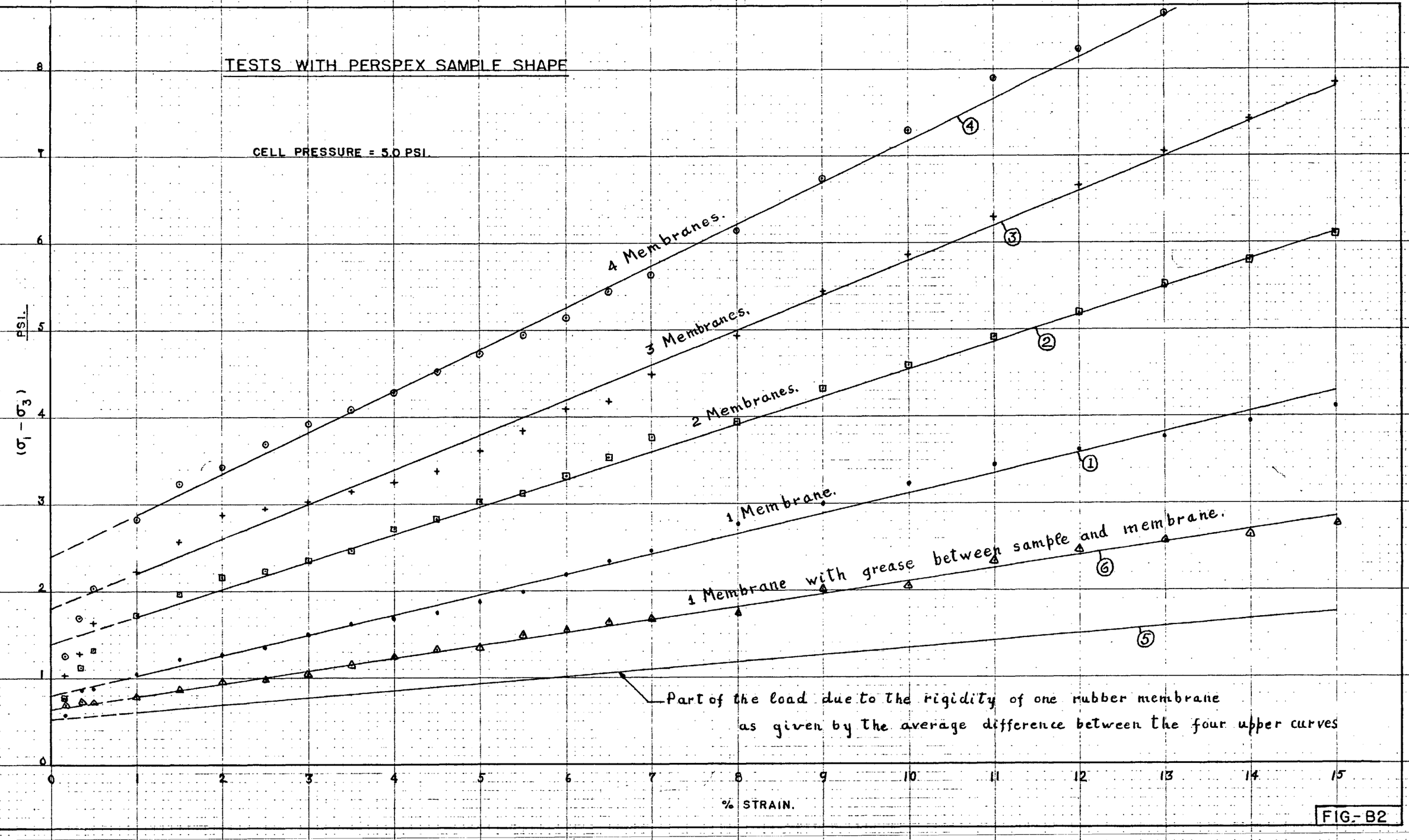


FIG.- B2

be said to represent the load due to the rigidity of one rubber membrane; this load amounts to only 40% to 60% of the total taken by one membrane (curve 1, Fig.B-2). The difference between curve 1 and curve 5 could be attributed to the friction between the membrane and the perspex sample.

To verify this explanation, one test was carried out using one membrane, and a thin coating of silicone grease was applied on the side of the perspex sample to reduce friction. The stress-strain curve obtained (curve 6, Fig.B-2) shows that the reduction of friction along the side of the sample has reduced the load taken by the membrane. Hence, the rubber membrane correction due to a shear plane failure can be divided into two components: one due to the rigidity of the membrane and one due to the friction between the membrane and the sample. The rigidity component should be independent of cell pressure while the frictional component should increase with cell pressure.

Tests with one membrane were carried out at 5, 10 and 20 p.s.i. to study the variation of load with cell pressure; corresponding stress-strain curves are given in

Fig.B-3. These curves show an increase in load with an increase in cell pressure.

Observations during testing on London clay from Bradwell have pointed out that the shear plane appears just before failure, that is within 1% strain before the maximum deviator stress is reached. Therefore the rubber membrane correction to be applied, as found from the tests with the perspex sample, should be taken from Fig.B-3 at a strain lower than 1% because the appearance of the plane corresponds to 0% strain in the tests on the perspex sample. For that purpose, the lines in Fig.B-3 have been extrapolated to 0% strain and their intercepts with the vertical axis are used as the needed correction.

The values of these intercepts for different cell pressures are plotted in Fig.B-4. It is seen that the load increases linearly with cell pressure. At zero cell pressure, the frictional component should theoretically be zero and the load of 0.6 p.s.i. could be attributed to the rigidity of the membrane; this compares with the values given by Fig.B-2 where the rigidity component is 0.6 p.s.i. at 1% strain. The increase of load with cell pressure can be considered as the frictional component and

TESTS WITH PERSPEX SAMPLE SHAPE

ONE MEMBRANE ONLY.

σ_3 = CELL PRESSURE.

$\sigma_3 = 20$ PSI.

$\sigma_3 = 10$ PSI.

$\sigma_3 = 5$ PSI.

$(b_1 - b_3)$ PSI.

0 1 2 3 4 5 6 7 8

0 1 2 3 4 5 6 7 8 9 10 11 12 13 14 15

% STRAIN.

FIG. - B3

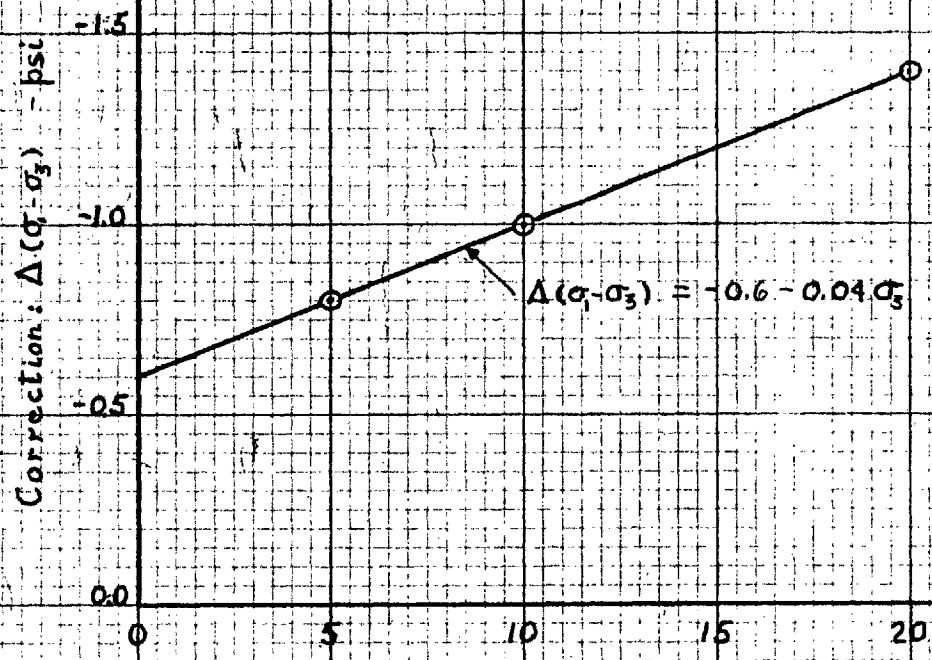
is given by 0.04 σ_3 where σ_3 is the cell pressure (see Fig.B-4).

Clearly, the frictional component will not increase indefinitely with cell pressure. To determine the limit of this increase, a rubber membrane was mounted around a porous bronze plate and placed in a shear box arrangement as shown in Fig. B-5. A perspex plate or an undisturbed sample of London clay was placed in the lower part of the box, and the rubber membrane placed in the upper part. This arrangement enabled the measurement of the friction between rubber and perspex or between rubber and clay. The results are given in Fig.B-5 and show that for a normal force lower than 20 p.s.i. the frictional forces are of the same order for rubber-clay and rubber-perspex, while for a normal pressure higher than 20 p.s.i. little increase can be expected in the frictional force between the rubber and clay. For a cell pressure or effective stress (σ'_3) at failure larger than 20 p.s.i., the value at 20 p.s.i. should be used to calculate the membrane correction.

Before the shear plane appears, the clay sample deforms by bulging; hence a small correction must be

RUBBER MEMBRANE CORRECTION

from tests with perspex sample shape.



Cell pressure σ_3 - psi.

NOTE: Points are taken from figure B-3 as the intercepts of the lines on the vertical axis.

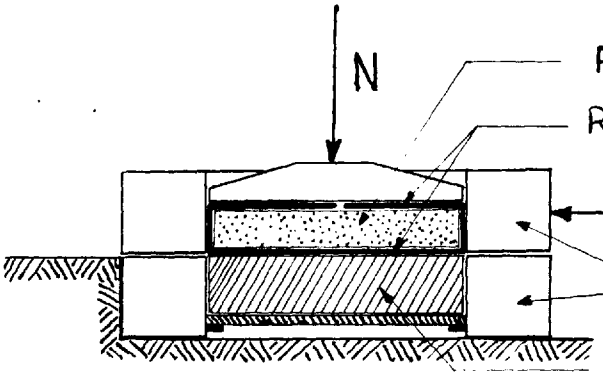
FIG B-4

SHEAR BOX ARRANGEMENT

TO STUDY FRICTION BETWEEN:

A) RUBBER MEMBRANE AND PERSPEX.

B) RUBBER MEMBRANE AND LONDON CLAY.



A = area of contact between rubber membrane and perspex or rubber membrane and London clay

η = unit normal pressure ($= N/A$)

f = unit frictional force ($= H/A$)

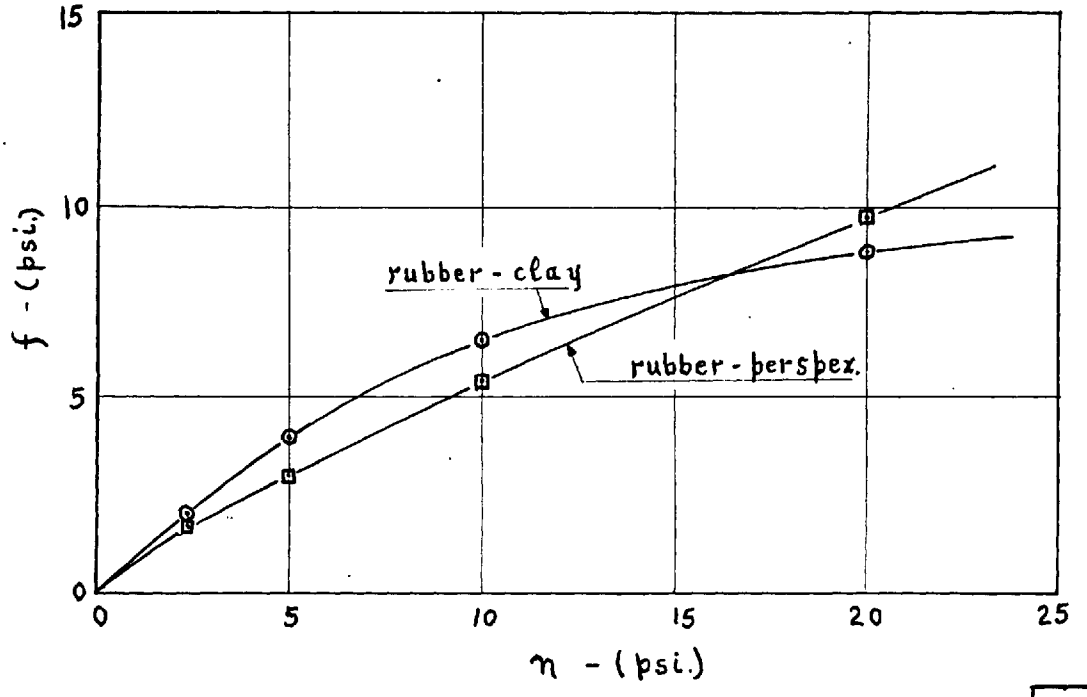


FIG.- B5

introduced to take this effect into account. Such a correction has been proposed by Henkel and Gilbert (1952) and for strains at failure smaller than 8%, it is approximately equal to 0.06 ϵ_f where ϵ_f is the per cent strain at failure and the correction is in p.s.i. Since in the case of the London clay from Bradwell the shear plane appears at a strain very close to the strain at failure, the failure strain has been used to calculate the correction due to bulging.

DRAIN CORRECTION

A test has been done at a cell pressure of 5 p.s.i. with a filter paper drain placed between the rubber membrane and the perspex sample. The corresponding stress-strain curve is given in Fig.B-6. From this figure it is evident that the drain correction amounts to 1.0 p.s.i.

SUMMARY

The rubber membrane and drain correction for a shear plane failure is summarised as follows:

Drain	= -1.0 p.s.i.
Bulging effect	= -0.06 ϵ_f(%) p.s.i.
Rigidity of membrane	= -0.60 p.s.i.
Friction(clay-membrane)	= -0.04 σ'_3 p.s.i. ($\sigma'_3 \leqslant 20$ p.s.i.)

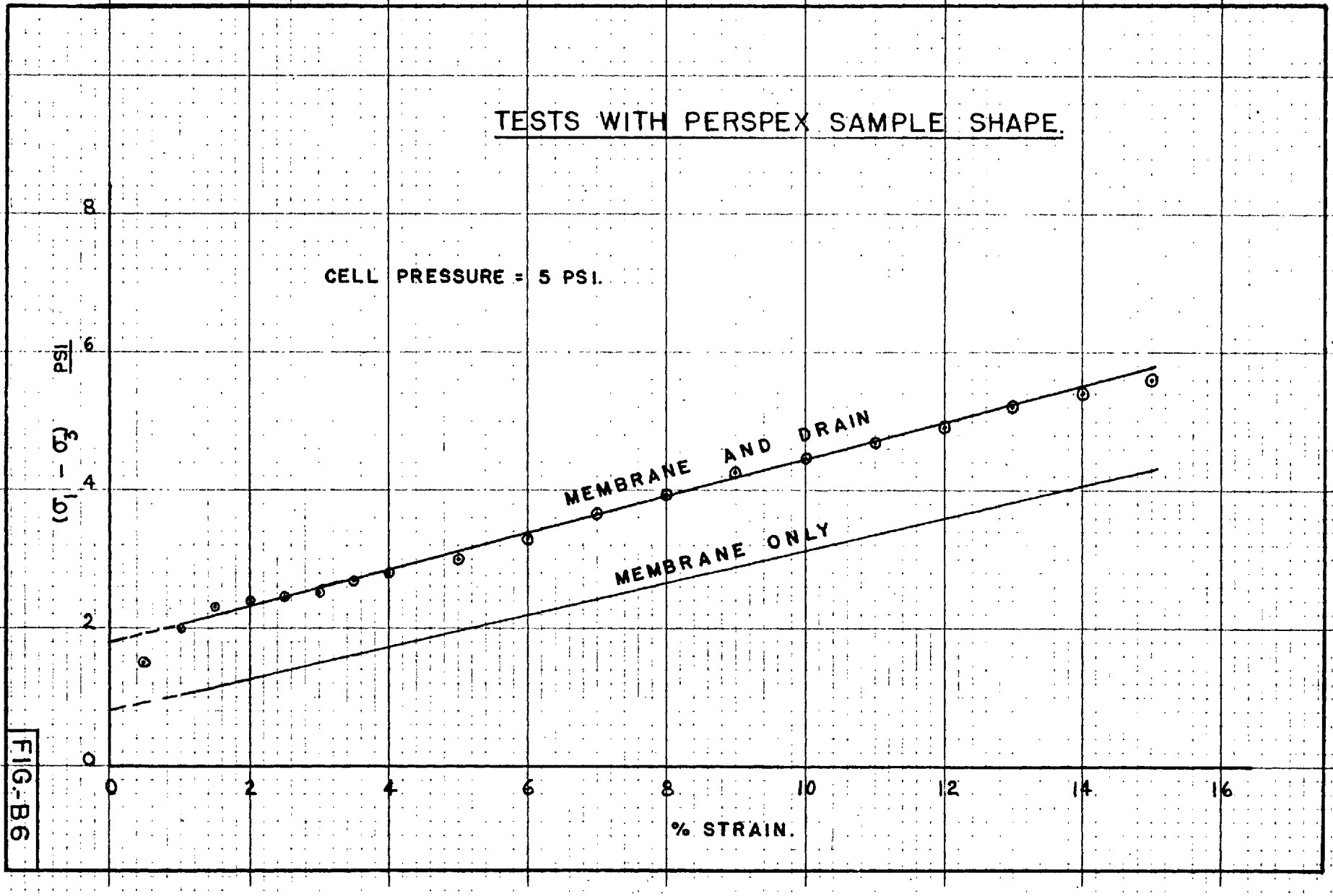

TESTS WITH PERSPEX SAMPLE SHAPE.
CELL PRESSURE = 5 PSI.
$(\sigma_1 - \sigma_3)$ PSI
MEMBRANE AND DRAIN
MEMBRANE ONLY
% STRAIN.
0
2
4
6
8
10
12
14
16

FIG.-B6

These values can be conveniently expressed by the equation:

$$\text{Correction (p.s.i.)} = \Delta(\sigma_1 - \sigma_3)$$

$$= -1.6 - 0.06\,\epsilon_f(\%) - 0.04\,\sigma'_3$$

APPLICATION OF THE RUBBER MEMBRANE AND DRAIN CORRECTION TO DIFFERENT TESTS

In the case of the London Clay from Bradwell, this correction has been adapted to the different tests:

(i) Drained tests:

In the drained tests, the volume change during shear accounts for 40% of the strain at failure (average of 17 tests) and the plane appears at about 1% strain before failure. Therefore the bulging correction has been reduced by 50%. Due to the very slow rate of strain and the volume change during shear, the frictional component has also been reduced by 50%.

Hence,

$$\text{Correction (p.s.i.)} = -1.6 - 0.03\,\epsilon_f(\%) - 0.02\,\sigma'_3$$

(ii) Consolidated-Undrained tests:

In these tests, the full correction has been

applied except when a very slow rate of strain was used. Then the frictional component was reduced by 50%. Hence

$$\text{correction (p.s.i.)} = -1.6 - 0.06\ \epsilon_f(\%) - x\ 0.04\ \sigma'_3$$

where $x = 1.0$ for 20 minutes at failure,

$= 0.5$ for 3 days at failure.

(iii) Undrained tests:

No drains were used in these tests and the frictional component has been reduced by 50% due to the air between the membrane and the sample, the talc on the inner side of the membrane and also due to the fact that the sample was sheared immediately after the application of the cell pressure.

Hence,

$$\text{correction (p.s.i.)} = -0.6 - 0.06\ \epsilon_f(\%) - 0.02\ \sigma'_3$$

The typical values calculated for different tests are:

Drained tests	:	correction = -2.1 p.s.i.
Consolidated-Undrained tests	:	correction = -2.5 p.s.i.
Undrained tests	:	correction = -1.3 p.s.i.

Bishop and Henkel (1957) have recommended a value of 2.0 p.s.i. for the rubber membrane and drain correction.

RUBBER MEMBRANE CORRECTION AT HIGH STRAIN

In order to determine the "post-failure" stress-strain characteristics in an undrained triaxial test, a rubber membrane correction was applied to allow for the severe deformation of the membrane at high strain.

First, the deviator stress was corrected as previously explained and thereafter a correction proportional to the slope of the lines in Fig.B-3 was added. The slopes of these lines were arbitrarily reduced depending on the severity of the deformation. Only the test results where the sample failed on a well defined plane were used.

AREA CORRECTION

In the drained tests, the area correction (Bishop and Henkel, 1957) is given by:

$$a = a_o \frac{1 + \frac{\Delta V}{V_o}}{1 - \epsilon}$$

where a = corrected cross-sectional area

a_o = cross-sectional area before shearing

V_o = volume of the sample before shearing

ΔV = volume change during shearing.

ϵ = strain.

For the undrained tests, where there is no volume change, the correction becomes:

$$a = \frac{a_o}{1 - \epsilon}$$

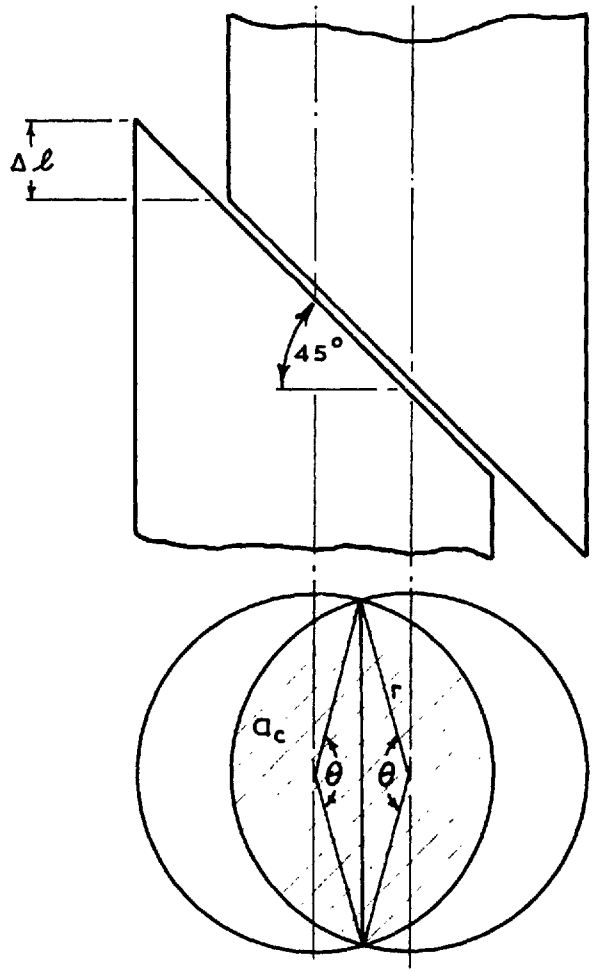
This correction which allows for the bulging of the sample was applied until the shear plane appeared; the area was then taken to be constant until failure. Once the shear plane has appeared the increase in strain produces a movement along the plane and the bulging effect is then very small.

Area Correction for High Strains

In fact, the effective area of a sample failing along a shear plane will decrease with increasing strain. For an ideally rigid sample where no bulging takes place (e.g. the perspex sample) this decrease would be as given by the shaded area in Fig. B-7.

In the undrained tests where the "post-failure" stress-strain characteristics of London Clay were studied

"POST FAILURE" AREA CORRECTION ON RIGID SAMPLE



FOR: d = DIAMETER OF THE SAMPLE $\left(=1\frac{1}{2}\text{ in}\right)$

ℓ = LENGTH OF THE SAMPLE $\left(=3\text{ in} = 2d\right)$

d' = STRAIN DUE TO SHEARING ALONG THE PLANE

$$= \frac{\Delta \ell}{\ell}$$

THEN: $\cos\frac{\theta}{2} = 2d'$

AND $a_c = \frac{d^2}{4}\left[\theta - \sin\theta\right]$

= CORRECTED AREA FOR A STRAIN d'

FIG-B 7

an area correction due to bulging was applied until failure and then the effective area was decreased by multiplying the area at failure, a_f, by a reduced value of the ratio $(\frac{a_c}{a_o})$, where a_c is the corrected area at a strain δ after failure (Fig.B-7)(equal to the actual strain minus the strain at failure) and a_o is the initial area of a sample 1½ in. in diameter.

Clearly this correction is approximate and rather severe for a sample of clay where there is a certain amount of bulging taking place, even after the appearance of the plane. Therefore the applied ratio $\frac{a_c}{a_o}$ was arbitrarily reduced to 80 or 60% of its value, depending upon the severity of the deformation.

APPENDIX C

DETAIL OF TOTAL STRESS ANALYSIS

The Reactor House and Turbine House excavations were analysed with different depths of tension crack. These different cases were solved for the maximum strength required in London Clay for a factor of safety of 1.0. Circle and plane analyses were used. As will be realised, some of the assumptions were rather extreme, but this was to insure that all possibilities were covered. The interpretation of these analyses is given in the present thesis, Chapter III, page 39.

1. REACTOR HOUSE EXCAVATION

The properties of the marsh clay are as follows:

density = 103 lb./cu.ft.

strength = 400 lb./sq.ft.

The densities of the fill and of the London clay are respectively 110 lb./cu.ft. and 120 lb./cu.ft.

In all the analyses, the ground water level was taken to be at the surface of the marsh clay or at the surface of the slope where there is no marsh clay. The dimensions of the slope are given in Fig. C-10.

Circles and planes were first assumed to pass through the toe of the slope. For this assumption the position of the critical circles with and without water in the cracks are shown in Fig. C-1 and C-2 and the positions of the critical planes in Fig. C-3; the required strengths in the different cases are given in Table C-1.

The different cases are as follows:

Case (1): Tension crack through fill

Case (2): Tension crack through Marsh clay.
In this case, the cracks are close or even under the fill and since a crack in marsh clay could not stand open under the fill, the fill was considered nonexistent in this case, as will be considered later.

Cases (3), (4) and (5): A tension crack through marsh clay and in London Clay at depths of 0.3H, 0.5H and 0.7H respectively, where H is the height of the slope in London Clay.

Case (6): Tension crack down to the junction of the brown and blue London Clay (= 0.84H).

Case (7): Tension crack to a level equal to the bottom of the excavation.

Since in case (2) a crack could not stand open

under the fill, a state of active pressure was considered to exist in marsh clay. This active pressure p_a is given by

$$p_a = q + \gamma_m z - 2c$$

where q is the pressure at the surface of marsh clay due to fill, γ_m is the density of the marsh clay and z is the depth from the surface of the marsh clay.

Hence, case (1a), Fig.C-4, consists of a tension crack through the fill and active pressure in marsh clay.

Case (2a), Fig.C-4, includes the same assumptions as case (1a) plus a tension crack in London Clay under the marsh clay, down to a depth of $0.3H$. This crack was assumed to be filled with water under hydrostatic pressure equal to the height of water up to the surface of the marsh clay.

These results are summarised in Fig.C-10 where the required strengths for the different cases are plotted against the depth of the tension crack. The shaded curve represents the maximum required strength for each depth of tension crack, and corresponding maximum ratios are also given in the same figure. The strength measured was taken

from the strength-depth curve (Fig.10) at the middle depth of the arc or plane in London Clay.

The same analyses were carried out with the assumption that the circles and planes passed through the junction of brown and blue London Clay. The position of the circles and planes are shown in Fig. C-4 to C-6 and the required strength for each case is given in Table C-2. It can be seen that for all cases the required strength is less than in the cases where the circles and planes pass through the toe of the slope.

2. TURBINE HOUSE EXCAVATION

For this slope, the ground water level was assumed to be at the surface.

The positions of the critical circles and planes are shown in Fig. C-8 and C-9, and the results are given in Table C-3.

For cases (1) to (6), the depths of tension cracks were taken as 0', 8', 12', 16', 19', and 23' respectively. The results are plotted in Fig.C-11, where the shaded curve represents the maximum required strength for all cases and the corresponding maximum ratios are tabulated in the same figure.

TABLE C-1

REACTOR HOUSE EXCAVATION
(Toe circles and planes)

CIRCLE ANALYSIS					
Case No. (Fig. C-1)	Required Strength lb./sq.ft.	Case No. (Fig. C-2)	Required Strength lb./sq.ft.	Case No. (Fig. C-7)	Required Strength lb./sq.ft.
1	1080	-	-	-	-
2	871	2w	886	1a	1100
3	943	3w	1030	2a	1100
4	893	4w	1145	-	-
5	726	5w	1270	-	-
6	487	6w	1370	-	-

PLANE ANALYSIS					
Case No. (Fig. C-3)	Required Strength lb./sq.ft.	Case No. (Fig. C-3)	Required Strength lb./sq.ft.	Case No. (Fig. C-7)	Required Strength lb./sq.ft.
1	900	-	-	-	-
2	714	2w	752	1a	975
3	776	3w	981	2a	1060
4	745	4w	1160	-	-
5	571	5w	1380	-	-
6	383	6w	1470	-	-
7	-	7w	1750	-	-

TABLE C-2

REACTOR HOUSE EXCAVATION

(Circles and Planes through junction of brown and blue London Clay)

CIRCLE ANALYSIS				PLANE ANALYSIS			
Case No. (Fig. C-4)	Required Strength lb./sq.ft.	Case No. (Fig. C-5)	Required Strength lb./sq.ft.	Case No. (Fig. C-6)	Required Strength lb./sq.ft.	Case No. (Fig. C-6)	Required Strength lb./sq.ft.
1	973	-	-	1	795	-	-
2	790	2w	810	2	640	2w	670
3	883	3w	955	3	665	3w	878
4	600	4w	1265	4	480	4w	1240
-	-	-	-	5	0	5w	1500

TABLE C-3

TURBINE HOUSE EXCAVATION

CIRCLE ANALYSIS				PLANE ANALYSIS			
Case No. (Fig. C-8)	Required Strength lb./sq.ft.	Case No. (Fig. C-8)	Required Strength lb./sq.ft.	Case No. (Fig. C-9)	Required Strength lb./sq.ft.	Case No. (Fig. C-9)	Required Strength lb./sq.ft.
1	560	-	-	1	426	-	-
2	650	2w	684	2	541	2w	596
3	653	3w	770	3	555	3w	718
4	588	4w	875	4	493	4w	923
5	490	5w	1020	5	370	5w	1170
-	-	-	-	6	0	6w	1435

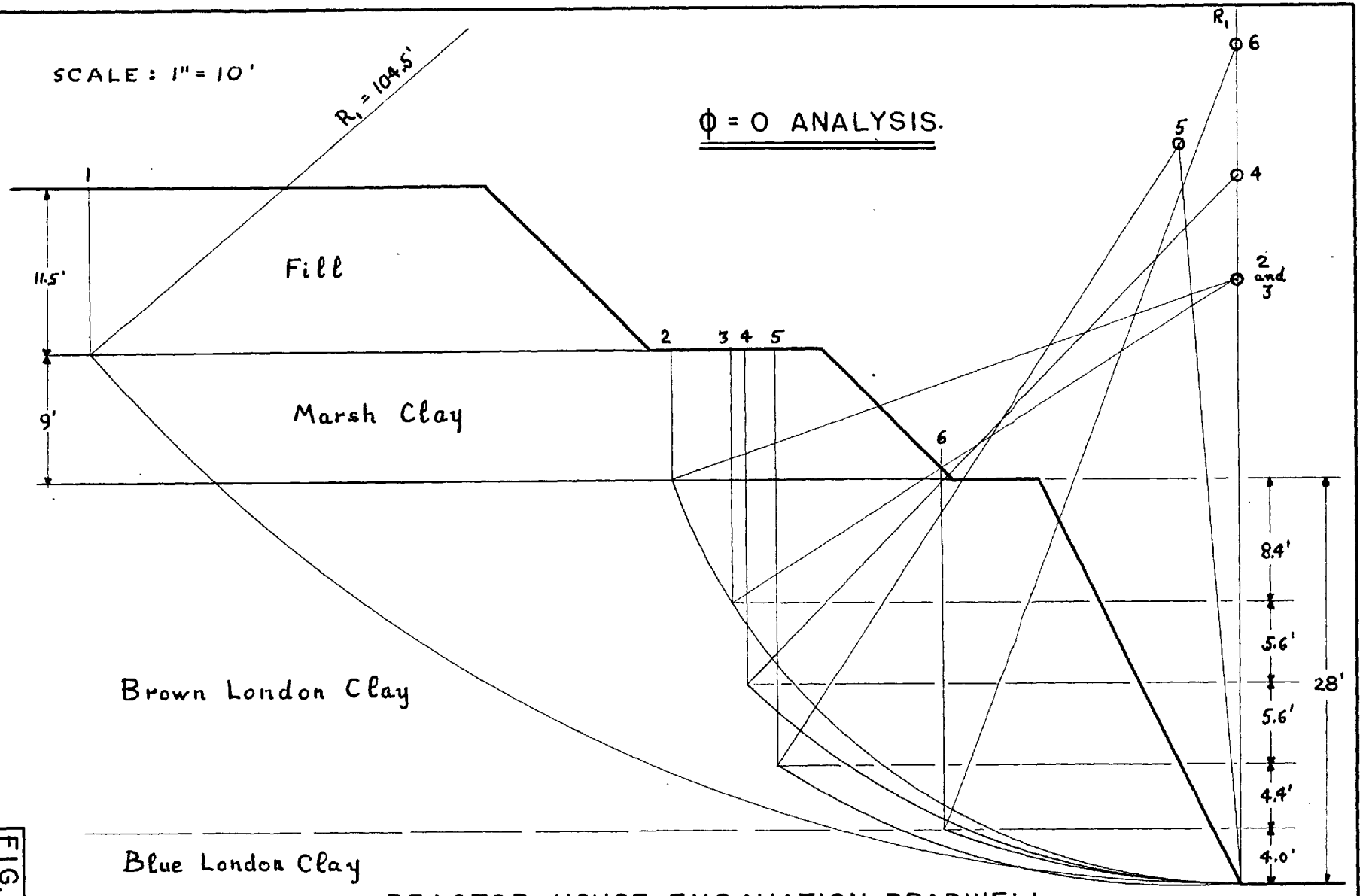


FIG. C-1

REACTOR HOUSE EXCAVATION, BRADWELL.

POSITION OF CRITICAL CIRCLES FOR DIFFERENT DEPTHS OF TENSION CRACKS.
(NO FREE WATER IN CRACKS)

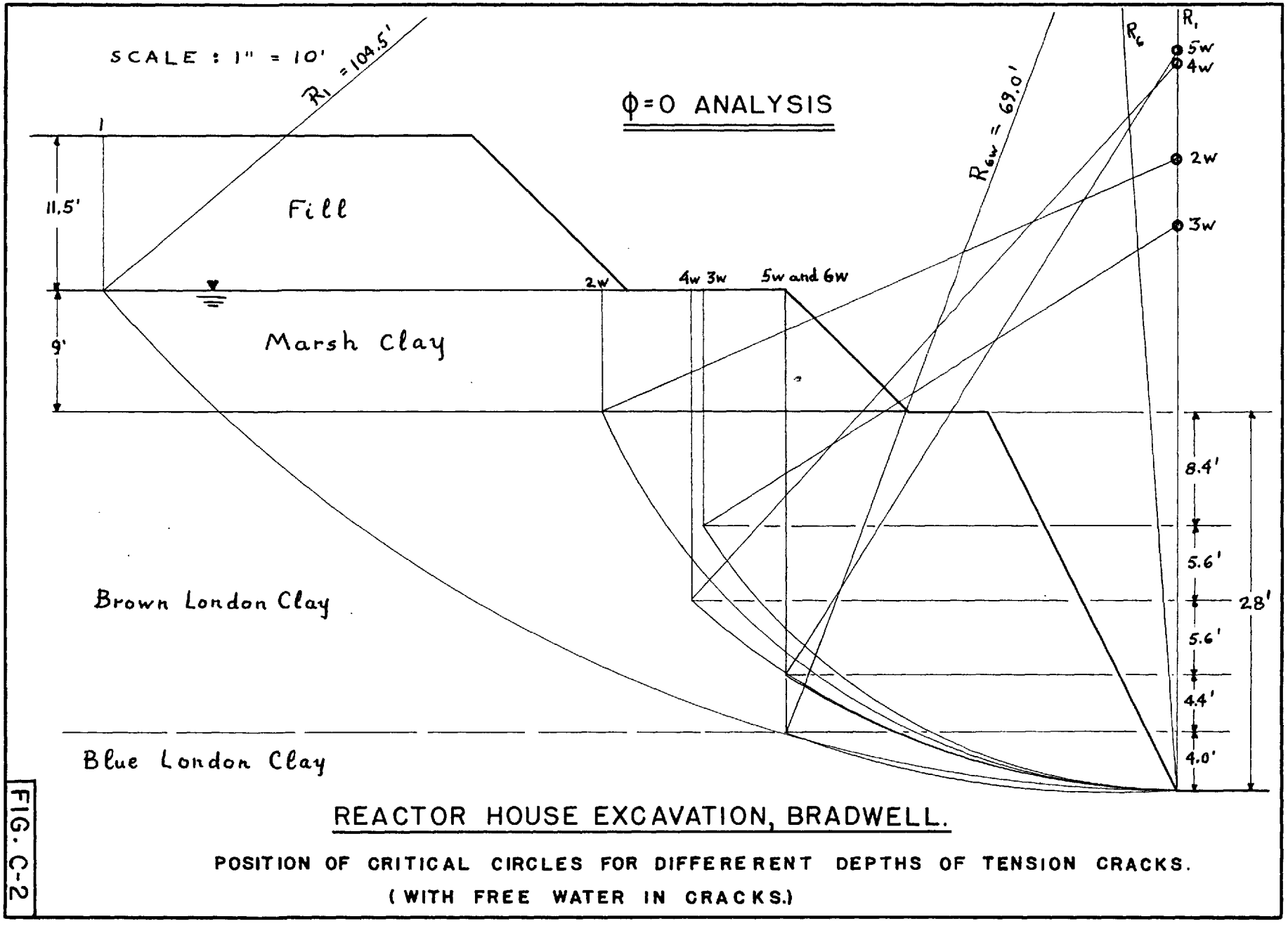


FIG. C-2

REACTOR HOUSE EXCAVATION, BRADWELL.

POSITION OF CRITICAL CIRCLES FOR DIFFERERENT DEPTHS OF TENSION CRACKS.
(WITH FREE WATER IN CRACKS.)

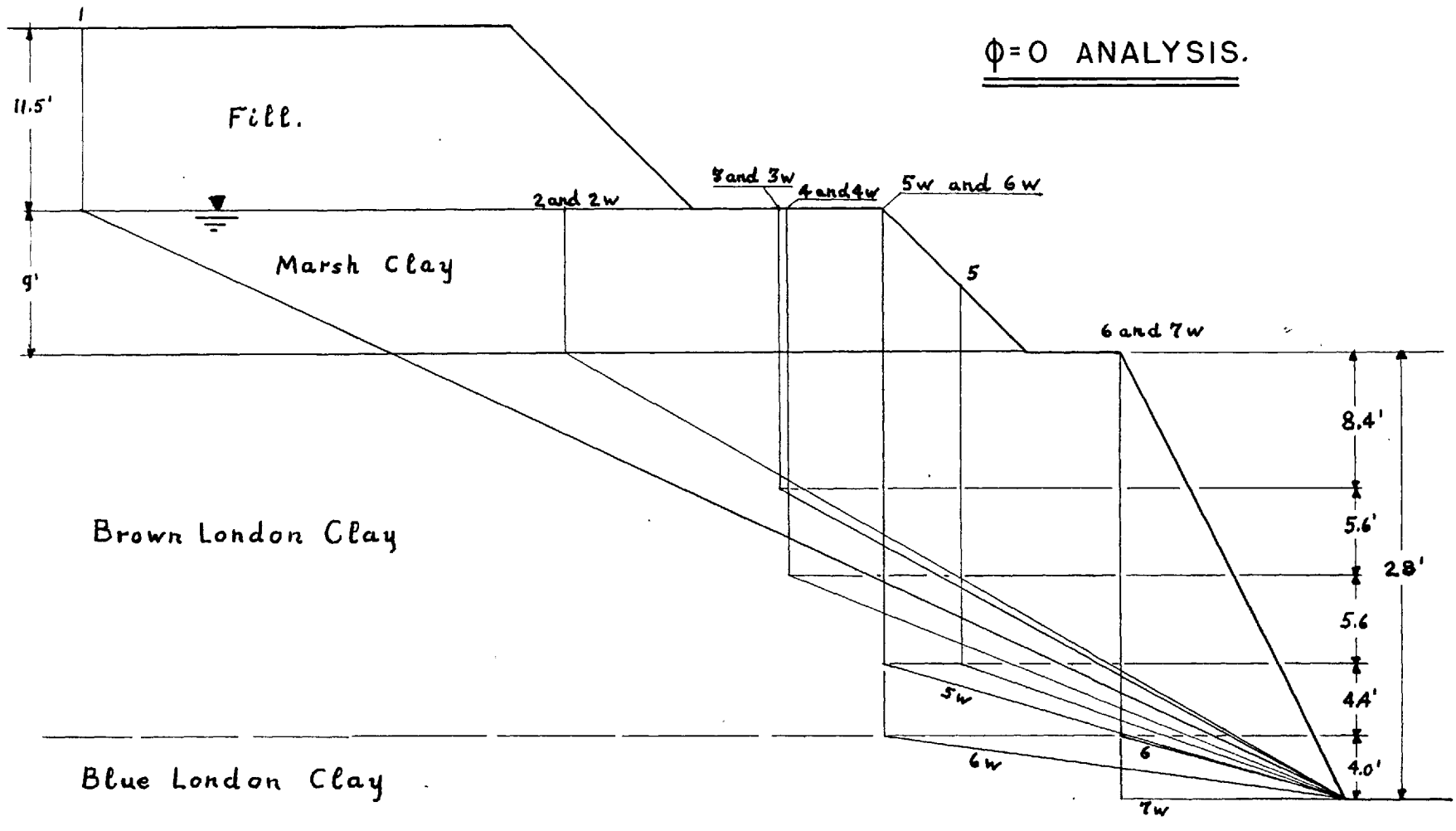


FIG. C-3

REACTOR HOUSE EXCAVATION, BRADWELL.

POSITION OF CRITICAL PLANES FOR DIFFERENT DEPTHS OF TENSION CRACKS.
(WITH AND WITHOUT FREE WATER IN CRACKS)

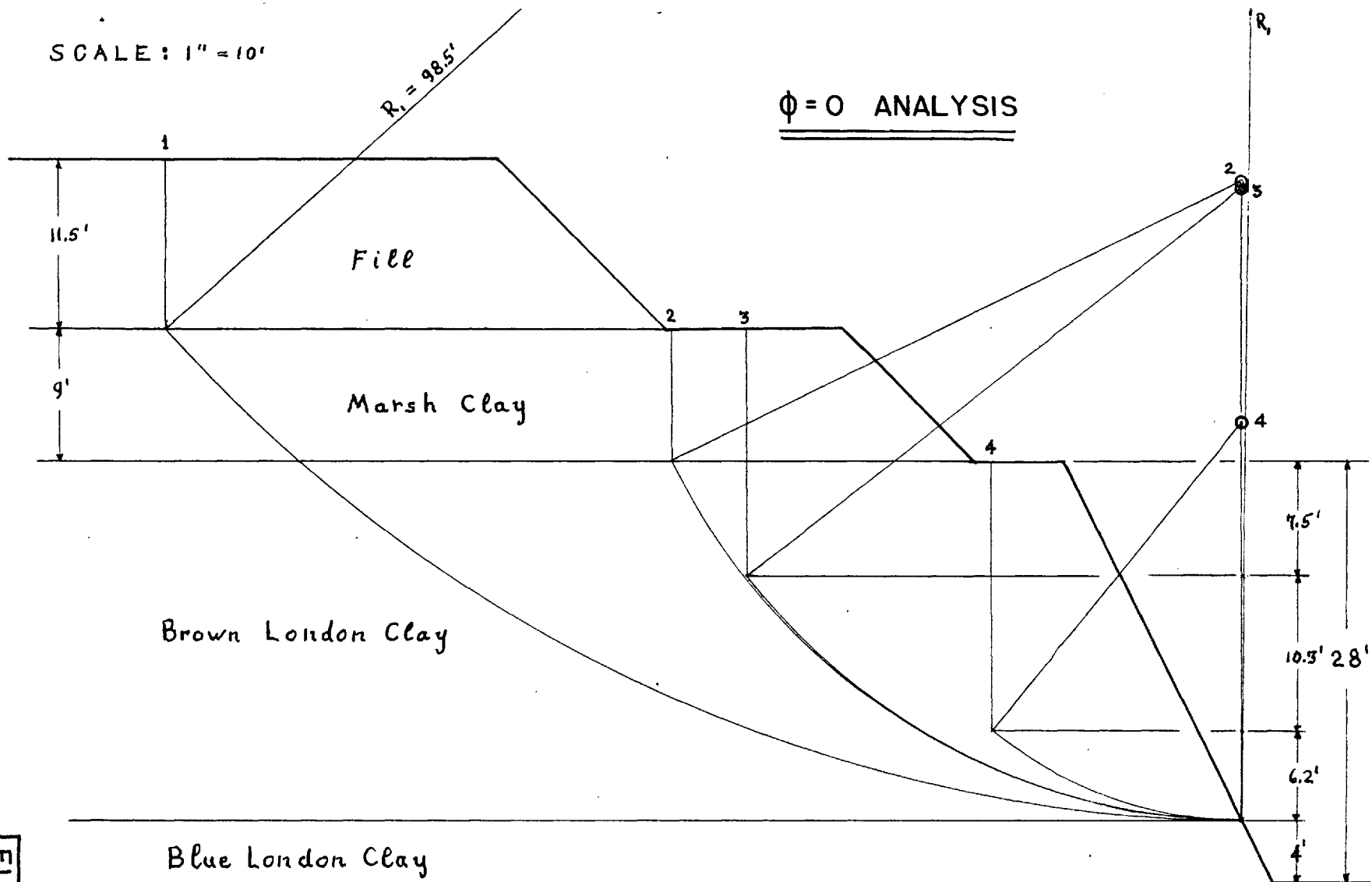


FIG. C-4

REACTOR HOUSE EXCAVATION, BRADWELL.

POSITION OF CRITICAL CIRCLES FOR DIFFERENT DEPTHS OF TENSION CRACKS
(NO FREE WATER IN CRACKS)

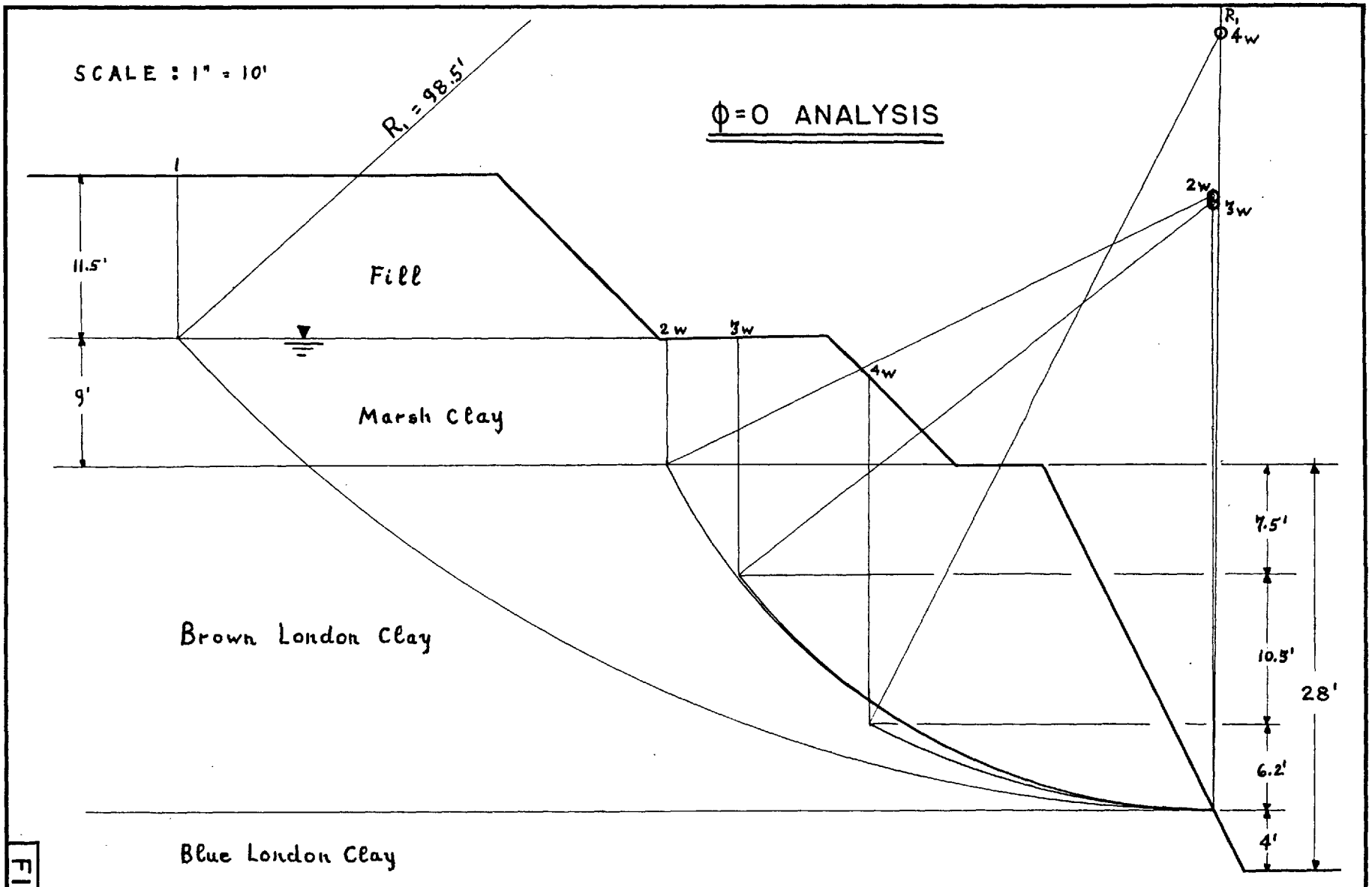


FIG. C-5

REACTOR HOUSE EXCAVATION, BRADWELL.

POSITION OF CRITICAL CIRCLES FOR DIFFERENT DEPTHS OF TENSION CRACKS
(WITH FREE WATER IN CRACKS)

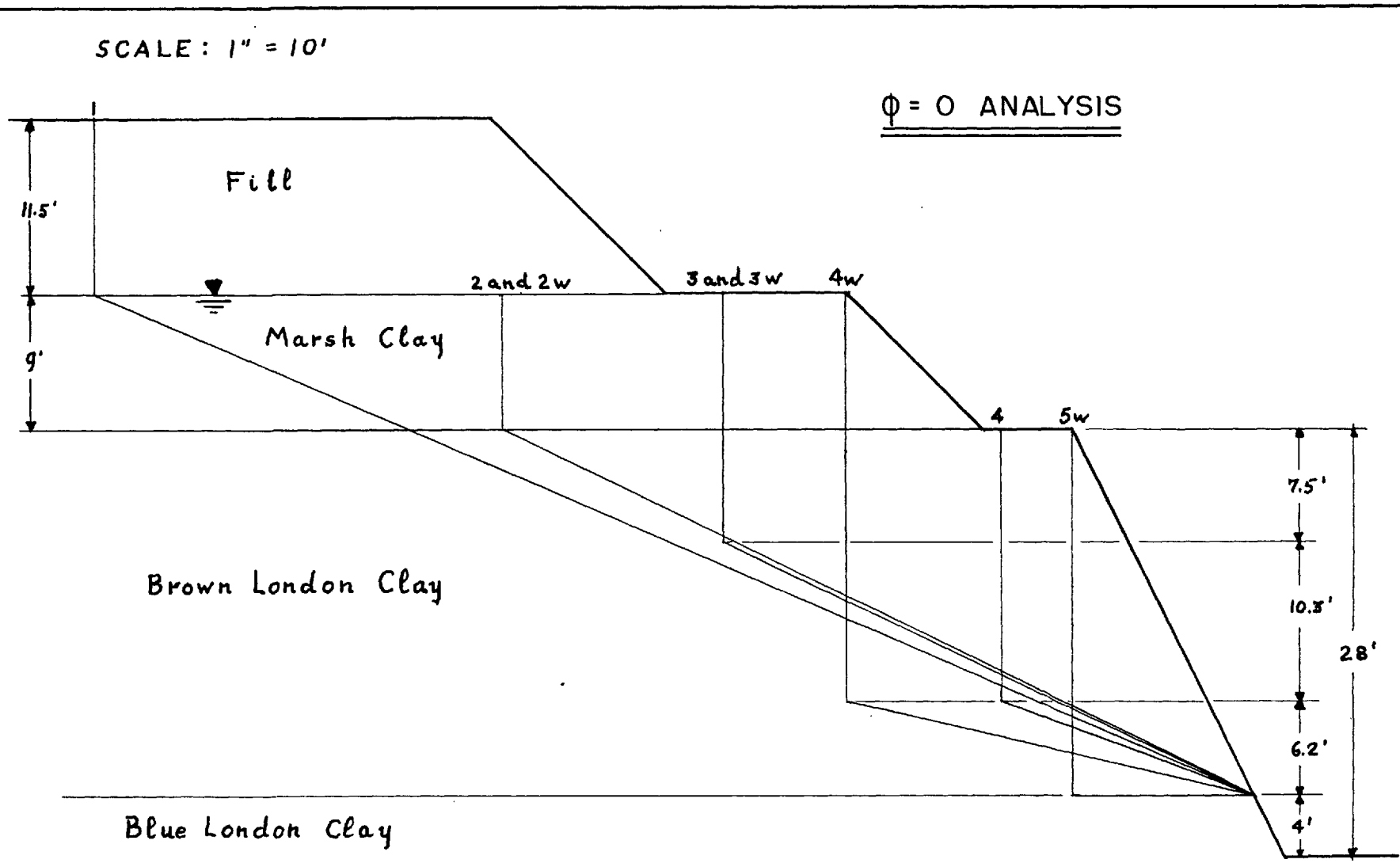


FIG.C-6

REACTOR HOUSE EXCAVATION, BRADWELL.

POSITION OF CRITICAL PLANES FOR DIFFERENT DEPTHS OF TENSION CRACKS.
(WITH AND WITHOUT FREE WATER IN CRACKS)

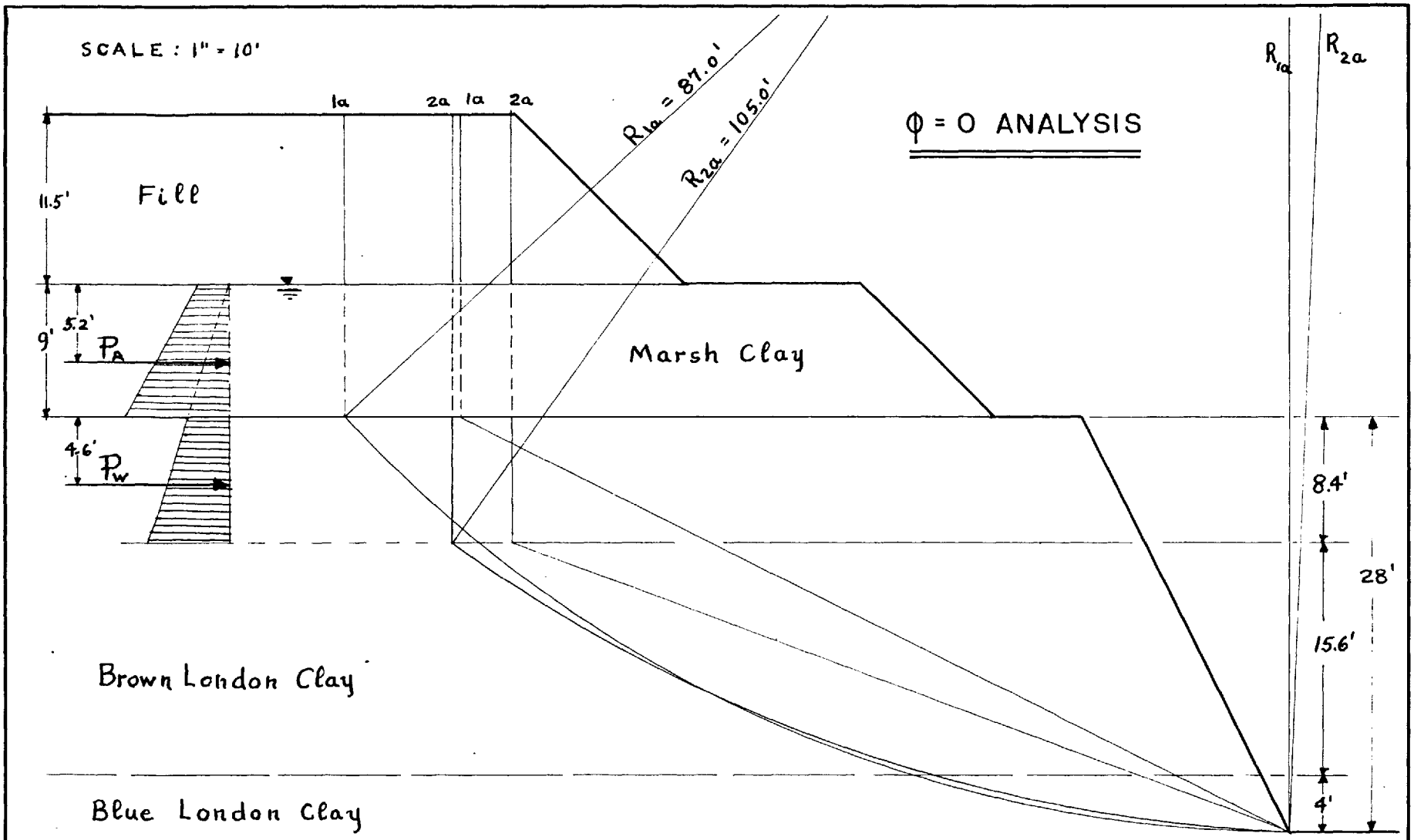


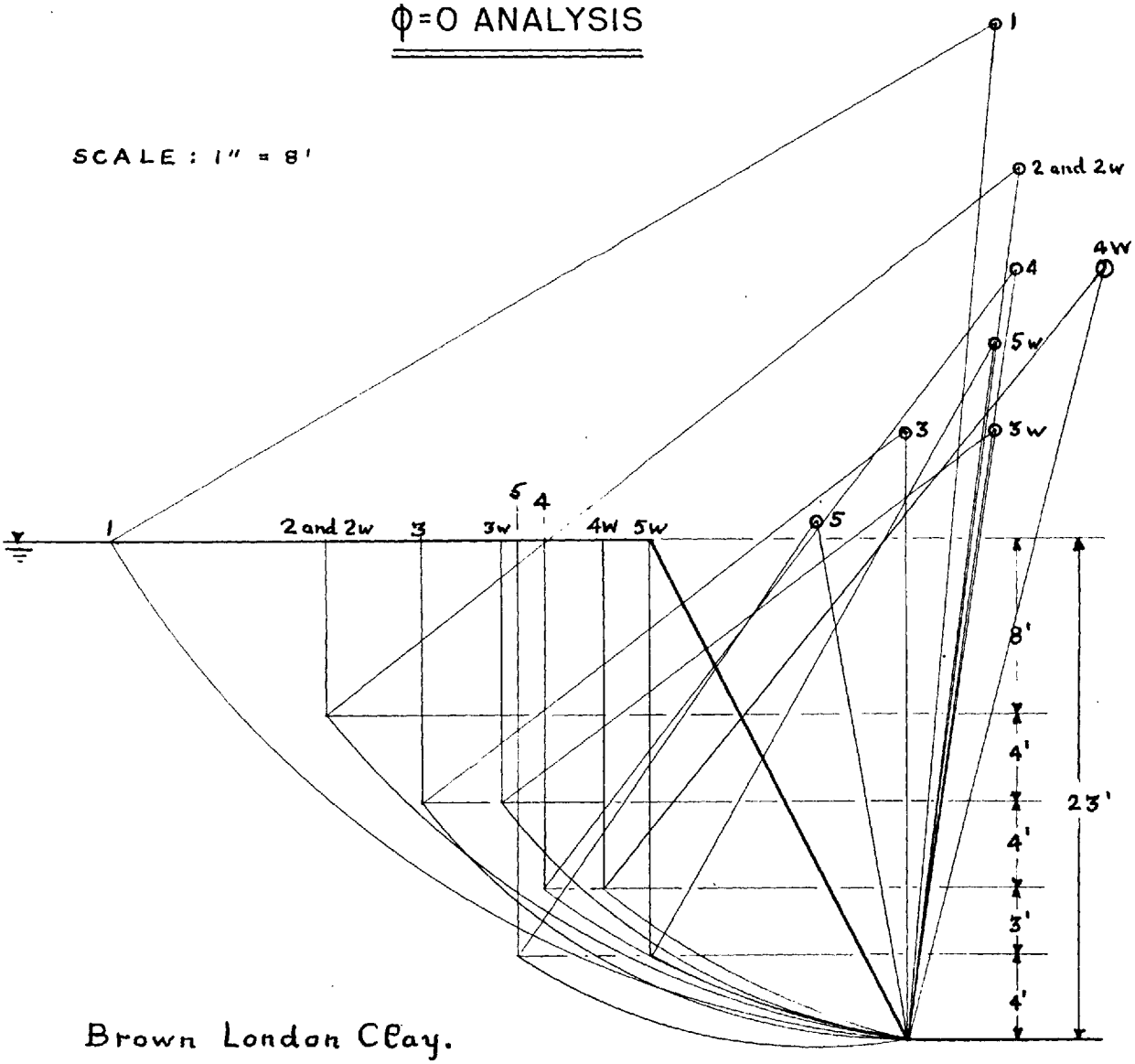
FIG. C-7

REACTOR HOUSE EXCAVATION, BRADWELL.

POSITION OF CRITICAL CIRCLES AND PLANES FOR DIFFERENT DEPTHS OF TENSION CRACKS.

(WITH MARSH CLAY IN ACTIVE STATE OF STRESS AND FREE WATER IN CRACK BENEATH.)

ϕ=0 ANALYSIS



TURBINE HOUSE EXCAVATION, BRADWELL.

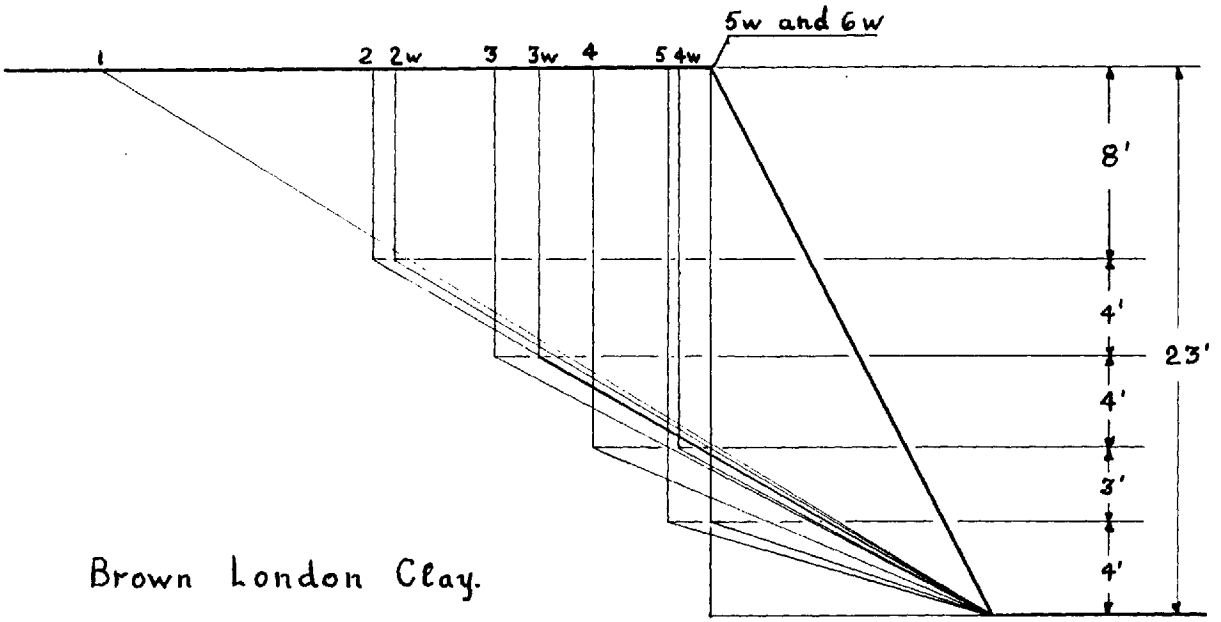
POSITION OF CRITICAL CIRCLES FOR DIFFERENT DEPTHS OF TENSION CRACKS.

(WITH AND WITHOUT FREE WATER IN CRACKS.)

FIG. C - 8

$\phi = 0$ ANALYSIS

SCALE : 1" = 8'



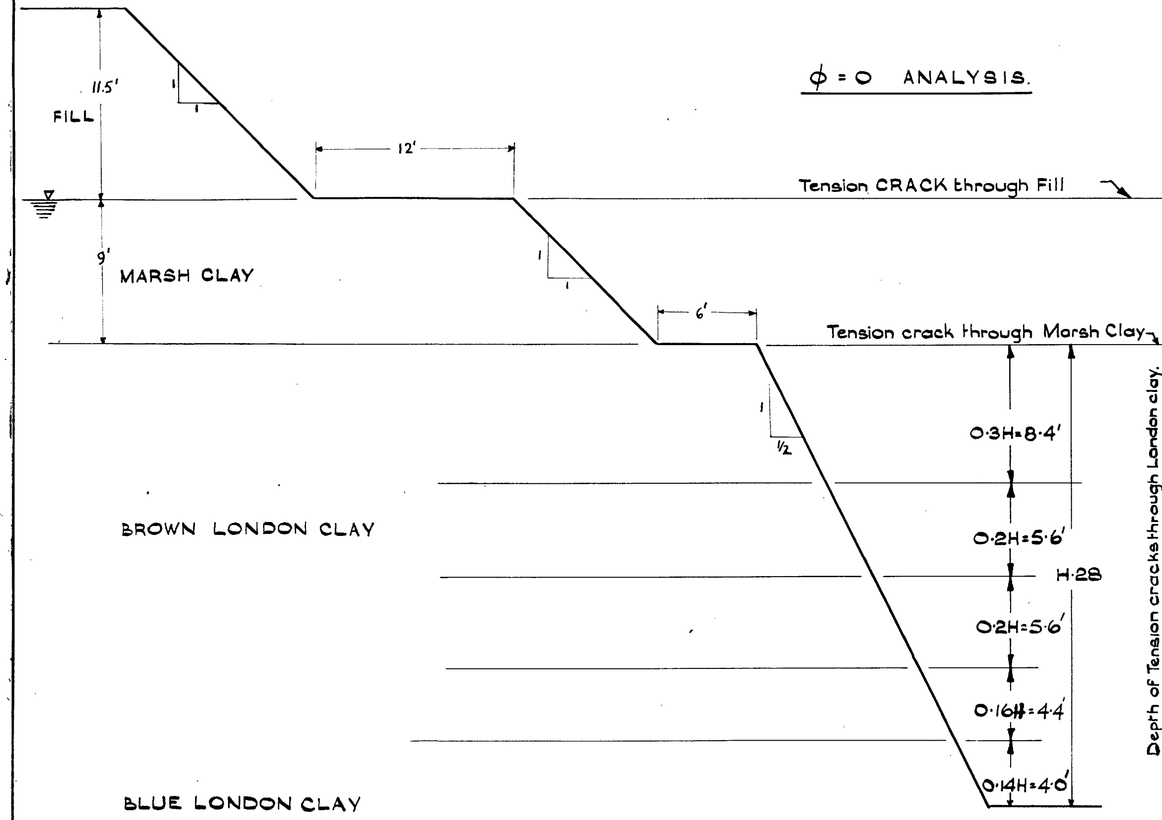
TURBINE HOUSE EXCAVATION, BRADWELL.

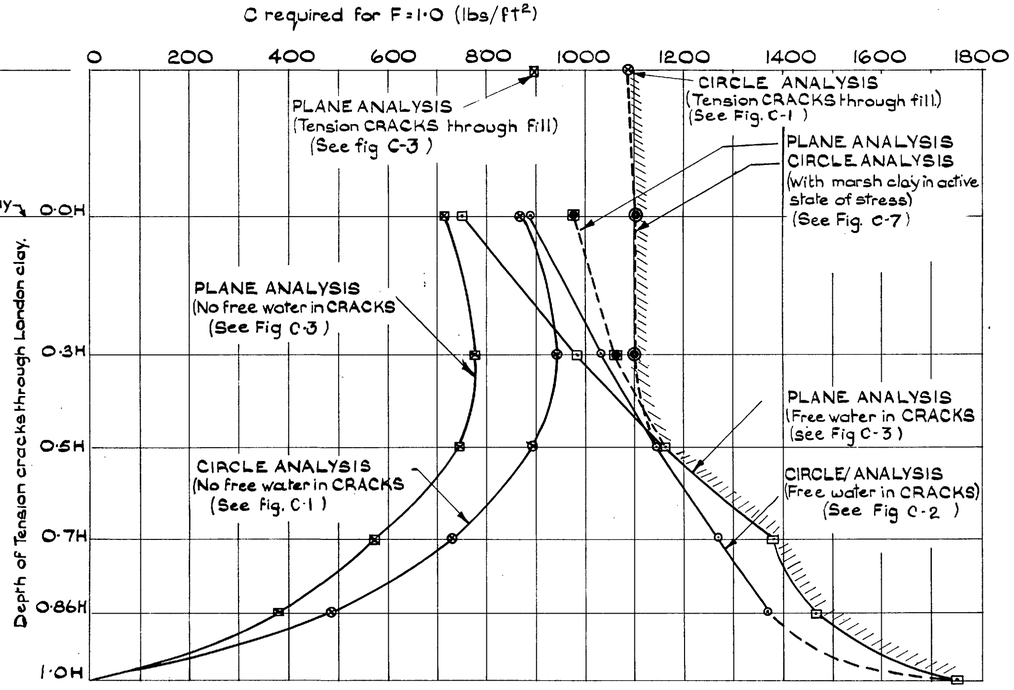
POSITION OF CRITICAL PLANES FOR DIFFERENT DEPTHS OF TENSION CRACKS.

(WITH AND WITHOUT FREE WATER IN CRACKS.)

FIG. C-9

$\phi = 0$ ANALYSIS.





Max. C required lbs/ft²	C Measured (note) lbs/ft.²	Max. C. Req / C. Meas.
1087	1800	·60
1100	1800	·61
1100	2030	·54
1160	2180	·53
1380	2320	·59
1470	2420	·61
1750	2500	·70

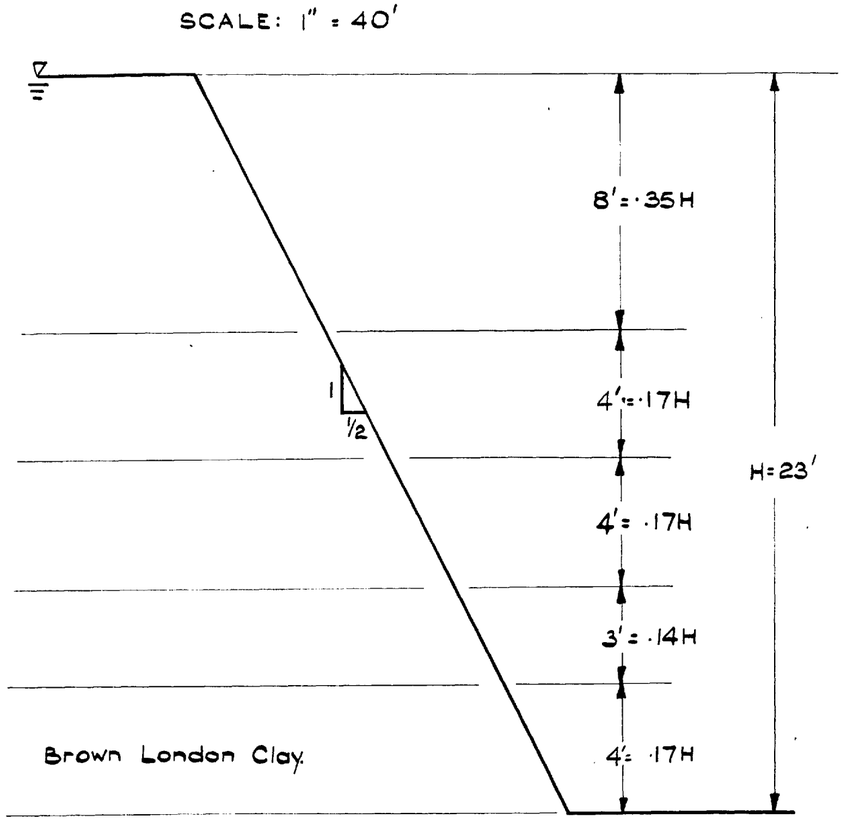
NOTE: C measured is taken at the average depth along the arc or the plane.

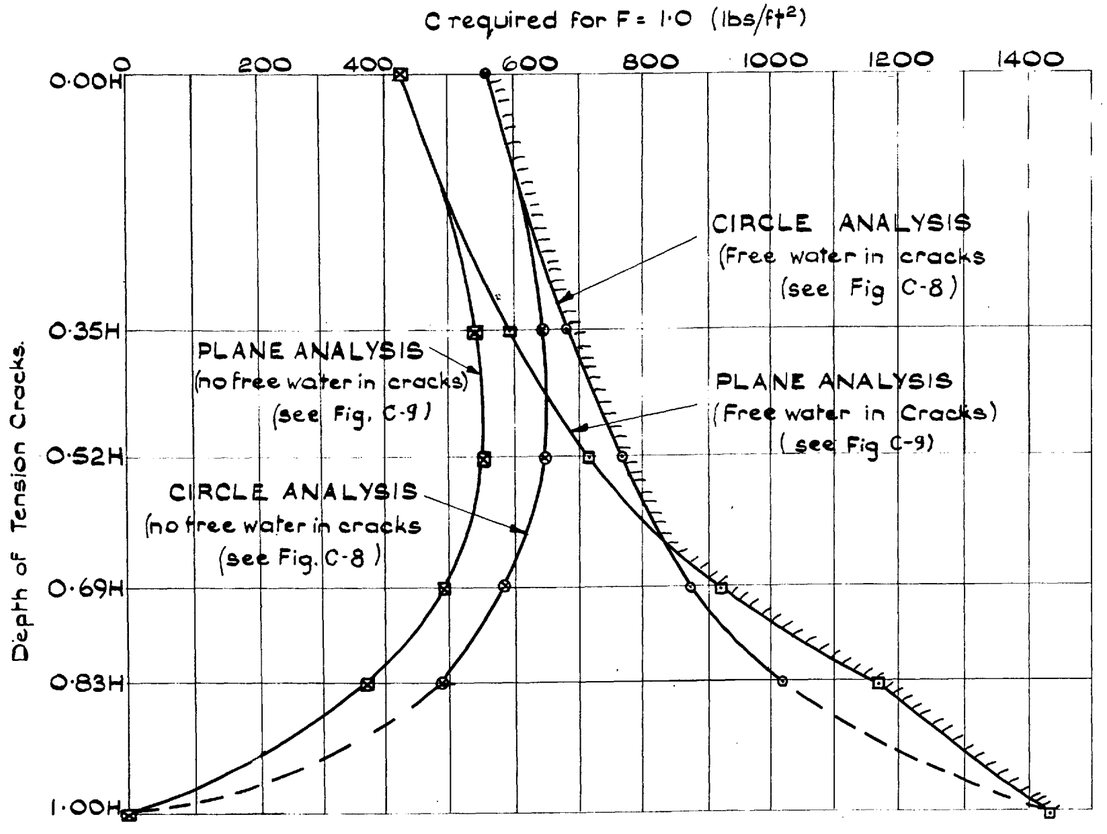
REACTOR HOUSE EXCAVATION BRADWELL

(SUMMARY OF ALL ANALYSIS FOR TOE CIRCLES & PLANES)

FIG. C-10

$\phi = 0$ ANALYSIS





max. C Required lbs/ft²	C measured (NOTE) lbs/ft²	Max C. Req. / C. meas
560	1380	·41
684	1650	·41
771	1780	·43
923	1990	·49
1170	1980	·59
1435	2080	·69

NOTE: C measured is taken at the average depth along the arc or the plane.

TURBINE HOUSE EXCAVATION BRADWELL

CIRCLE AND PLANE ANALYSIS, DIFFERENT DEPTHS OF TENSION CRACKS
(WITH AND WITHOUT WATER IN CRACKS)

FIG. C-11

APPENDIX D

PHOTOELASTIC ANALYSIS OF STRESSES IN THE BANK OF AN EXCAVATION BY MEANS OF A GELATINE MODEL

1. INTRODUCTION

The only photoelastic material sensitive enough to give a stress pattern due to its own weight, in a reasonably small model, is gelatine, whose extreme sensitivity is probably connected with its very low modulus of elasticity. This low modulus is a disadvantage for small-deflection studies, but is equally an advantage in allowing fairly thin transparent face plates to maintain a gelatine model in a state of plane strain.

There is evidence (Farquharson and Hennes 1940) that gelatine obeys Hooke's law, so that the stress field in it will correspond to linear elasticity. Unfortunately some of the boundary conditions in the present problem are of zero displacement, and as a result the stresses will depend upon Poisson's ratio, ν. For gelatine $\nu = \frac{1}{2}$ (Farquharson and Hennes 1940), which is a much higher value than would ideally be chosen for an elastic material to give the best simulation of soil.

Gelatine models for photoelasticity are made by casting in a mould with transparent faces. Before setting the liquid, gelatine is of course subject only to hydrostatic stresses which produce no photoelastic pattern in a polariscope because the photoelastic fringe order is proportional to the difference between the principal stresses in the plane normal to the light rays, and for hydrostatic stresses this difference is everywhere zero. When the gelatine set in the present experiments, the stresses were unchanged, for the fringe order remained zero everywhere, so that the initial situation corresponded to $K_o = \sigma_3/\sigma_1 = 1$. While in some soils, for example some overconsolidated clays, $K_o = 1$ may be close to reality, in others, such as very soft clays, this value is more likely to be $K_o = 0.5$ (Bishop 1958).

It will be realised from the difficulties discussed above that gelatine experiments are only introduced into soil problems for want of any better approach, and the results should be applied with caution and a clear appreciation of the idealisations and discrepancies involved.

Furthermore, the elastic stress analysis cannot be used for predicting the state of stress at failure, since failure is preceded by non-linear stresses near the failure

surface; but it can be used for an approximate determination of some of the factors influenced by the stress distribution, such as the distribution of pore water pressures immediately after excavation.

2. EXPERIMENTAL TECHNIQUE

(a) Mixture

The first problem was the determination of the mixture to be adopted. For this purpose a perspex casting tank 3" x 3" x 8" high was built, and different mixtures were calibrated for photoelastic sensitivity by extending cast gelatine prisms from the tank and letting them stand under their own weight in the polariscope. The stress at any level was given by the weight of material above, so that the stress pattern consisted of horizontal fringes, whose vertical spacing gave the photoelastic sensitivity from the following formula:

$$f = \frac{(\sigma_1 - \sigma_3)t}{2n} = \frac{\gamma t}{2}\left(\frac{d}{n}\right)$$

where f = "Material fringe value" (the photoelastic constant for the material)

t = thickness of prism (inches)

n = fringe value

d/n = vertical spacing of fringes (in./fringe)

γ = density of material (lb./sq.in.)

Farquharson and Hennes (1940) have described the variation of photoelastic sensitivity with the modulus of elasticity for different proportions of gelatine, glycerine and water. In the light of this work several mixtures were tried and salts were also added in an effort to improve the properties (Leick 1904), without apparent effect.

On the basis of these preliminary tests the following proportions were adopted as giving good working values of the modulus of elasticity and of the material fringe value:

Leaf gelatine:	12%	(by weight)
Glycerine :	28%	" "
Water :	60%	" "

The material fringe value for this mixture was typically f = 0.12 lb./in./fringe, and the density γ = 0.0396 lb./cu.in.

(b) Mould

The size of the mould had then to be decided on.

It was calculated that for a vertical bank 5 in. high a thickness of 4 in. would give approximately three fringes in the height of the bank. The use of a higher bank would probably have resulted in too severe a deformation.

To minimize the influence of the supporting boundaries on the general pattern of the stresses around the excavation, 2H (where H = height of the vertical bank) was adopted as the distance between these boundaries and the bottom corner of the slope.

According to Saint-Venant's principle, an excavation would produce negligible changes of shear stress at distances which are large in comparison with the depth of the excavation. Thus, for a model test of finite size the appropriate boundary condition will be zero shear at boundaries remote from the excavation bank. A distance of 2H from the bank, which is twice the depth of the excavation, could be considered as sufficient, while being a practical dimension.

Hence, the chosen dimensions of the mould were 15" x 20" x 4", and an illustration of it is given in Fig. D-1; it will be seen that the excavation is represented by a removable wooden block.

MOULD FOR PHOTOELASTIC TESTS ON GELATINE

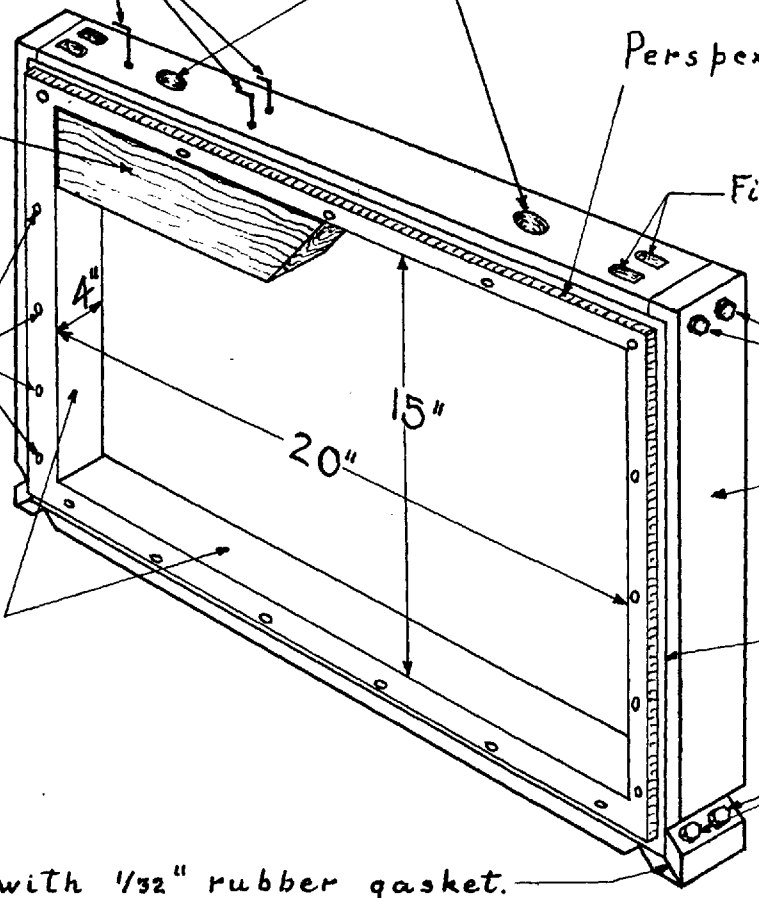


FIG. D-1

(c) Preparation of the Mixture

The total quantity of mixture needed was 50 lb. A 10 gallon barrel coated inside with tin was used over three bunsen burners at low level to heat distilled water to 40°C. The gelatine was then gradually added while the mixture was gently stirred. Once the gelatine dissolved the temperature was brought to 60°C, the glycerine was added, and the temperature was finally increased to 80°C for 10 minutes. The mixture was then weighed and hot water added to correct for the evaporation which had taken place during the process.

The mixture was cooled to 40°C with occasional stirring before being poured into the mould.

(d) Preparation of the Mould

The inside surfaces of the perspex plates were covered with a thin coating of silicone grease and the inside surface of the frame and of the wooden block were given a thick coating.

The gelatine was then poured into the mould through a ¼" inside diameter rubber tube. The calibration tank was also filled and a small amount of oil was deposited on the surface of the gelatine to avoid shrinking due to surface drying.

The castings were left to set and some hot mixture was occasionally added to account for the decrease of volume due to shrinking. This incidentally made sure that the gelatine at the inlet would be the last part to set. After two hours most of the shrinking had taken place and a small amount of oil was added on the surface of the gelatine at the inlet to prevent drying.

(e) Testing

The model was tested after having been allowed to to set for at least 36 hours. One plate was removed with the mould lying on its side and its contact surface was covered with heavy gear oil. The plate was replaced and the mould turned on the other side to repeat the operation. At this point the wooden block was removed and the gelatine was cut at the mouth of the inlet tube.

The model ready for testing was placed in a 15" polariscope with a sodium light source. The isochromatics and isoclinics were recorded directly on the perspex plate with a wax pencil, making sure that the eye of the operator was looking in a direction normal to the plane of the model. This was insured by observing the reflection of the eye of the operator in the glass of the polariscope.

Four different sections were studied, but only two castings were needed: the model with a slope of ½:1 was tested and then cut back to the vertical by a greased spatula on a 90° brass-plate guide. Similarly the Bradwell section model was cut back to give a 1:1 slope.

3. EXPERIMENTAL DETAILS

(a) Clarity

Clarity of a 4" thick model presented a problem because of air bubbles in the mixture. It was found essential to avoid any turbulence during stirring and during pouring.

The same mixture could be melted and used again with a good clarity if after the first test all the gelatine surfaces which had been in contact with oil were carefully cleaned with alcohol.

(b) Creep and Temperature Effects

It was found that a certain amount of creep which occurs in fresh gelatine effectively ceases after a day. Consequently at least 36 hours was allowed to elapse after mixing before testing.

It has been suggested (Crisp 1952) that the

material fringe value of gelatine is very sensitive to temperature variation. The room temperature variation during the two hours duration of a test never exceeded 3° F and no appreciable change of the calibration resulted.

(c) Friction

It is thought that friction was effectively eliminated by the use of silicone grease and heavy oil on the surfaces. This point was verified in a pilot test by inclining the mould on either side at an angle of about 45°, hence producing a movement of the gelatine, and then bringing it back to its original position. In all cases the fringes came back to their original positions, which had been recorded on the perspex face plate.

The importance of friction reduces rapidly with increasing thickness of the model, and it is felt that the present 4" thickness involved much less frictional trouble than the 1" thickness adopted by some previous experimentalists.

(d) Deformation

In the case of the vertical bank a severe deformation was encountered at the bottom corner of the slope; the deformation caused the corner to bend sharply inwards. This was effectively corrected by using a slightly rounded

(⅛" diameter) corner. Some deformation of the overall height (up to 5%) still remained, and could have been partly eliminated only by using a stiffer mixture, with a consequent loss in sensitivity.

(e) Initial Stresses

Before removing the wooden block, the models were checked for initial stresses. They were found to be stress-free except for a localised effect against the inlet in the upper part of the bank. This effect was reduced when the gelatine was cut at the mouth of the inlet tube, but the remaining effect caused a small local error in the stress reading.

4. RESULTS

Four different sections were studied:

1. Vertical bank
2. ½:1 slope
3. 1:1 slope
4. Bradwell section.

An example of the results as recorded is shown in Fig.D-2 for the ½:1 slope. The "isochromatic" lines give contours of constant difference in principal stresses

$(\sigma_1 - \sigma_3)$, while the isoclinics are contours of constant direction of the major principal stress. The numerical value of the isochromatics, or "fringe orders", were mostly found by interpolation, but on the free boundaries they were determined by means of the Sénarmont ¼ wave plate compensation technique, giving fringe orders to two places of decimals.

The results were first corrected to the initial geometry, which is shown as a fine line in Fig.D-2. For doing this the points of contact of the fringes with the boundaries were scaled out proportionally to the initial dimension of the boundary. From these corrected points the fringes were then redrawn to corrected positions, Fig.D-3, following the general layout of the observed fringes. Using the calibration, the results were expressed in terms of γH, and contours along which $(\sigma_1 - \sigma_3) = 0.1\,\gamma H$, $0.2\,\gamma H$, etc. were found by interpolation; they are given in Fig. D-7, D-11, D-15 and D-19.

The isoclinics also required correction because of the change of geometry and this involved more possibility of error. For example, in the case of the ½:1 slope the direction of the major principal stress which, at the

surface of the slope, is parallel to the surface is measured as around 30° with the horizontal on the deformed section (Fig.D-2), whereas it should be at 26.5° on the corrected section (Fig.D-3). The free boundaries, where the directions of the principal stresses are known, were used as a basis for the correction and the corrected isoclinics are shown in Fig. D-10, D-14, D-18 and D-22.

5. SEPARATION OF PRINCIPAL STRESSES

(a) Governing equation

The best method of separating the principal stresses in gelatine work is by a numerical solution of the Laplace equation for the sum of the principal stresses $(\sigma_1 + \sigma_3)$. In the case of plane strain where the body forces are the only forces the compatibility equation takes the form of Laplace's equation (Timoshenko and Goodier, 1951, page 25).

$$\left(\frac{\partial^2}{\partial x^2} + \frac{\partial^2}{\partial y^2}\right)(\sigma_x + \sigma_y) = \nabla^2(\sigma_x + \sigma_y) = 0$$

where σ_x and σ_y are the stresses parallel to the X and Y axes.

Since $(\sigma_x + \sigma_y) = (\sigma_1 + \sigma_3)$ always,

$$\nabla^2(\sigma_1 + \sigma_3) = 0$$

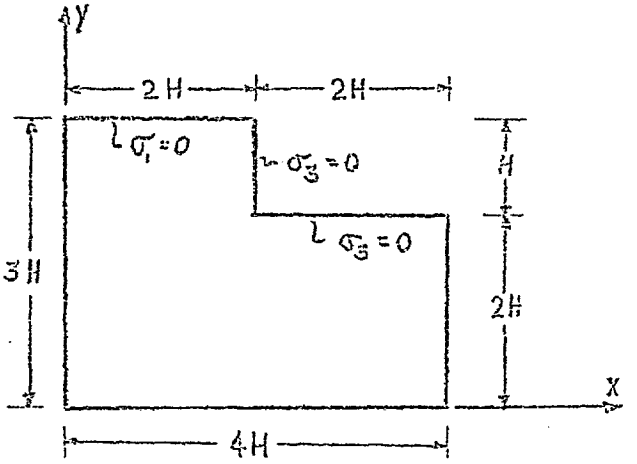
With appropriate boundary conditions this equation can be solved by the Relaxation method (Allen, 1955).

(b) Boundary Conditions

The boundary conditions can be determined as follows:

(i) Free Boundaries:

On the free boundaries the sum of principal stresses $(\sigma_1 + \sigma_3)$ is numerically equal to the value of $\pm(\sigma_1 - \sigma_3)$ because the stress normal to the boundary is a principal stress and is zero. Adopting $\sigma_1 > \sigma_3$ always, considerations of the isoclinics give the free boundary conditions shown in the following diagram:



(ii) Boundary y = 0:

The conditions along this boundary are:

$$\left.\begin{aligned} v &= 0 \\ \tau_{xy} &= 0 \end{aligned}\right\} \qquad (1)$$

where v is the displacement parallel to the y-axis and τ_{xy} is the shear stress in the x-y plane.

This means that for all x,

$$\frac{\partial v}{\partial y} = 0 \;,\quad \frac{\partial^2 v}{\partial x^2} = 0 \quad , \quad \text{and} \quad \frac{\partial \tau_{xy}}{\partial x} = 0 \qquad \cdots\cdots\cdots (2)$$

Now, the shearing strain γ_{xy} in the x-y plane along this boundary is expressed as follows:

$$\gamma_{xy} = \frac{\partial u}{\partial y} + \frac{\partial v}{\partial x} = \frac{1}{G}\,\tau_{xy} \qquad \cdots\cdots\cdots (3)$$

where G is the modulus of elasticity in shear.

(1), (2), (3) imply

$$\frac{\partial u}{\partial y} = 0 \qquad \cdots\cdots\cdots\cdots\cdots (4)$$

Differentiating eq.(3), we have

$$\frac{\partial \gamma_{xy}}{\partial x} = \frac{\partial^2 u}{\partial x \partial y} + \frac{\partial^2 v}{\partial x^2} = \frac{1}{G}\frac{\partial \tau_{xy}}{\partial x} \qquad \cdots\cdots (5)$$

(2) and (5) give

$$\frac{\partial^2 u}{\partial x \partial y} = 0 \qquad \cdots\cdots\cdots\cdots\cdots (6)$$

Hooke's law for plane strain

$$\frac{\partial u}{\partial x} = \frac{1}{E}\left[-\nu(1+\nu)\sigma_y + (1-\nu^2)\sigma_x\right] \qquad \ldots (7)$$

which can be differentiated and combined with (6) to give

$$\frac{\partial^2 u}{\partial x \partial y} = \frac{1}{E}\left[-\nu(1+\nu)\frac{\partial \sigma_y}{\partial y} + (1-\nu^2)\frac{\partial \sigma_x}{\partial y}\right] = 0 \qquad \ldots (8)$$

Equilibrium requires that

$$\frac{\partial \sigma_y}{\partial y} + \frac{\partial \tau_{xy}}{\partial x} + Y = 0 \qquad \ldots\ldots\ldots (9)$$

where Y is the vertical body force per unit volume.

(9) and (2) imply

$$\frac{\partial \sigma_y}{\partial y} = -Y \qquad \ldots\ldots\ldots\ldots (10)$$

(10) and (8) give

$$\frac{\partial \sigma_x}{\partial y} = -\frac{\nu}{(1-\nu)} Y \qquad \ldots\ldots\ldots\ldots (11)$$

From (10) and (11),

$$\frac{\partial}{\partial y}(\sigma_x + \sigma_y) = -\frac{Y}{1-\nu} \qquad \ldots\ldots\ldots\ldots (12)$$

Finally, noting that $(\sigma_x + \sigma_y) = (\sigma_1 + \sigma_3)$ equation (12) becomes

$$\frac{\partial}{\partial y}(\sigma_1 + \sigma_3) = -\frac{Y}{1-\nu} \qquad \ldots\ldots\ldots (13)$$

Equation (13) is the required boundary condition. Y, the body force, is equal to γ, the density of the material.

(iii) Boundaries $x = 0$, $x = 4H$.

By an exactly similar analysis for the vertical boundaries where $u = 0$ and $\tau_{xy} = 0$, it can be shown that

$$\frac{\partial}{\partial x}(\sigma_1 + \sigma_3) = -\frac{X}{1-\nu} \qquad \ldots\ldots\ldots (14)$$

The body force $X = 0$, so that the resulting boundary condition is

$$\frac{\partial}{\partial x}(\sigma_1 + \sigma_3) = 0 \qquad \ldots\ldots\ldots\ldots (15)$$

6. RELAXATION OF LAPLACE'S EQUATION

Using the mixed boundary conditions given above, Laplace's equation was solved by the Relaxation method.

Due to the localised concentration of stresses at the bottom corner of the slope it was important to use a fine mesh around this point; an example of such a net is given in Fig.D-6, where a mesh length of 1/12 H is used near the corner of the 1:1 slope.

Contours of the sum of the principal stresses were then constructed by interpolation and are given in Fig.D-10, D-14, D-18 and D-22.

7. FINAL RESULTS

The final results are presented in more useful graphs giving the individual values of σ_1 and σ_3 in Fig.D-9, D-13, D-17 and D-21.

As a general check of the calibration and calculations the normal pressure at the bottom of the model was computed and its resultant compared with the total weight of the gelatine. Every case checked within 45%.

8. DISCUSSION

The position and properties of the supporting boundaries which are adopted in a model test must be taken into account in the interpretation of the results. In the present tests, "shear-free" boundaries were placed typically

at a distance of 2 H from the bottom corner of the vertical bank.

To estimate the influence of the boundary conditions on the general pattern of the stresses, tests were made using "fixed" boundaries, on which $u = v = 0$. This condition was simulated by fixing a fine aluminium grid on the inner faces of the frame of the mould (Fig.D-1).

The isochromatics and isoclinics from such a test for the ½:1 slope are given in Fig.D-4, and the isochromatics for the two types of boundary condition are superposed in Fig.D-5. It is seen that the results are qualitatively the same in the middle part of the section, and since the fringe values are the same for the two tests, the stress differences must also be quantitatively similar.

Hence the boundaries can be said to have had little influence on the shear stresses around the slope. The "shear-free" boundaries were preferred for their simpler boundary conditions in the Relaxation solution.

The 2% accuracy of the normal pressure at the bottom of the model does not imply that the same accuracy can be expected of the stresses around the excavation. Due to the large deformations of the slope and the difficulty

of correcting the section to its initial geometry, the part around the slope was probably the most erratic and an error of 10% would more likely be representative.

This 10% error is apparent for the vertical bank and the ½:1 slope if the value of σ_1 is considered at a point close to the boundary behind the slope, at a depth H below the surface. At this point, which is on the same level as the bottom of the excavation, the value measured should be $\sigma = 1.0\ \gamma H$, while in fact it was measured as $1.1\ \gamma H$, Fig.D-9, D-13. On the other hand, the measured values for the 1:1 slope, Fig.D-17, and for the Bradwell section, Fig.D-21, give exactly the expected values.

This may also be indicative that the boundaries were far enough from the wall of the excavation for the results not to be too affected by them. On the other hand, in the case of the vertical bank, a tension crack opened at the surface between the gelatine and the mould to a depth of nearly H/5.

Another factor affecting the accuracy of the results is the width of the fringes which in some part of the model would become large enough to form a shady area as can be seen in Fig.D-2.

Finally, it is difficult to estimate the influence of the large deformations on the shear stresses measured. They might very well lead to serious errors, but more data are needed before their influence can be properly appreciated.

FIG. D-2

1/2:1 SLOPE

RESULT SHEET

SHEAR-FREE BOUNDARIES

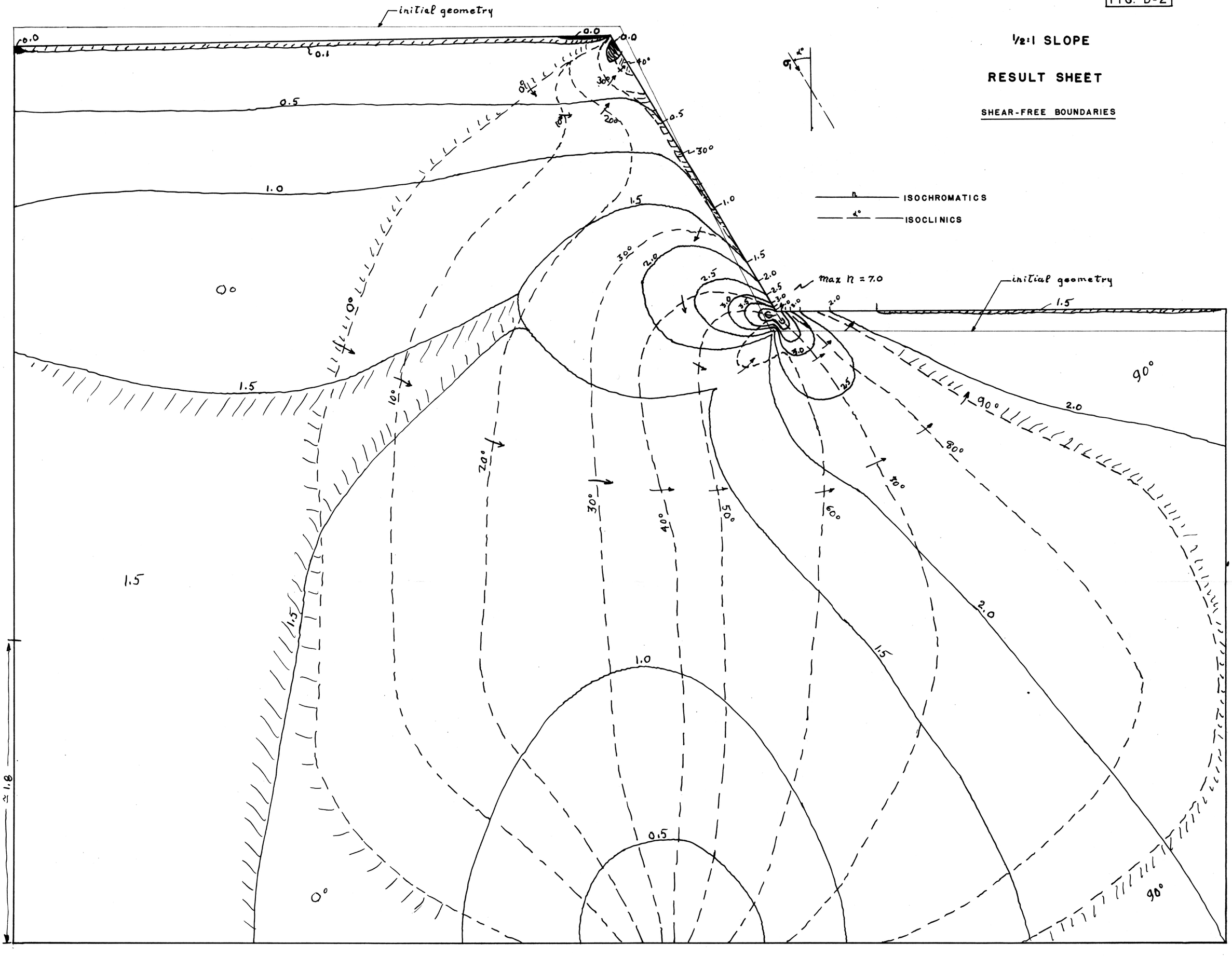


FIG. D-3

1/2:1 SLOPE

CORRECTED RESULTS

SHEAR-FREE BOUNDARIES

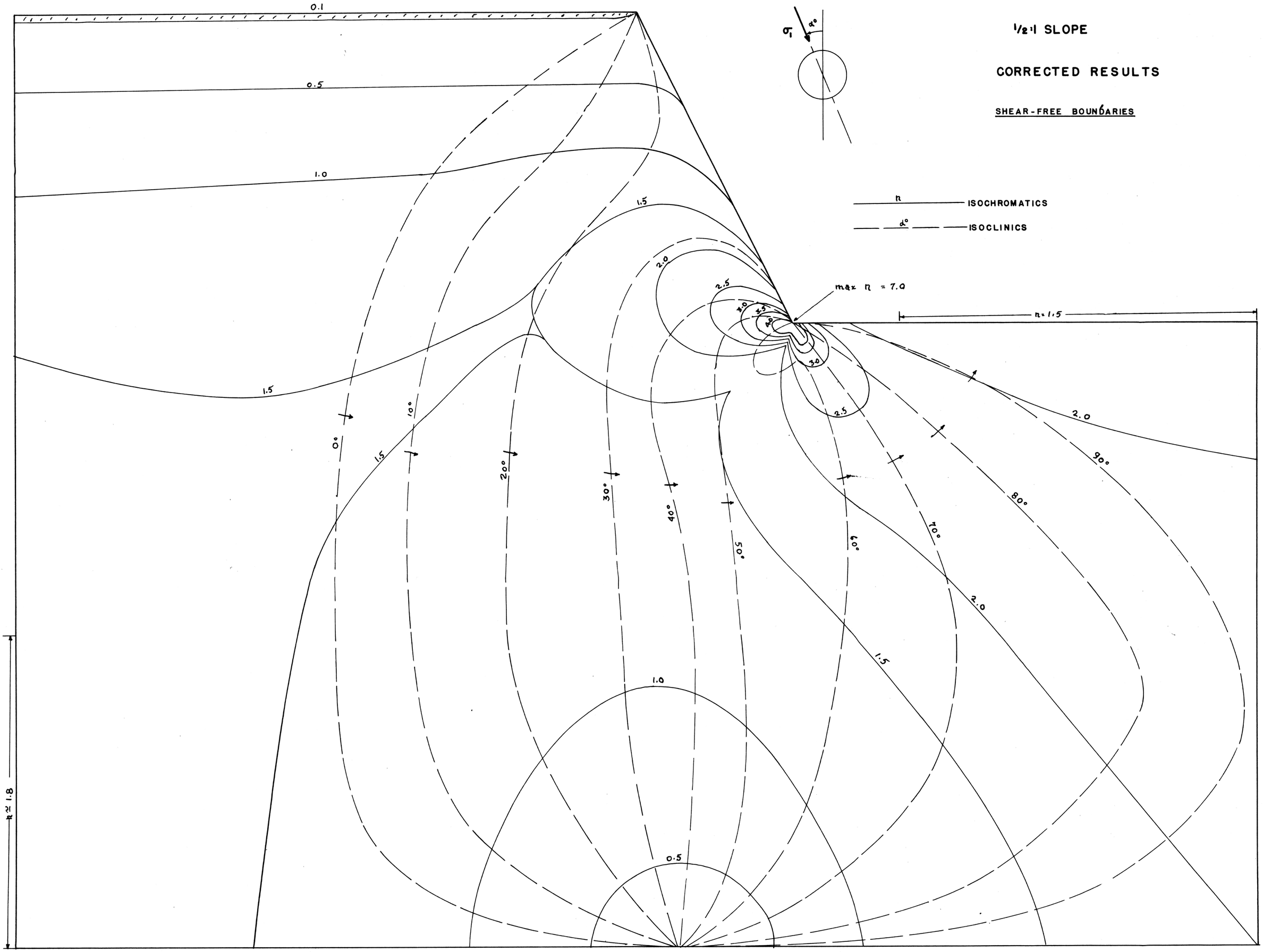


FIG. D-4

1/2:1 SLOPE.

RESULTS FOR "FIXED" BOUNDARIES.

n ——— ISOCHROMATICS.

α° — — — ISOCLINICS.

n = fringe order

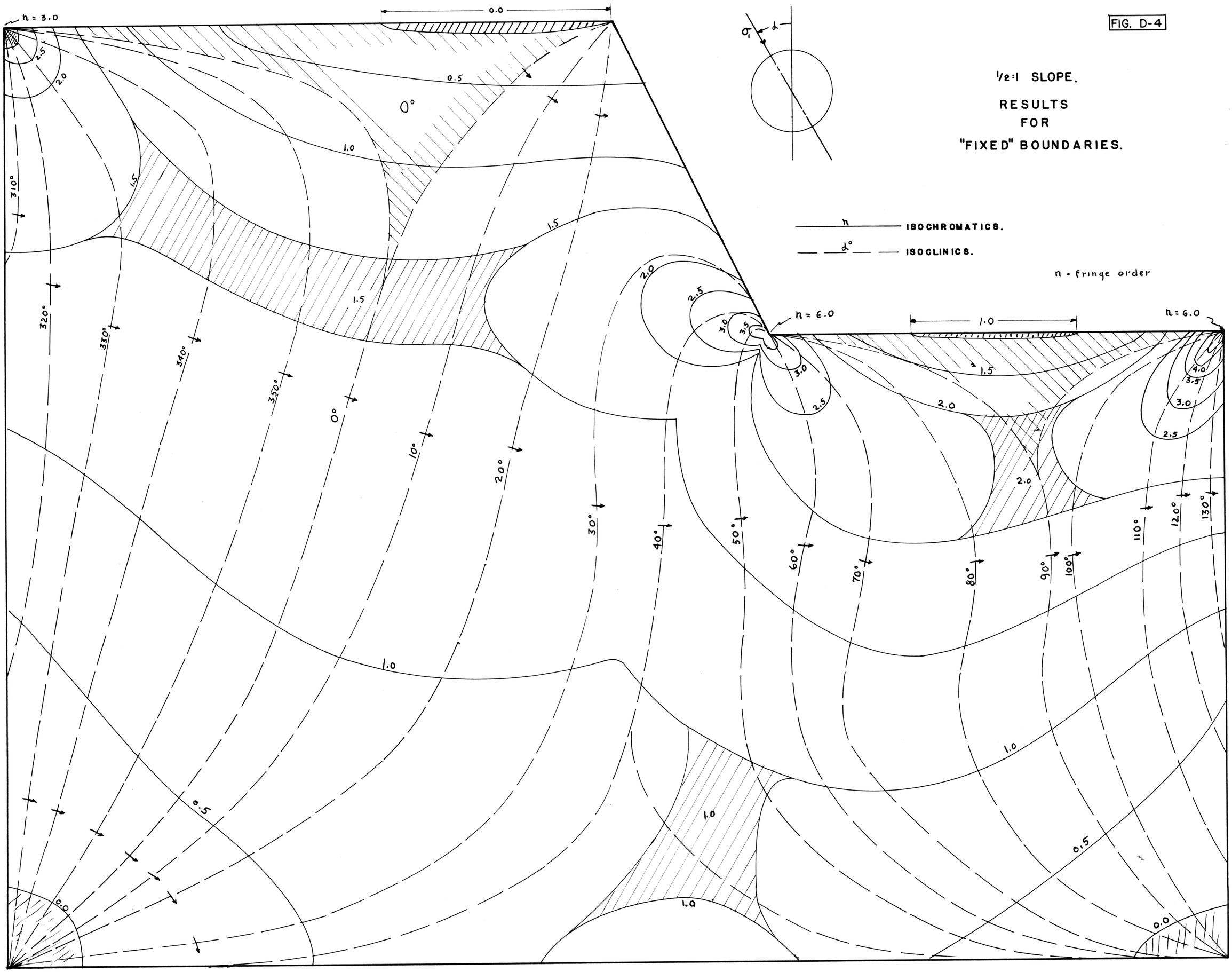


FIG. D-5

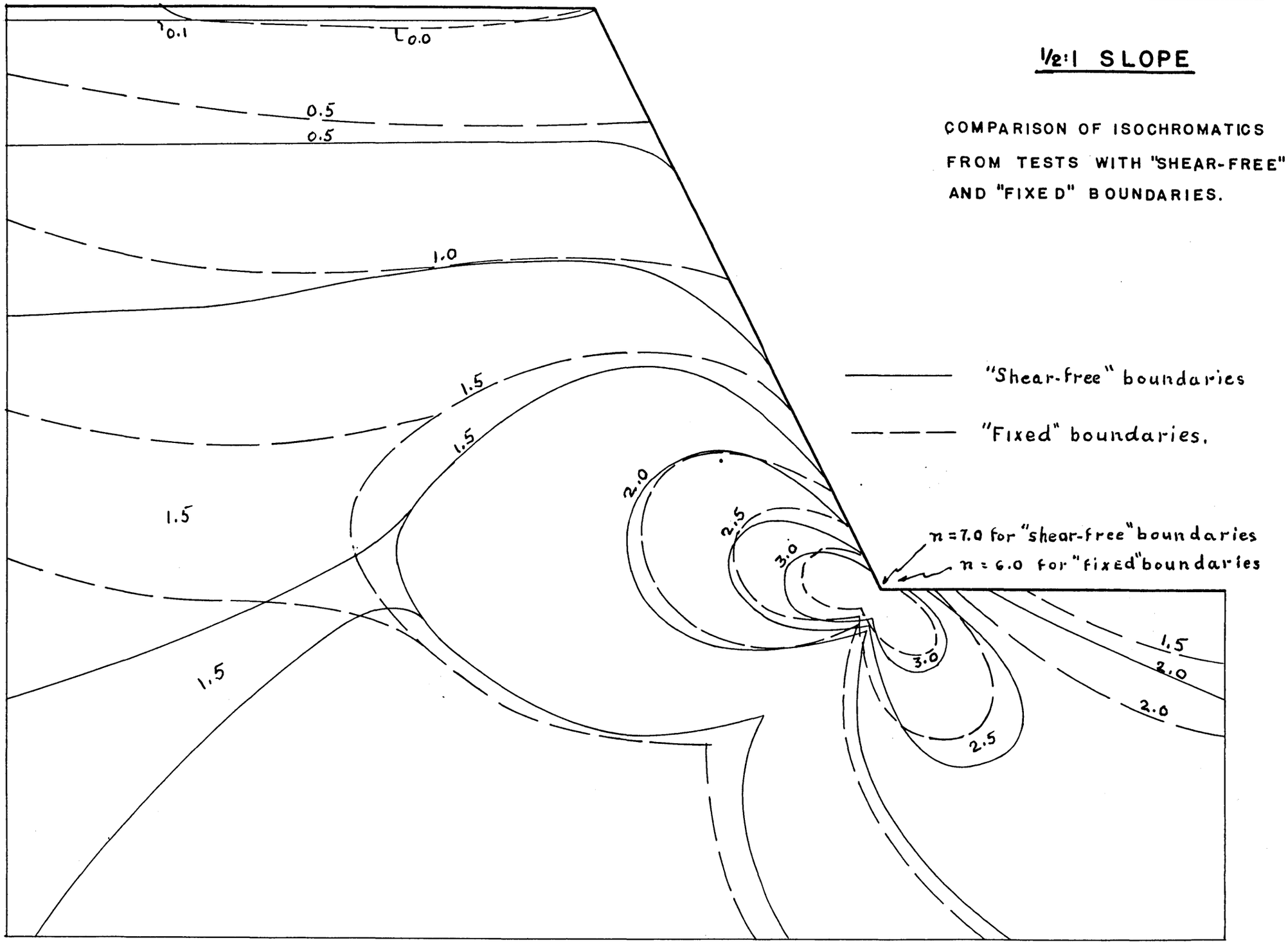

1/2:1 SLOPE
COMPARISON OF ISOCHROMATICS FROM TESTS WITH "SHEAR-FREE" AND "FIXED" BOUNDARIES.
"Shear-free" boundaries
"Fixed" boundaries.
n = 7.0 for "shear-free" boundaries
n = 6.0 for "fixed" boundaries
0.1
0.0
0.5
0.5
1.0
1.5
1.5
1.5
1.5
2.0
2.5
3.0
3.0
2.5
2.0
2.0
1.5

FIG D-6

RELAXATION SOLUTION for the 1:1 slope.

$$\nabla^2(\sigma_1 + \sigma_3) = 0$$

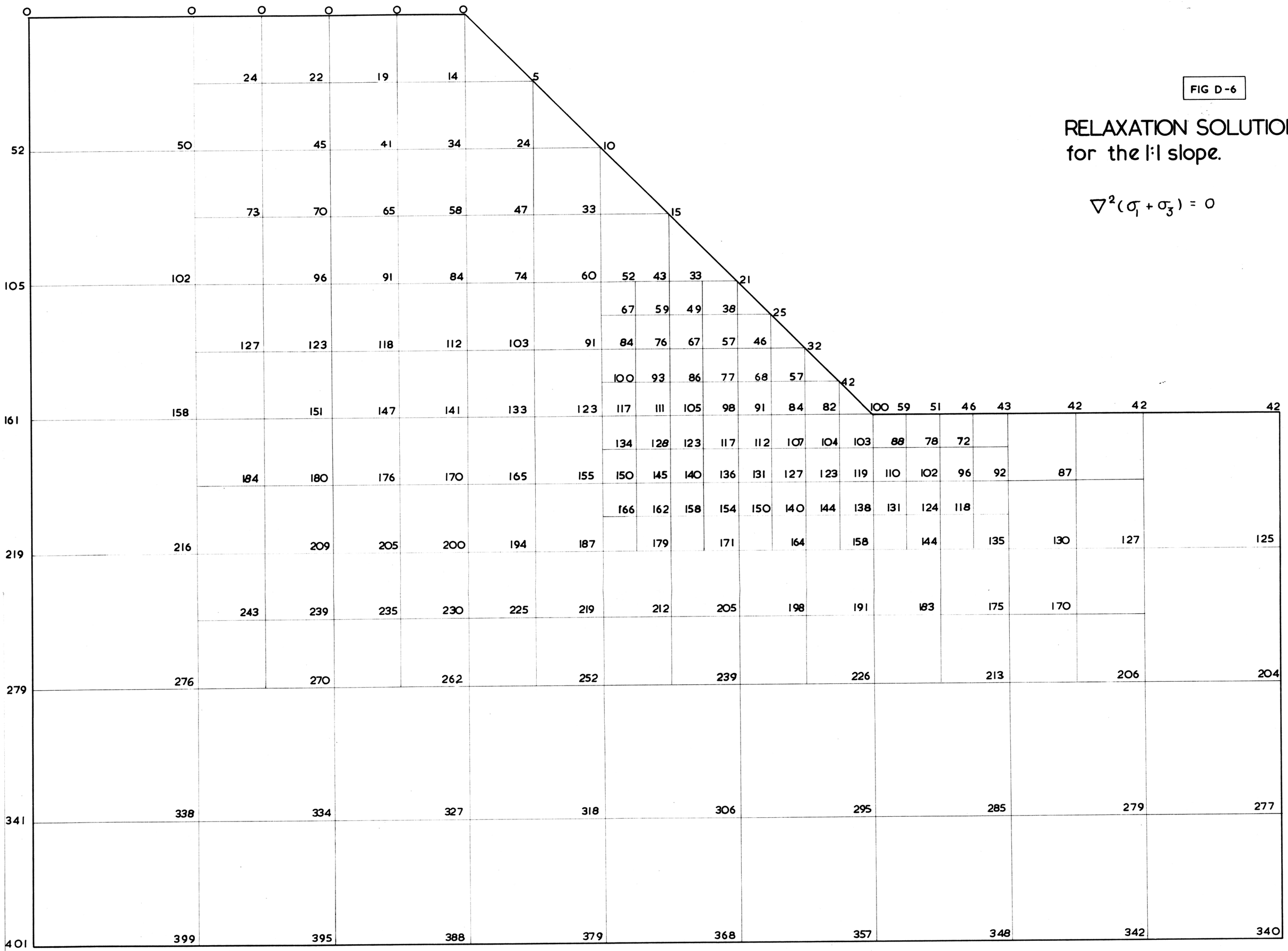


FIG-D7

VERTICAL SLOPE

$(\sigma_1 - \sigma_3)$

$N = \frac{\sigma_1 - \sigma_3}{\gamma H}$

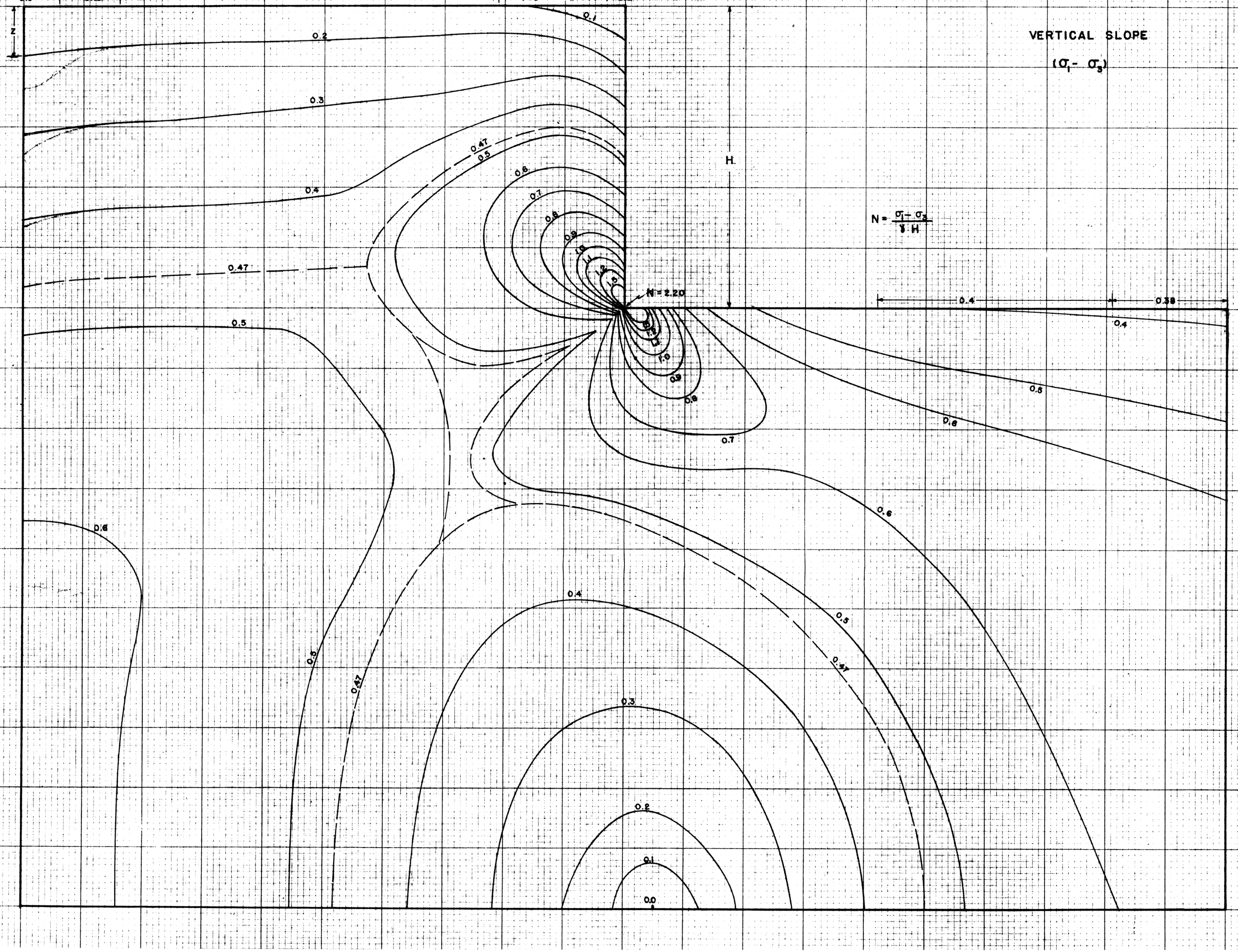


FIG D8

VERTICAL SLOPE

$(\sigma_1 + \sigma_3)$

$N = \frac{\sigma_1 + \sigma_3}{\gamma H}$

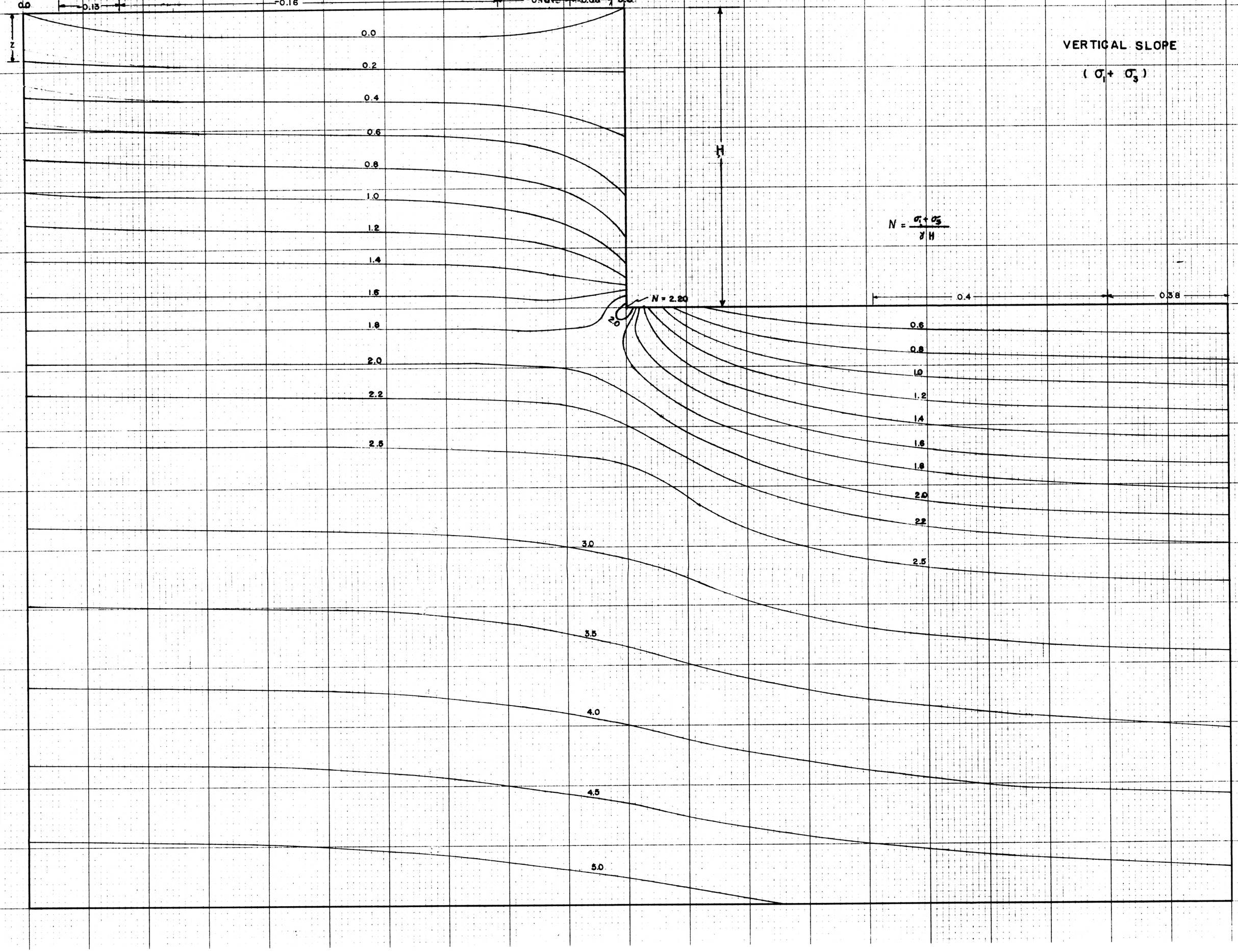


FIG D9

VERTICAL SLOPE

σ_1 AND σ_3

H

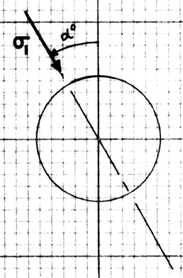
0.0 ——→ $N = \frac{\sigma_3}{\gamma H}$

0.1 ——→ $N = \frac{\sigma_1}{\gamma H}$

FIG. D-10

VERTICAL SLOPE

ISOCLINICS



0°

0°

5°

10°

20°

30°

40°

45°

50°

60°

70°

80°

90°

90°

0°

FIG D11

1/2 : 1 SLOPE

$(\sigma_1 - \sigma_3)$

$$N = \frac{\sigma_1 - \sigma_3}{\gamma H}$$

H

N = 2.20

0.03

0.0

0.1

0.2

0.3

0.4

0.47

0.5

0.6

0.7

0.8

0.9

1.0

1.1

1.2

0.47

0.5

0.6

0.7

0.8

0.9

0.47

0.5

0.57

0.47

0.4

0.3

0.2

0.1

0.0

0.4

0.5

0.6

0.47

0.5

FIG. D12

1/2:1 SLOPE

$(\sigma_1 + \sigma_3)$

$$N = \frac{\sigma_1 + \sigma_3}{\gamma H}$$

H

N= 2.20

-0.03

0.0

0.0

0.1

0.2

0.4

0.6

0.8

1.0

1.2

1.4

1.6

1.8

2.0

2.2

2.5

3.0

3.5

4.0

4.5

5.0

5.5

0.47

0.5

0.6

0.8

1.0

1.2

1.4

1.6

1.8

2.0

2.2

2.5

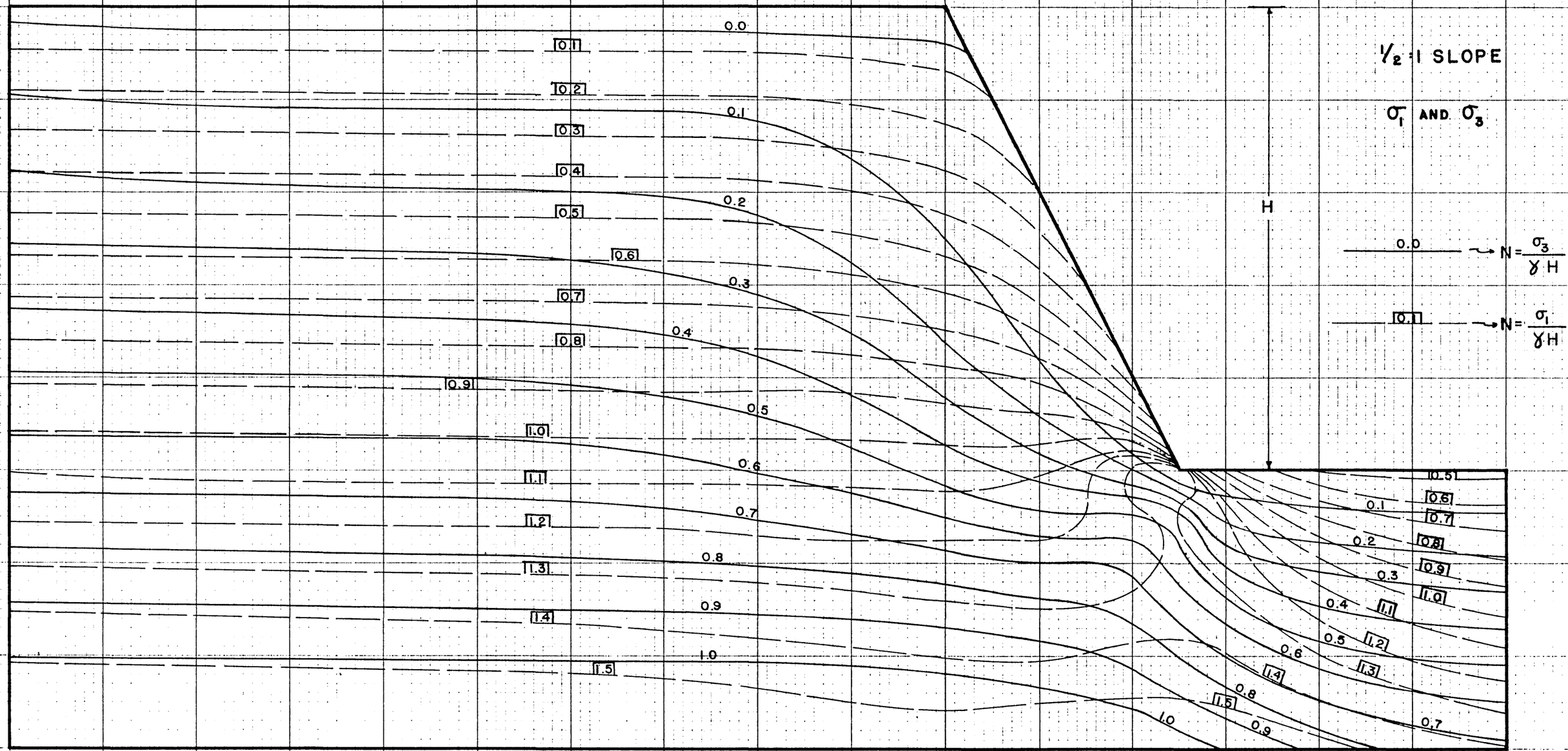
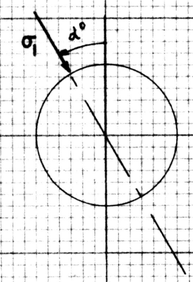

1/2 : 1 SLOPE
σ1 AND σ3
H
0.0 → N = σ3 / γH
0.1 → N = σ1 / γH
0.0
0.1
0.2
0.3
0.4
0.5
0.6
0.7
0.8
0.9
1.0
1.1
1.2
1.3
1.4
1.5

FIG. D-14

1/2:1 SLOPE

ISOCLINICS



0°

0°

10°

20°

30°

40°

50°

60°

70°

80°

90°

90°

0°

90°

FIG-D15

1:1 SLOPE

$(\sigma_1 - \sigma_3)$

$$N = \frac{\sigma_1 - \sigma_3}{\gamma H}$$

H

0.0
0.1
0.2
0.3
0.35
0.4
0.45
0.5
0.57
0.6
0.7
N= 1.0
0.42
0.5
0.57
0.4
0.35
0.3
0.2
0.1
0

FIG-D16

1:1 SLOPE

$(\sigma_1 + \sigma_3)$

$N = \frac{\sigma_1 + \sigma_3}{\gamma H}$

H

0.0 0.0 0.0

0.2

0.4

0.6

0.8

1.0

1.2

1.4

1.6

1.8

2.0

2.5

3.0

3.5

N = 1.0

0.42

0.5

0.6

0.8

1.0

1.2

1.4

1.6

1.8

2.0

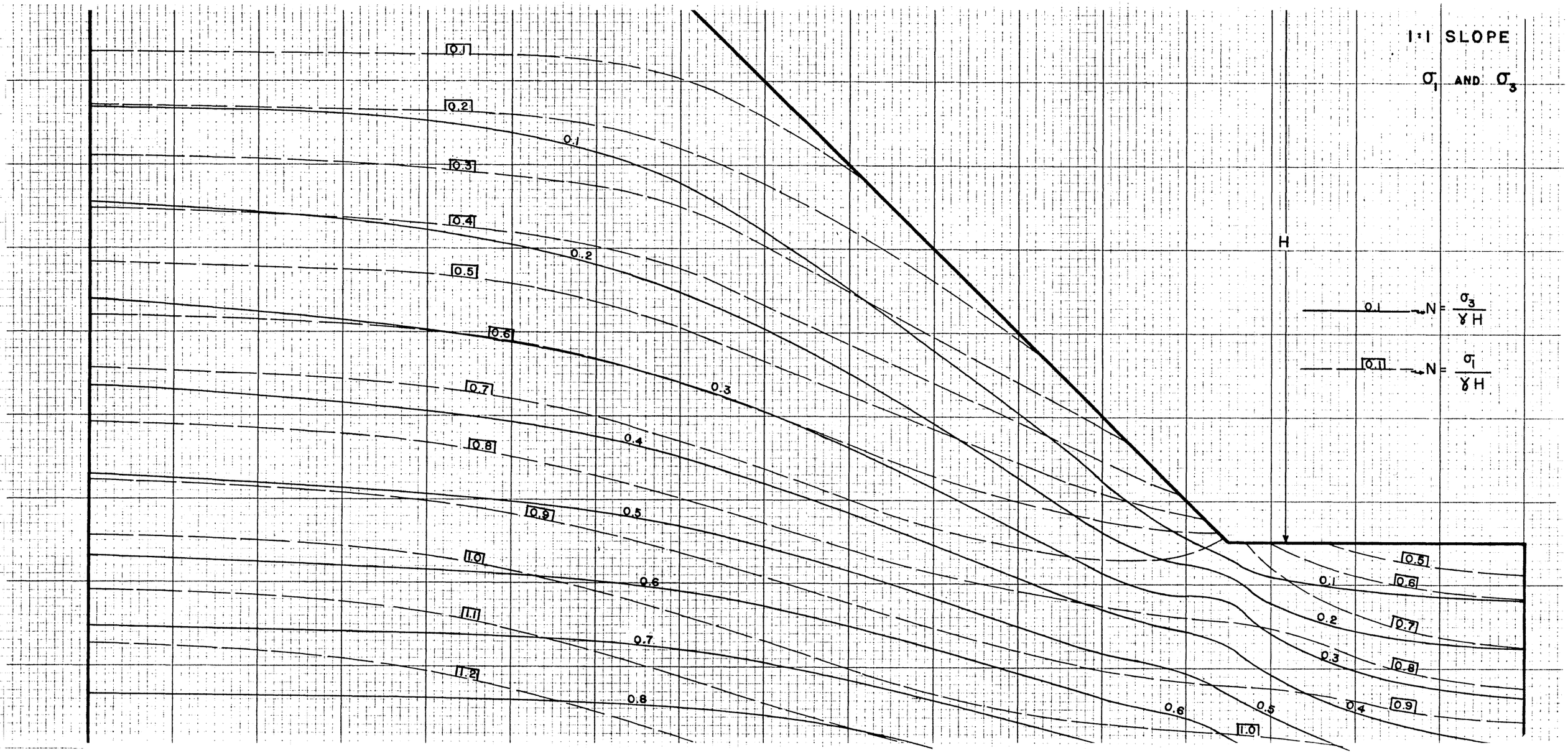
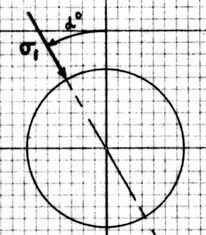

1:1 SLOPE
σ_1 AND σ_3
H
0.1 → $N = \frac{\sigma_3}{\gamma H}$
[0.1] → $N = \frac{\sigma_1}{\gamma H}$
[0.1]
[0.2]
[0.3]
[0.4]
[0.5]
[0.6]
[0.7]
[0.8]
[0.9]
[1.0]
[1.1]
[1.2]
0.1
0.2
0.3
0.4
0.5
0.6
0.7
0.8
0.6
0.5
0.4
[1.0]
[0.5]
[0.6]
[0.7]
[0.8]
[0.9]
0.1
0.2
0.3

FIG. D-18

1:1 SLOPE

ISD CLINICS



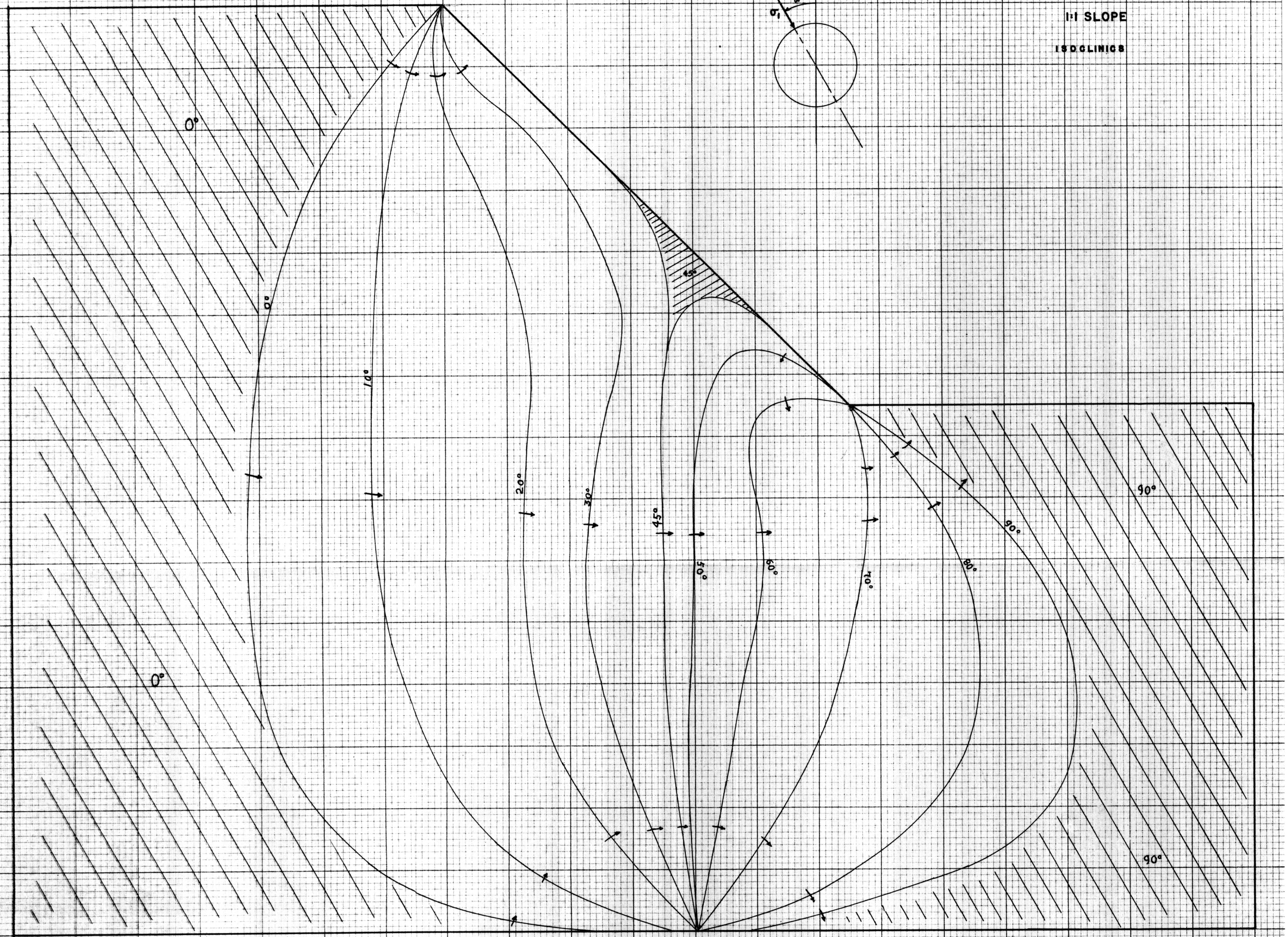


FIG D19

BRADWELL SLOPE

$(\sigma_1 - \sigma_3)$

$N = \frac{\sigma_1 - \sigma_3}{\gamma H}$

H

N= 2.90

00 0.03 0.0 0.06 0.10 0.0 0.06 0.09 0.0

0.1 0.2 0.3 0.4 0.5 0.55 0.6 0.7 0.8

0.1 0.2 0.3 0.4 0.5 0.55 0.6 0.8 0.94 1.1 1.3 1.5

0.66 0.7 0.8 0.94 0.94

0.8 0.6 0.55 0.8 0.4 0.3 0.2 0.1 0.0 0.4 0.65 0.8 0.9 0.94

0.6

FIG-D20

BRADWELL SLOPE

$(\sigma_1 + \sigma_3)$

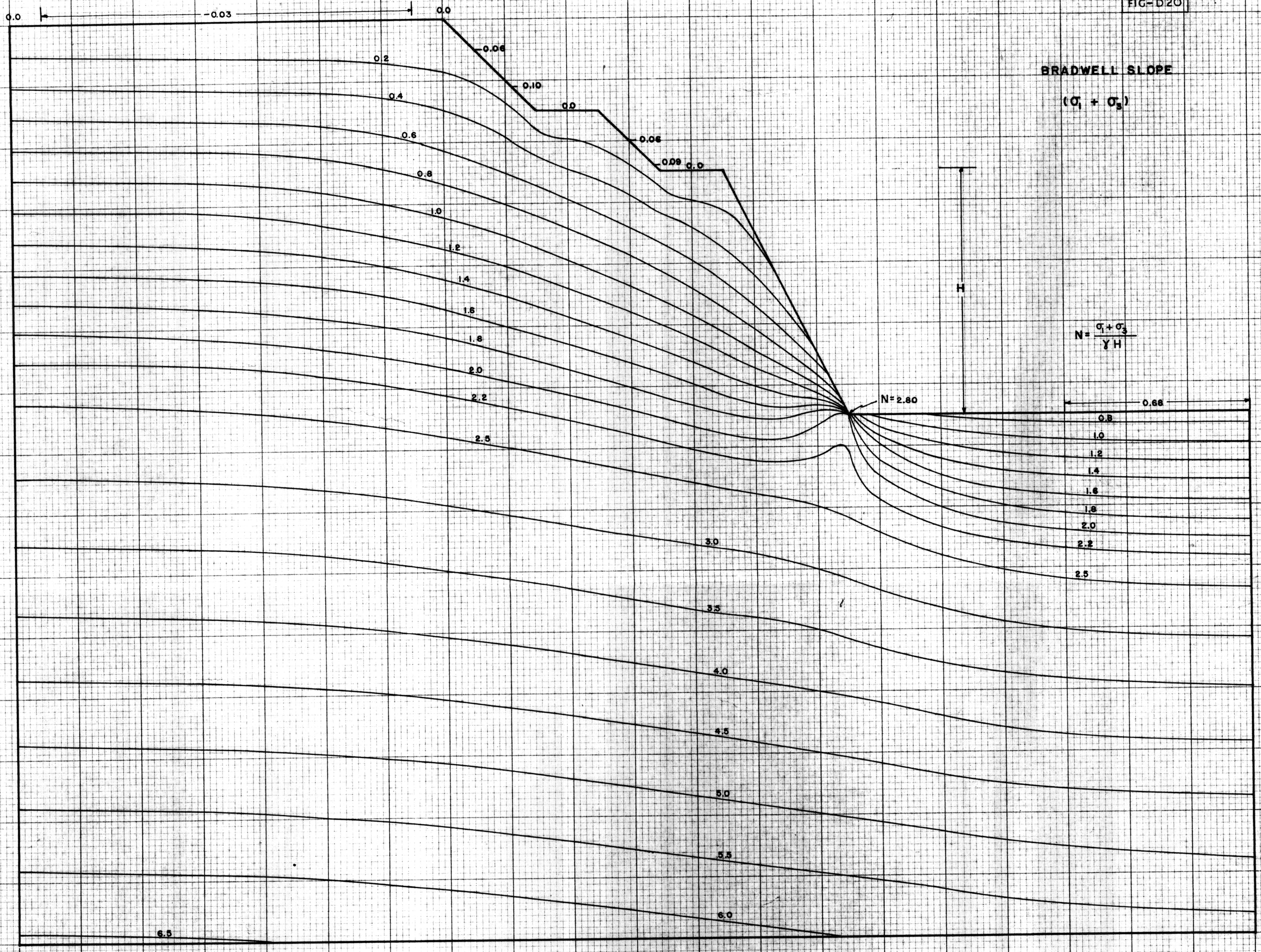


FIG-D21

BRADWELL SLOPE

σ_1 AND σ_3

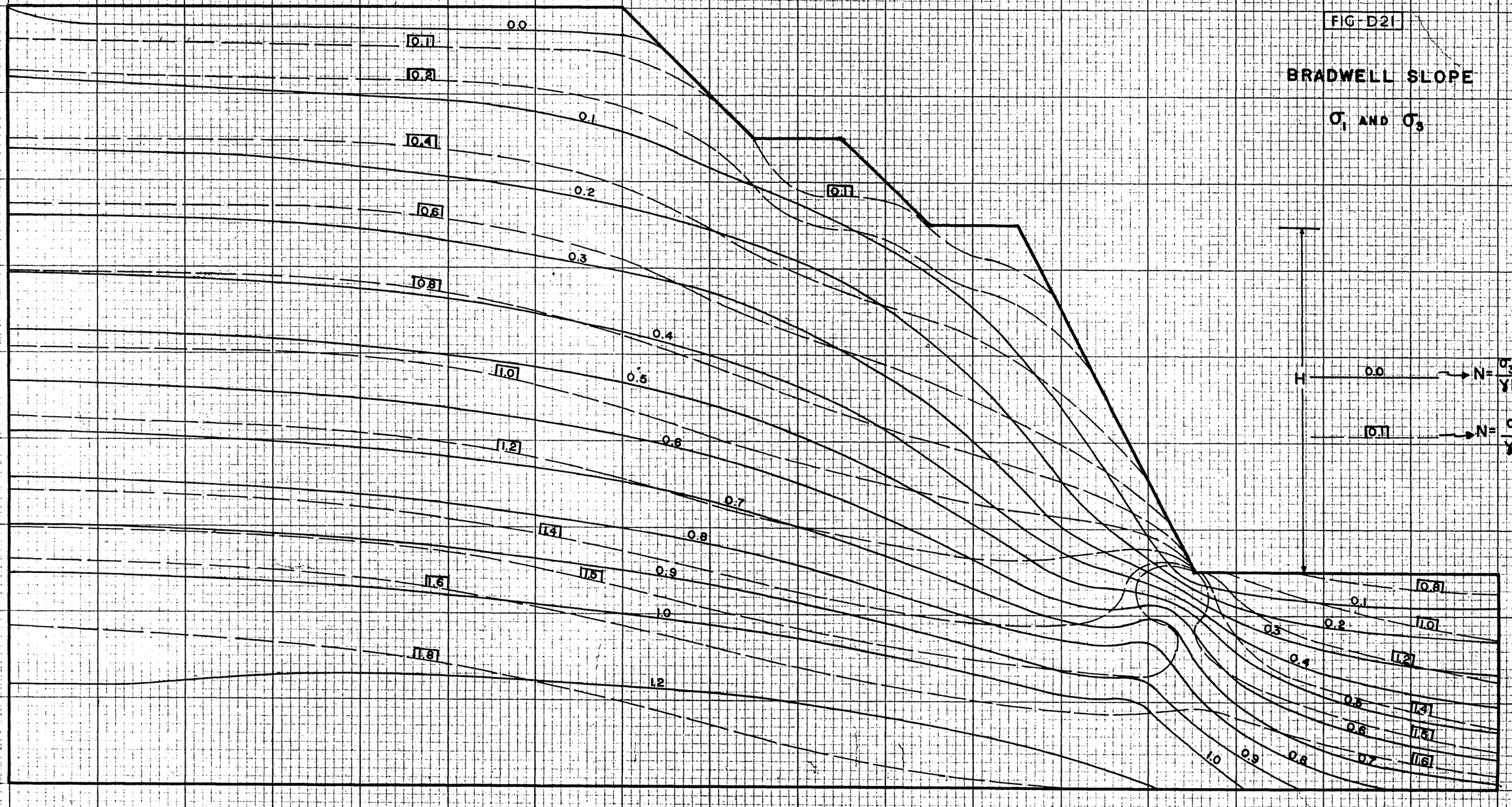
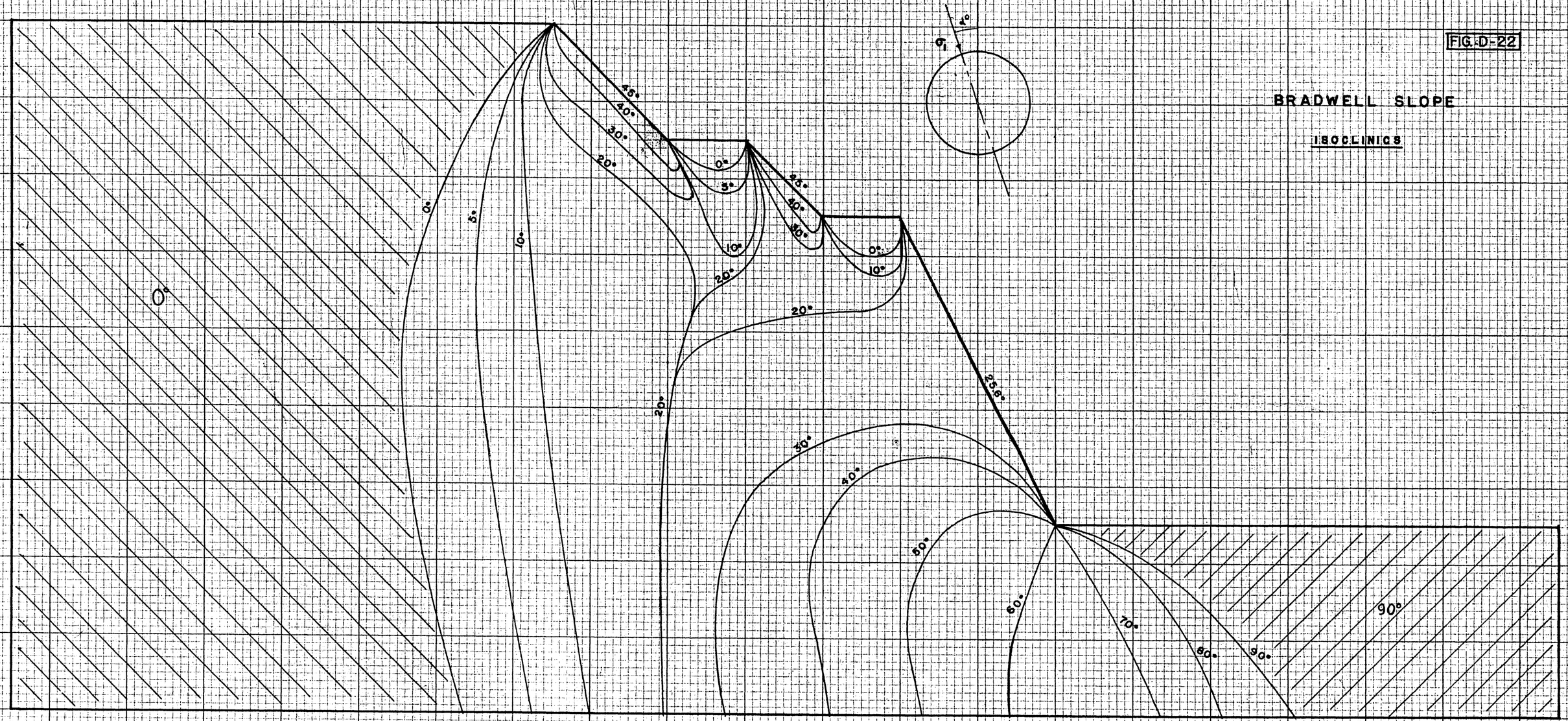


FIG. D-22

BRADWELL SLOPE

ISOCLINICS



REFERENCES

Allen, D. N. (1955) "Relaxation Methods"
McGraw-Hill Publishing Company, London.

Bishop, A. W. (1955) "The Use of the Slip Circle in the Stability Analysis of Slopes"
Geotechnique, Vol.5, pp.7-17.

Bishop, A. W. (1958) "Test Requirements for Measuring Earth Pressure at Rest"
Brussels Conference, Vol.1, pp.2-14.

Bishop, A. W. and Henkel, D. J. (1957) "The measurement of Soil Properties in the Triaxial Test"
Edward Arnold Ltd., London.

Brees, S. C. (1837) "Railway Practice"
John Williams, London.

Crisp, J. D. C. (1952) "The Use of Gelatine Models in Structural Analysis"
Proc. Inst. Mech. Eng. Vol.1B, No.12.

DeLory, F. A. (1957) "Long-Term Stability of Slopes in Over-consolidated Clays"
Ph.D. Thesis, University of London.

Farquharson, F. B. and Hennes, R. G. (1940) "Gelatine Models for Photoelastic Analysis of Stress in Earth Mass"
Civil Engineering.

Glossop, R. (1948) "The London Clay. Part I - Field and Laboratory Technique"
Verres et Silicates Industriels, Vol.13, No.7, pp.93-98.

Golder, H. Q. and Skempton, A. W. (1948) "The Angle of Shearing Resistance in Cohesive Soils for Tests at Constant Water Content"
2nd Conf. Soil Mech. Vol.I, pp.185-192.

Henkel, D. J. (1957) "Investigations of Two Long-Term Failures in London Clay Slopes at Wood Green and Northolt"
Proc. 4th Int. Conf. Soil Mech. Vol.II, p.315.

Henkel, D. J. and Gilbert, G. D. (1952) "The Effect of the Rubber Membrane and the Measured Triaxial Compression Strength of Clay Samples"
Geotechnique, Vol.III, p.20.

Hill, R. (1956) "The Mathematical Theory of Plasticity"
Clarendon Press, Oxford. Footnote, p.296.

Hvorslev, M. J. (1951) "Time Lag and Soil Permeability in Ground Water Observations"
Waterways Experiment Station, Bulletin No.36.

Jukes-Brown, A. J. (1911) "The Building of the British Isles"
Stamford, London.

Leick, A. (1904) Uber künstliche Doppelbrechung und Elastizitat von Gelatineplatten"
Ann. Phys. IV, 14, pp.139-152.

Skempton, A. W. (1948) "The Rate of Softening in Stiff Fissured Clays, with Special Reference to London Clay"
Proc. 2nd Int. Conf. Soil Mech. Vol.II, p.50.

Skempton, A. W. (1953) "The Colloidal Activity of Clays"
Proc. 3rd Int. Conf. Soil Mech. Vol.I, pp.57-61.

Skempton, A. W. (1954) "The Pore-Pressure Coefficients A and B"
Geotechnique, Vol.4, No.4, pp.143-147.

Skempton, A. W. (1959) "Cast In-situ Bored Piles in London Clay"
Geotechnique, Vol.9, pp.153-173.

Triaxial Shear Report, April 1947,
Waterways Experiment Station, Vicksburg.